2006

Robust Estimation of Reliability in the Presence of Multiple Failure Modes

Phani R. Adduri
Wright State University

ROBUST ESTIMATION OF RELIABILITY IN THE PRESENCE OF MULTIPLE FAILURE MODES

A dissertation submitted in partial fulfillment of the
requirements for the degree of
Doctor of Philosophy

By

PHANI R ADDURI

B. E., Andhra University, India, 1999
M.E., Lamar University, 2001

2006
Wright State University

WRIGHT STATE UNIVERSITY

SCHOOL OF GRADUATE STUDIES

November 15, 2006

I HEREBY RECOMMEND THAT THE DISSERTATION PREPARED UNDER MY SUPERVISION BY Phani R Adduri ENTITLED Robust Estimation of Reliability in the Presence of Multiple Failure Modes BE ACCEPTED IN PARTIAL FULFILLMENT OF THE REQUIREMENTS FOR THE DEGREE OF Doctor of Philosophy.

_____

Ravi C. Penmetsa, Ph. D
Dissertation Director

_____

Ramana V. Grandhi, Ph. D
Director, Ph.D. Program in Engineering

_____

Joseph F. Thomas, Jr., Ph. D
Dean, School of Graduate Studies

Committee on Final Examination

_____

Ravi Penmetsa, Ph. D., WSU

_____

Ramana Grandhi, Ph. D., WSU

_____

Nathan Klingbeil, Ph. D., WSU

_____

Frank Ciarallo, Ph. D., WSU

_____

Robert Canfield, Ph. D., AFIT

ABSTRACT

Adduri, Phani Ram. Ph. D., Department of Mechanical and Materials Engineering, Wright State University, 2006. Robust Estimation of Reliability in the Presence of Multiple Failure Modes.

In structural design, every component or system needs to be tested to ascertain that it satisfies the desired safety levels. Due to the uncertainties associated with the operating conditions, design parameters, and material systems, this task becomes complex and expensive. Typically these uncertainties are defined using random, interval or fuzzy variables, depending on the information available. Analyzing components or systems in the presence of these different forms of uncertainty increases the computational cost considerably due to the iterative nature of these algorithms. Therefore, one of the objectives of this research was to develop methodologies that can efficiently handle multiple forms of uncertainty.

Most of the work available in the literature about uncertainty analysis deals with the estimation of the safety of a structural component based on a particular performance criterion. Often an engineering system has multiple failure criteria, all of which are to be taken into consideration for estimating its safety. These failure criteria are often correlated, because they depend on the same uncertain variables and the accuracy of the estimations highly depend on the ability to model the joint failure surface. The evaluation of the failure criteria often requires computationally expensive finite element analysis or computational fluid dynamics simulations. Therefore, this work also focuses on using

high fidelity models to efficiently estimate the safety levels based on multiple failure criteria.

The use of high fidelity models to represent the limit-state functions (failure criteria) and the joint failure surface facilitates reduction in the computational cost involved, without significant loss of accuracy. The methodologies developed in this work can be used to propagate various types of uncertainties through systems with multiple nonlinear failure modes and can be used to reduce prototype testing during the early design process.

In this research, fast Fourier transforms-based reliability estimation technique has been developed to estimate system reliability. The algorithm developed solves the convolution integral in parts over several disjoint regions spanning the entire design space to estimate the system reliability accurately. Moreover, transformation techniques for non-probabilistic variables are introduced and used to efficiently deal with mixed variable problems. The methodologies, developed in this research, to estimate the bounds of reliability are the first of their kind for a system subject to multiple forms of uncertainty.

TABLE OF CONTENTS

LIST OF FIGURES

LIST OF TABLES

ACKNOWLEDGEMENT

First, I would like to specially thank my academic advisor, Dr. Ravi Penmetsa, for his academic guidance and support during all these years of my Ph. D. program. I am deeply grateful for his mentoring, advice and research support. His stimulating suggestions and encouragement has helped me during this research and writing this dissertation. I also truly appreciate his patience during my numerous mishaps.

I would also like to thank Dr. Ramana Grandhi for his productive comments and suggestions. I would like to extend my gratitude to my committee members for their advice and help during my study and also for their time in reviewing this dissertation.

Also, a very special thanks goes to my wife for her patient love and support during my good days and encouragement through my bad ones. Finally, I would like to thank my parents for their love and continuous support during all these years.

1. INTRODUCTION

Every structural component that is designed using computer models has to be experimentally validated and the level of safety has to be predicted. The cost of testing complex physical systems becomes increasingly expensive in today's competitive market, driving the need for analytical certification. Uncertainty analysis is a computational tool that enables analytical certification by determining the safety of the component subject to various uncertainties in the design process. These uncertainties may be due to operating conditions, material properties, or geometric properties of the component. The uncertainty can be quantified based on the information available about that particular parameter.

If sufficiently large amount of data about a particular variable is available, then its variation can be approximated by using a probability distribution. These variables that can be assigned a probability distribution to represent the associated uncertainty are classified as random variables. But, if the information about a particular variable is sparse, then its variation cannot be approximated reliably using a probability distribution. These types of variables are classified as non-probabilistic variables. Based on the amount of information available, these variables can be modeled as interval variables or possibility functions.

Depending on the type of uncertain variables in the problem, a quantification technique is chosen to propagate the uncertainty through the system. If the information is available as just the lower and upper bounds on an uncertain variable, interval analysis techniques are used. Likewise, possibility theory is used when possibilistic information is available. And when the variables are random, probability analysis methods can be used

to estimate the probability of failure. The various methods that can be used for propagation are shown in figure 1.1.

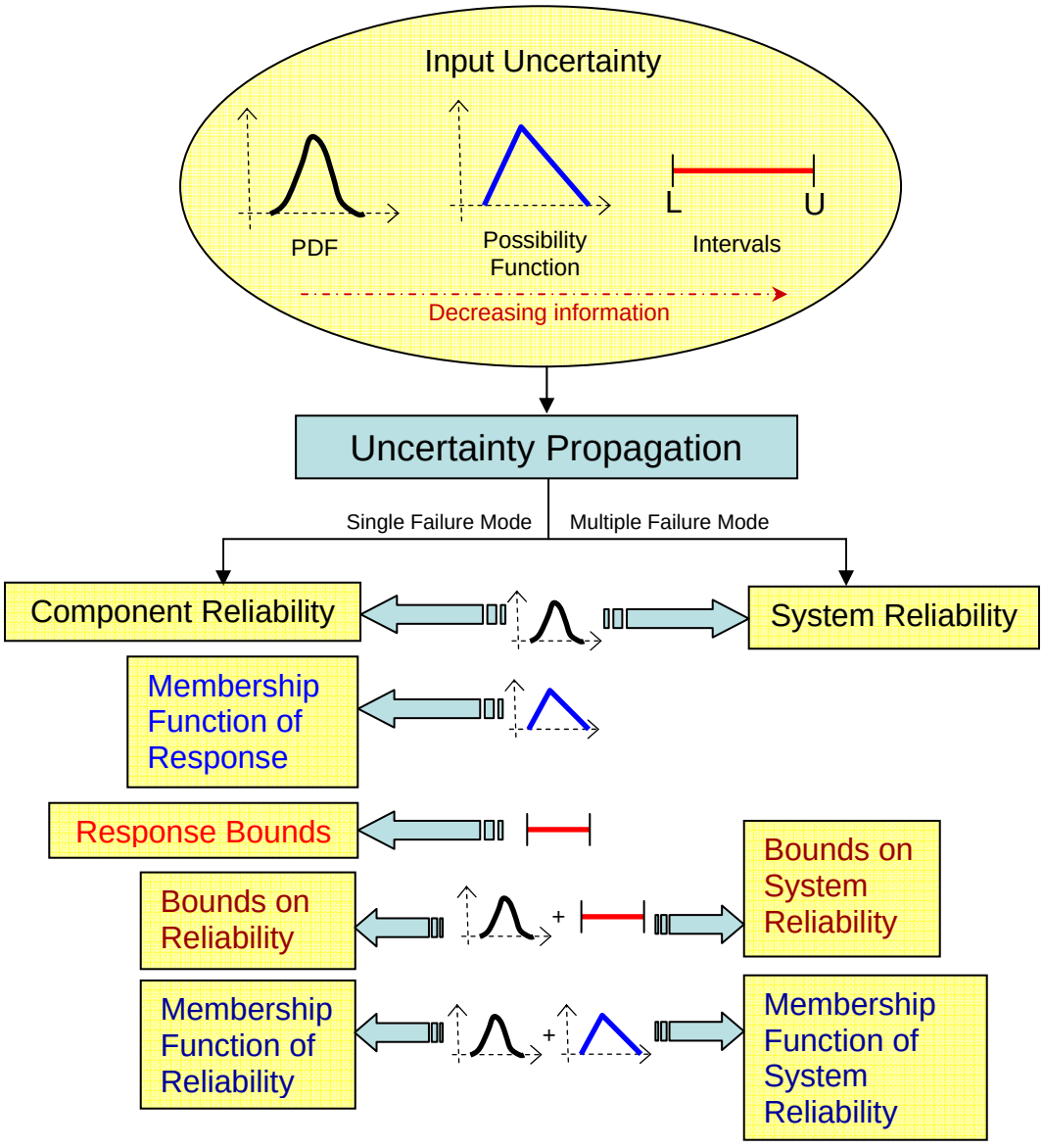

Figure 1.1: Various Techniques for Propagating Uncertainty

Traditional structural design approaches simplify the problem by considering all the variables as deterministic and accounts for the uncertainties by using safety factors. This approach does not provide any information about the influence of the variations of different parameters on the safety of the system. On the other hand, using a probabilistic

approach, the information about the influence of these uncertainties on the safety of the system can be quantified. This information can be used to optimize structures for maximum reliability and minimum weight or other important design criteria. Due to this advantage, reliability analysis is finding increased application in the design environment over the past few years. The following sections identify various forms of uncertainty that were considered in this research.

1.1. Probabilistic Techniques

These techniques are used when all the uncertain variables are modeled using probability density functions representing large amount of test data. Using these techniques, the reliability of the structure is estimated based on a single or multiple failure criteria. In this dissertation, component reliability is defined as the reliability when dealing with a single failure criterion and when based on multiple failure criteria the reliability is defined as system reliability.

1.1.1. Component Reliability

Reliability is defined as the probabilistic measurement of satisfactory performance of a system based on a particular performance criterion. Another way to look at the problem is to consider the unsatisfactory performance. The probability associated with this unsatisfactory performance is called the probability of failure. Most often in probabilistic analysis, the main goal is to calculate the probability of failure of the component based on a particular performance criterion. The probability of failure is estimated using the following relation:

$$p_f = \int_{\Omega} f_x(\boldsymbol{X})\, d\boldsymbol{X} \tag{1.1}$$

where, $f_x(\boldsymbol{X})$ denotes the joint probability density function of the vector of basic random variables, $\boldsymbol{X} = (x_1, x_2, \ldots, x_n)^T$ representing uncertain quantities such as loads, geometry, material properties, and boundary conditions. Also, Ω is the failure region modeled by the limit-state function or performance function $g(\boldsymbol{X})$. The failure region is defined by $g(\boldsymbol{X}) \leq 0$, and p_f is the probability of structural failure.

Monte Carlo simulation [1] can be used to estimate the failure probability numerically. But, if the limit-state function is implicit, this simulation involves tremendous computational cost, as a large number of exact function evaluations are required, which come from a computationally expensive Finite Element Analysis (FEA) or Computational Fluid Dynamics (CFD) simulations. To reduce the computational cost involved, the approximations of the limit-state functions can also be used in the Monte Carlo simulation. But, the random sampling used in Monte Carlo produces inaccuracy in the results [2]. This is because the random numbers generated using pseudo random number generators tend to form clusters and are not uniformly distributed over the entire design space [3]. Moreover, the accuracy of the estimated failure probability is also dependent on the number of samples used in the Monte Carlo simulation. So, to estimate low orders of failure probabilities, the number of samples needed are higher which in turn increases the computational cost involved. Therefore, alternate analytical or semi-analytical methods that make use of approximations are required for the estimation of structural failure probability.

Mathematically, it is often difficult to construct the joint probability density function, $f_x(\boldsymbol{X})$ for a given set of random variables, because of the scarcity of statistical data. Even if the joint probability density function could be determined, it is highly impractical to perform the multi-dimensional integration over the failure region, Ω, to estimate the failure probability. These difficulties lead to the development of methods to evaluate the failure probability based on function approximations.

Several methods were developed to estimate the failure probability using function approximations. The most common is the First-Order Reliability Method (FORM) [4]. In FORM, the limit-state function is approximated by a tangent plane at the Most Probable Point (MPP). The MPP is the point on the limit-state function that is closest to the origin in the standard normal space and has the maximum likelihood of failure. Using FORM, the first order estimation of the failure probability is given by $p_f = \Phi(-\beta)$, where $\Phi(\bullet)$ is the standard normal cumulative distribution function and β is the safety index, which is the distance of the MPP from the origin. The use of FORM in the estimation of failure probability is justified when the random variables are normally distributed and the limit-state function is linear around the MPP. However, if the failure surface is nonlinear, then the estimation of the failure probability using FORM gives inaccurate results. To improve the accuracy, advanced mean value methods [5] have been developed.

One method that takes into account the curvature of the limit-state function at the MPP is the Second-Order Reliability Method (SORM) [6-8]. In SORM, the limit-state function is approximated using a quadratic approximation at the MPP. In most cases, SORM provides a better estimate of the failure probability than FORM. But for using the quadratic approximation for the limit-state function, second-order derivatives of the limit-

state function are needed, which require significant computational effort. Moreover, the formulae derived for the estimation of failure probability are based on specific characteristics of a standard normal distribution function. Therefore, non-normal random variables are to be normalized, which introduces additional error.

Wang and Grandhi [9] used a high quality approximation of the failure region to accurately estimate the MPP for a highly nonlinear limit-state function. This methodology does not need the evaluation of the exact performance function, as the approximate model is constructed and used for the MPP search. Therefore, the computational time in finding the MPP is greatly reduced for problems with highly nonlinear and implicit performance functions. Several authors [10-14] have also explored the use of approximations in computing the failure probability.

One methodology for estimating the failure probability is the evaluation of the convolution integral using Fast Fourier Transforms (FFT). In the literature the use of FFT for estimating the probability of failure for a particular limit-state function has been demonstrated. In order to use FFT, the limit-state function must be separable and in closed-form. Sakamoto, et al. [15] used a response surface approximation to get a closed-form expression for a particular implicit limit-state function. Penmetsa and Grandhi [16] used a Two-point Adaptive Nonlinear Approximation (TANA2) at the MPP for obtaining a closed-form expression for a limit-state function. The accuracy of the estimated probability of failure depends entirely on the validity of the approximation around the MPP of the limit-state function. The procedural details of using FFT to estimate the failure probability are given below, as this is the basis for a methodology developed in this work to estimate the failure probability of a structural system.

Fast Fourier Transforms can be applied to solve the convolution integral if the limit-state function is a linear combination of independent variables. To obtain a linear function, the original limit-state function can be approximated by using a first-order Taylor series expansion, but this gives very poor estimates. If the second-order terms are considered in the approximation, the cost of evaluation of the second-order gradients is very high. Therefore, Sakamoto et al. [15] implemented the response surface methodology and used intervening variables in the response surface to make the response surface a linear combination of these intervening variables. In the response surface approach, the approximate limit-state function considered is expressed as

$$\tilde{g}(\boldsymbol{X}) = \beta_0 + \sum_{i=1}^{n} \beta_i x_i + \sum_{i=1}^{n} \beta_{ii} x_i^2 \tag{1.2}$$

where, $\boldsymbol{X} = (x_1, x_2, ..., x_n)^T$ are the basic independent random variables in reliability analysis and β_0, β_i's and β_{ii}'s are constants. Eq. (1.2) is a second-order response surface model without the interaction terms. This was used so that the approximate limit-state can be express as a linear combination of the intervening variables is in the following form

$$\tilde{g}(\boldsymbol{Y}) = y_1 + y_2 + \ldots + y_n \tag{1.3}$$

$$y_i = \beta_i x_i + \beta_{ii} x_i^2 \tag{1.4}$$

where, y_i is an intervening variable.

If the distribution of the random variables x_i is known, Eq. (1.5), using the chain rule gives the probability density function of the intervening variables y_i.

$$f_y(y) = \frac{dx}{dy} f_x(y) \tag{1.5}$$

where f_y is the PDF of the variable y and f_x is the PDF of the variable x.

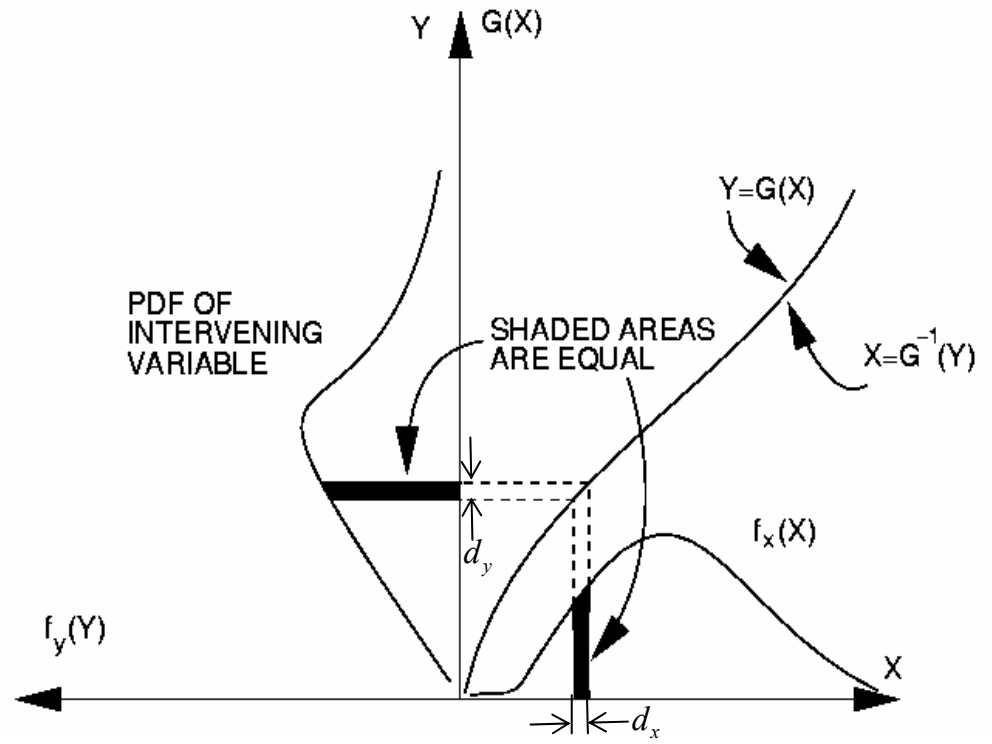

Figure 1.2: Transformation of PDF

As shown in Fig. 1.2, the PDF of the transformed variables can be obtained by matching the area under the original PDF to the area under the transformed PDF. The above statement that the areas are equal implies that, the likelihood that Y takes on a value in an interval of width d_y is equal to the likelihood that X takes on a value in an interval centered on a corresponding value $x = g^{-1}(y)$ but of width $d_x = d_{g^{-1}(y)}$. Figure 1.2 is a graphical representation of Eq. (1.5)

Eq. (1.4) transforms the approximation into a linear combination of the intervening variables. Therefore, the PDF of $\tilde{g}$ which is the convolution of the individual PDFs of the intervening variables y_i, can be expressed as follows:

$$f_{\tilde{g}}(\tilde{g}) = f_{y_1}(y_1) * f_{y_2}(y_2) * \ldots f_{y_n}(y_n) \tag{1.6}$$

Applying the Fast Fourier Transform on both sides of Eq. (1.6), we get

$$FFT[f_{\tilde{g}}] = FFT[f_{y_1}] \cdot FFT[f_{y_2}] \ldots FFT[f_{y_n}] \tag{1.7}$$

By the inverse FFT, the PDF of the limit-state $\tilde{g}$ is obtained. The probability of failure is given by the following equation

$$p_f = \int_{-\infty}^{0} f_{\tilde{g}}(\tilde{g})\, d\tilde{g} \tag{1.8}$$

By evaluating the area under the probability density function for all values in the failure region, the failure probability is estimated. In this approach, the probability density functions are assumed to be time dependent signals enabling the use of FFT to perform efficient convolution.

Probability Density and Characteristic Functions:

As discussed earlier, the limit-state function is transformed using intervening variables into a linear combination of the random variables. The PDF of the linear limit-state is obtained by the convolution integral [17]. For carrying out this multifold integration, the FFT technique is implemented. The characteristic function, which is the Fourier transform of the PDF, and the PDF of a random variable, can be expressed as a pair of Fourier transforms [18]. The formulation of the Fourier transform pairs is as follows

$$M_Y(\theta) = \int_{-\infty}^{\infty} P_Y(y)\,.\, e^{i2\pi\theta y}\, dy \tag{1.9}$$

$$P_Y(y) = \int_{-\infty}^{\infty} M_Y(\theta).e^{-i2\pi\theta y}\, d\theta \tag{1.10}$$

in which $P_Y(y)$ and $M_Y(\theta)$ are the probability density and characteristic function of Y, respectively, and $i = \sqrt{-1}$. These equations define the direct and the inverse Fourier transforms with $M_Y(\theta)$ as the direct Fourier Transform of $P_Y(y)$, and $P_Y(y)$ as the inverse Fourier Transform of $M_Y(\theta)$.

The properties of a characteristic function are summarized in the following:

1. $|M_Y(\theta)| \le 1, M_Y(-\theta) = \overline{M_Y(\theta)}$

   in which $|\bullet|$ and $\overline{\bullet}$ are the absolute value and the complex conjugate of $\bullet$, respectively.

2. The characteristic function of a random variable $X = a \cdot Y + b$ is expressed as,

   $M_x(\theta) = e^{ib2\pi\theta} \cdot M_Y(a\theta)$

3. The characteristic function of a random variable Y, which is the sum of statistically independent random variables $y_1, y_2, \ldots, y_n$, is given by the product of the characteristic function of each random variable,

   $M_Y(\theta) = M_{y_1}(\theta) \cdot M_{y_2}(\theta) \cdots M_{y_n}(\theta)$.

Due to the above properties, Fourier Transform techniques can be used to evaluate the complex convolution integral. The use of this technique for correlated random variables was also demonstrated by Sakamoto et al. [15]. As the technique can be applied for different kinds of distributions and even for correlated random variables, it has broad utility.

1.1.2. System Reliability

A structure consists of many individual components that have the potential to fail. Failure of any of these individual components might lead to structural failure. The reliability analysis of structural systems involves the simultaneous consideration of multiple limit-states from different disciplines, which might be correlated. Each limit-state might be an implicit function and requires expensive computations to evaluate the function value and the gradients that are needed for reliability analysis. Therefore, in the presence of multiple limit-states, the computational effort involved in estimating the failure probability increases tremendously. The failure probability of the system is the integration of the joint probability density function over the joint failure region obtained by the intersection of all of the limit-states. Monte Carlo simulation can be used to estimate the joint probability density function numerically. However, this simulation involves tremendous computational cost, as a large number of exact function evaluations are required. Therefore, alternate methods that make use of approximations are required for the estimation of structural system failure probability.

Structural systems can be idealized into two simple categories: series and parallel systems [19]. A series system is one in which, if even one component fails, the whole system fails. These systems are also called weakest link systems. Every component of the system should function satisfactorily for the system to be reliable. A statically determinate structure is a series system, as the failure of one of its members implies the failure of the structure. Figure 1.3 (a) shows a series system, which clearly shows that the failure of anyone of the components leads to structural failure.

In the case of parallel systems, the system survives even if one or more of the components have failed. The system fails to function satisfactorily only when every component has failed. Parallel systems are also called redundant systems. Redundancy in parallel system is of two types, active and passive redundancy. Active redundancy occurs when the redundant members participate in the structural behavior even at low loading. Passive redundancy occurs when the redundant elements do not participate in structural behavior until the structure has suffered a sufficient degree of degradation or failure of its elements. Figure 1.3 (b) shows a model of a parallel system. A system that has a combination of series and parallel components is called a mixed system.

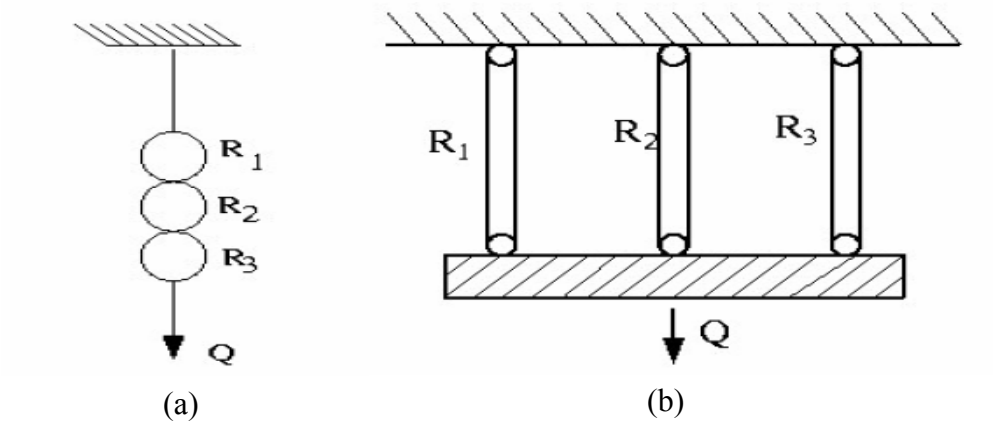

Figure 1.3: (a) Series System, (b) Parallel System

The system failure probability can be obtained easily if its components are assumed to be independent. However, in practical problems, the failure conditions depend on the same random variables, therefore, the components are correlated. Several authors have developed methods to determine the bounds on the failure probability of a structural system. Cornell [20] has developed bounds on the failure probability for a system subjected to multiple failure modes that have been extensively used in the

literature. The upper bound was obtained by assuming the components are perfectly correlated, whereas the components were assumed to be uncorrelated for obtaining the lower bound.

For a series system, the bounds are given by

$$\text{Max [Component } P_{f_i}\text{]} \le P_f \text{ of system} \le \sum_{i=1}^{n} \text{ [Component } P_{f_i}\text{]} \tag{1.11}$$

Bennett and Ang [21] developed the bounds for a parallel system that are given by

$$\text{Max } [\sum_{i=1}^{n} \text{ [1-(Component } P_{f_i}\text{)]}, 0] \le P_f \text{ of system} \le \text{ Min [Component } P_{f_i}\text{]} \tag{1.12}$$

where n is the number of failure modes. However, the component P_f has to be quantified accurately in order to obtain an accurate system reliability bound. The failure probability of the components is typically estimated using either FORM or SORM. This estimation results in an inaccurate representation of the failure region for nonlinear limit-state functions. This error in the component failure probability is propagated into the bounds of the system failure probability, making them inaccurate.

Ditlevsen [22] proposed a method of narrow bounds based on the correlation between the failure modes. However, these bounds are accurate when the limit-state functions are linear. A methodology was developed by Feng [23] to improve the accuracy of the Ditlevsen's bounds using third-order joint probability. The resulting accuracy is high for problems for which the third-order joint probability can be estimated accurately; but, in most cases, the formula for the estimation of the third-order joint probability has significant errors. Song [24] has proposed a method using numerical integration in a reduced domain. This method reduces the actual number of simulations and gives

accurate results for a low number of failure modes. However, when the structure has many failure modes, this methodology cannot be used directly. He proposed a method to deal with this drawback, but that required second and third-order probabilities or the use of the failure probability estimated by using FORM, both of which introduces errors. Several other techniques [25-27] have been developed for estimating the bounds on system reliability based on the type of system under consideration.

Some techniques [28-32] have been developed to estimate the system reliability as a single value rather than as bounds. Melchers and Ahammed [30] proposed a methodology to estimate the failure probability of a parallel system. In this method, the closest intersection point is estimated by using successive approximations. As this is the point of maximum likelihood within the zone of interest, a first-order approximation is constructed at this point for each of the limit-states and the failure probability is estimated based on these approximations. Using this method, the intersection point that is closest to the origin in the standard normal space can be estimated accurately, but a first-order approximation at this intersection point would result in an erroneous approximation of a nonlinear limit-state function. This, in turn, would result in a poor approximation of the joint failure region, as shown in Figure 1.4. Therefore, a high fidelity model is required to capture the nonlinear joint failure region. In this work, a methodology for estimating the reliability of a structural system was developed. This methodology was developed to primarily handle series systems but can be modified to approximate the intersection region required for parallel systems as well.

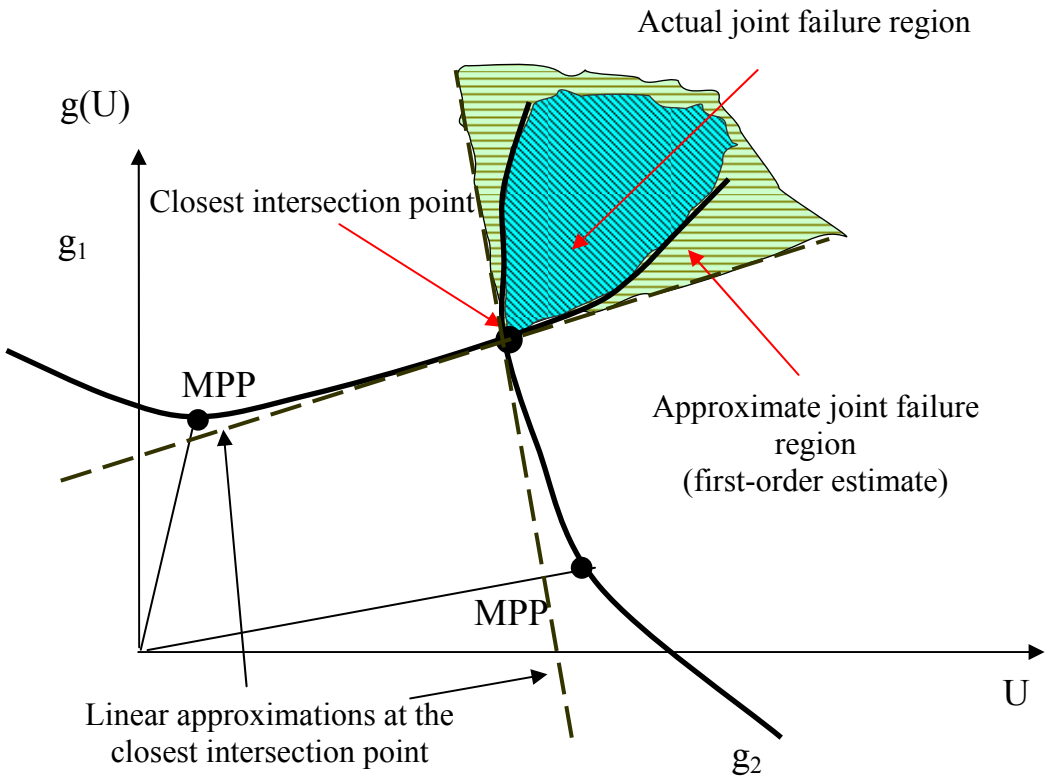

Figure 1.4: Joint Failure Region

However, when dealing with a series system, the estimation of the probability of failure is not as straightforward as that of a parallel system. This is because the MPP for each of the limit-state functions, as well as the intersection points, make a significant contribution to the failure probability integral. The joint failure region should be modeled accurately for estimating the failure probability of a series system. Therefore, there is a need to develop a methodology to estimate the failure probability of a structural system, whether the system is a series or a parallel system.

Importance sampling techniques [31, 32] can also be used to handle this integration, but an appropriate sampling function should be used to take full advantage of this method. Mori and Kato [31] proposed an importance sampling function for performing the integration for a series system. Based on the fact that an optimal

importance sampling function can be determined for a linear limit-state function in a standard normal space, an importance sampling function was presented as a linear combination of the optimal sampling functions for each of the limit-states. This sampling technique produces accurate results for linear limit-state functions. Due to the overlapping of the domains of the sampling functions for each of the limit-states, their linear combination differs from the optimal sampling function. This decreases the accuracy of the sampling function. Thus, the number of simulations needed for the convergence of the failure probability increases.

System reliability estimation is a complex and computationally expensive task. In this research, a methodology is developed to efficiently estimate the reliability by using surrogate representations of the limit-state functions to reduce the computational cost. This methodology uses Fast Fourier Transforms (FFT) to solve the convolution integral. As the entire failure region cannot be modeled using a single approximation, a methodology was developed so that the convolution integral can be solved using several approximations, each of which are valid within a certain region over the entire space.

1.2. Non-Probabilistic Techniques

In many cases, uncertainty does not necessarily imply randomness. If the information available is not sufficient to model a PDF, assuming one in order to apply reliability estimation methods leads to erroneous results. Therefore, non-probabilistic techniques are used to propagate these kinds of uncertainties through the system and obtain the bounds on the system response. These bounds can be used to validate a design

or suggest additional testing to gather more data on the response. The following two types of models are considered in this research.

1.2.1. Fuzzy Membership Functions

Fuzzy theory facilitates the representation of imprecise and vague information in an analytical form. Zadeh [33] introduced these concepts of fuzzy sets in 1965. Since then, these concepts have been used in different fields for representing unclear information. In uncertainty analysis, these concepts are being used for representing uncertain parameters when the information is limited. Using fuzzy theory, these variables can be represented by membership functions based on their possibility of occurrence. The membership function is a functional representation of the missing information extrapolated from the available information, which is typically the lower and upper bounds and the central value. Therefore, numerous models are fit to this minimal data depending on the problem and intuition of the designer.

Fuzzy information can be propagated through a system using two different techniques. One technique is to include the fuzzy uncertainties in the finite element formulation [34- 36]. This results in a linear fuzzy system of equations as a function of α, which is the degree of possibility. The degree of possibility is defined such that 0% represents the lower and upper bounds and the 100% possibility represents the central value of the peak of the membership function. The advantage of this technique is that these equations need to be solved only once to obtain the membership function of the response. These methods are still under development and have not been well tested.

Another technique explores all the binary combinations of the extreme values of the fuzzy variables at each possibility level to obtain the bounds on the response. As one

exact finite element analysis is required for each configuration, the computational effort involved increases exponentially, but the bounds on the response are captured accurately in the absence of extreme values within these bounds.

1.2.2. Interval Bounds

If the information about a variable is available only as an upper and lower bound, then interval analysis techniques [37, 38] can be used to estimate the lower and upper bounds on the response. Interval arithmetic provides an exact bound if all the variables occur only once in the function. This problem of dependency [39] estimates a wider bound for the response if a variable occurs more than once.

Interval uncertainties can also be propagated through the structure by including them in the finite element formulation [40-44]. A static structural problem can be expressed in the form of a system of linear interval equations which are solved to obtain the bounds on the structural response. As each variable appears more than once, the bounds obtained are wider than the actual bounds.

Braibant et al [45] presented possibilistic approaches for structural optimization and design which establishes a connection between fuzzy analysis and interval arithmetic. They proposed that it is possible to evaluate fuzzy variables by the use of α-cuts or membership levels, as shown in figure 1.5. α is the degree of possibility of the fuzzy set. At each level, the variation of an uncertain parameter is defined by a lower and an upper bound. Once the variables are defined as membership functions, the bounds on the response at various α-cuts can be obtained.

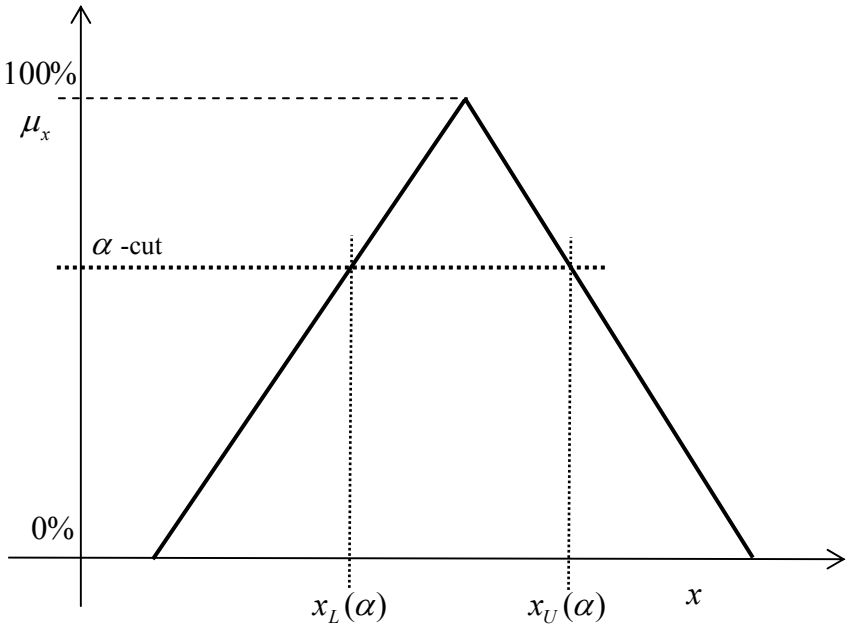

Figure 1.5: Membership Function Showing an α-cut

The Vertex method [46] evaluates the function value at each of the vertices of the design space, represented by the bounds on the variables, to obtain the minimum and maximum values of the response. This method works well for linear problems, but fails to capture the minimum and maximum for nonlinear non-monotonic responses. Some of the other methods [47, 48] use optimization techniques to calculate the minimum and maximum value of the response within the specified bounds.

All these methods discussed above cannot accommodate a combination of random as well as fuzzy input variables. Therefore, methods need to be developed for dealing with problems comprised of mixed uncertain variables. Moller et al [49] introduced a methodology for estimating the membership function of the safety index by considering fuzzy randomness. They formulated a Fuzzy First Order Reliability Method (FFORM) that simultaneously permits the usage of fuzzy variables and random variables. Using this

method, the membership function of the reliability index can be estimated accurately. But the calculation of the failure probability from the safety index values is prone to errors. The estimated safety index is independent on the nonlinearity of the failure surface and this surface is approximated using a linear approximation in the calculation of failure probability.

In this current work, a methodology to deal with problems with both random as well as fuzzy variables is developed. Typically, obtaining the minimum and maximum values of a nonlinear response requires the use of optimization techniques at each α-cut. The proposed technique estimates the membership function of the reliability accurately without the use of optimization techniques.

In a multidisciplinary environment, the failure of the structure is governed by several limit-state functions. But when the knowledge about some of the uncertain variables is limited, the entire range of these bounds should be explored while estimating the bounds on the reliability. This increases the computational cost exponentially with the increase in the number of nonrandom variables. Moreover, for each combination of the nonrandom parameters a new joint failure region should be modeled accurately for the prediction of the reliability. So for dealing with problems where some variables are random and some are nonrandom, the methodology for estimating the reliability of a structural system is extended to estimate the bounds on the system reliability.

1.3. Reliability-based Design Optimization

While designing a structure, the uncertainties, which might arise in the design process due to the operating conditions, boundary conditions, material properties, etc,

need to be taken into consideration. These uncertainties contribute to the probability that the structure does not perform as intended. Therefore, when dealing with uncertain parameters in the design process, additional constraints are placed on the optimization problem to satisfy a prescribed reliability level. These constraints facilitate the optimal design to be both economical as well as reliable. The coupling between reliability analyses and optimization methods leads to high computational cost due to the iterative nature of both methods. Therefore, methodologies that make use of function approximations have been developed to improve their efficiency [50-56].

As the calculation of the failure probability requires the solution of the convolution integral, different approximation techniques have been used to compute the reliability index. In the optimization problem, this reliability index is constrained to achieve the target reliability. If the failure of the structure is based on a single failure mode, then the reliability index based on that particular failure mode is constrained in the optimization problem. In the case of multiple performance functions, each of the reliability indices can be constrained, leading to the same number of reliability constraints as the performance functions. So the optimization formulation is given by

$$\text{Minimize } f(\boldsymbol{X},\boldsymbol{B})$$

$$\text{subject to } \beta[g_i(\boldsymbol{X},\boldsymbol{B}) \geq 0] \geq \beta_{t\_i},\ i = 1....n$$

$$b_j^L \leq b_j \leq b_j^U,\ j = 1...m$$

where $f(\boldsymbol{X},\boldsymbol{B})$ is the objective function, and $\beta[g_i(\boldsymbol{X},\boldsymbol{B}) \geq 0]$ is the safety index of the limit-state function $g_i(\boldsymbol{X},\boldsymbol{B}) < 0$. The objective function and the limit-state might

depend on both the design variables, $\boldsymbol{B}$, and the uncertain random variables, $\boldsymbol{X}$. The β_{t_i} are the target reliability indices.

The safety or reliability index is defined as the distance of the MPP from the origin in the normalized space of the random variables. So, the safety index is independent of the nonlinearity of the failure surface at the MPP. As shown in Figure 1.6, for the given value of the safety index, the linear failure surface at the MPP differs from the actual surface based on the nonlinearity of the limit-state function. So the actual failure probability differs from the failure probability corresponding to the safety index.

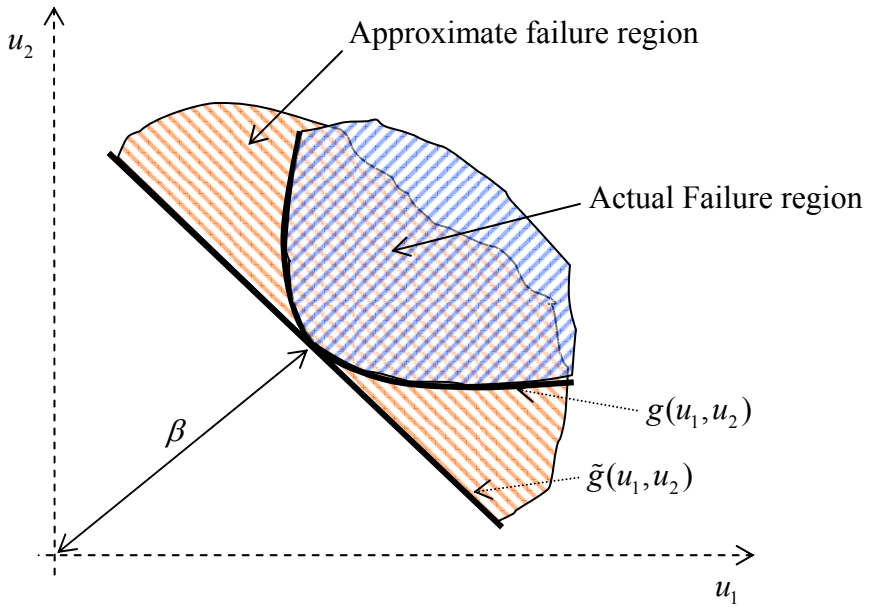

Figure 1.6: Failure Surface Based on Safety Index

To overcome this difficulty, the same optimization problem can also be formulated with a failure probability constraint for each limit-state. The reliability constraints in the optimization problem can now be formulated as the probability of failure of each of the components to be less than a predetermined probability level. So,

the optimization problem based on one probability constraint for each failure mode can be generally defined as

$$\text{Minimize } f(\boldsymbol{X}, \boldsymbol{B})$$

$$\text{subject to } P[g_i(\boldsymbol{X}, \boldsymbol{B}) < 0] \le p_i,\ i = 1....n$$

$$b_j^L \le b_j \le b_j^U,\ j = 1...m$$

where p_i are the target probability of failures. This formulation needs an efficient algorithm to estimate the failure probability accurately. Moreover, when dealing with multiple limit-states, the definition of failure of the structural system cannot be taken into consideration in the design process because each failure probability or reliability index is constrained. So in this work, the methodology for estimating the system reliability is used along with optimization to design a structure using one system reliability constraint. The design space for a reliability-based optimization problem formulated with a system reliability constraint is not as restricted as the one with a constraint for each failure mode. This is because a combination of constraints has to be satisfied rather than each individual constraint. Therefore, using the system reliability constraint, there will be an improvement in the optimal design obtained when compared with that obtained using multiple component reliability constraints.

1.4. Overview

This section summarizes the outline of the chapters in the context of the various uncertainty analysis techniques used to propagate different types of uncertainties. Chapter 1 introduced the various propagation techniques available based on how the uncertain

parameters are modeled. Also, a brief introduction on optimizing a structure in the presence of uncertainties to obtain an optimal design which is also reliable is presented. Chapter 2 deals with an innovative technique for obtaining the membership function of the response by the use of transformation technique for membership functions. This technique was extended for problems with a combination of fuzzy and random uncertain variables. Chapter 3 deals with estimating the reliability of a structural system subjected to multiple failure modes. For dealing with high nonlinearity of the joint failure region, a methodology was developed so that the convolution can be solved based on multiple approximations over several disjoint regions in the design space. In chapter 4, the system reliability estimation algorithm was extended to handle a combination of random as well as interval variables. Chapter 5 combines the technique for transforming membership functions along with the algorithm for estimating the system reliability for handling problems with random as well as fuzzy variables. The advantages of using a system reliability constraint in reliability-based optimization is demonstrated by considering a lightweight composite torpedo model in chapter 6. Finally, chapter 7 summarizes the work done and presents some directions for future work. A brief description of function approximations used in this work to reduce computational cost is given in the appendix.

1.5. Contributions

Based on the information available about the uncertain quantities, different forms of uncertainties might be present in a given problem. The computational cost increases tremendously while dealing with problems with mixed forms of uncertainties. Moreover, most of the work available in the literature on uncertainty analysis deals with a single

failure criterion. But an engineering system often has multiple failure criteria and all of these criteria are to be taken into consideration while estimating its safety. Therefore, the primary objectives of this research work are:

1. Develop methodologies to efficiently handle problems with a combination of random as well as nonrandom (fuzzy or interval) variables
2. Develop techniques to estimate the safety in the presence of multiple failure modes

High fidelity approximate models are used to model implicit limit-state functions as well as the joint failure surface to reduce the computational cost without loss of accuracy. Fast Fourier transforms based reliability estimation technique has been developed to estimate the reliability based on multiple failure modes. In this algorithm, the convolution integral is solved in parts over multiple disjoint regions spanning the entire design space. Transformation techniques for nonrandom variables is also introduced and used to efficiently deal with mixed variables problems. The methodologies, developed in this work, for dealing with multiple forms of uncertainties as well as multiple failure modes are the first of their kind to estimate the bounds on system reliability.

2. MEMBERSHIP FUNCTION OF COMPONENT RELIABILITY

The uncertainties in a physical system can be modeled and analyzed by using probability theory or possibility theory depending on the amount of information available. In probability theory, the uncertain variables are modeled using Probability Density Functions (PDF) and then propagated through the system to obtain its reliability. In the absence of sufficient data to model a PDF, possibility theory, in which variables are represented using fuzzy membership functions, can be used to propagate uncertainty. But when dealing with a combination of both probability distributions and fuzzy membership functions, the computational cost involved in estimating the membership function of reliability increases exponentially because one reliability analysis, which is a computationally expensive procedure, is performed at each possibility level to obtain the bounds on the reliability of the structure. To improve the computational efficiency, a technique that uses response surface models and transformations of possibility functions is presented here. The efficiency and accuracy of the proposed methodology is demonstrated using numerical examples.

2.1. Transformation of Membership Functions

Obtaining the minimum and maximum values of a nonlinear response within certain bounds requires the use of optimization techniques at each α-cut. This procedure is computationally expensive for problems with implicit limit-state functions, as optimization requires the function value and gradient information at several points in the iterative process. But if the response is expressed as a linear combination of the fuzzy variables, then at each α-cut the bounds of the response can be obtained by using

interval arithmetic algorithm. Therefore, a nonlinear function is expressed as a linear combination of intervening variables in order to apply an interval arithmetic algorithm. If the membership functions of the intervening variables are available, then at each α-cut, the bounds of the response at that level can be determined.

Let the intervening variable, y, be a function of x given by, $y = G(x)$. The membership function of y is obtained by using the membership function of x. The membership function gives the possibility of occurrence. For this reason, the possibility of occurrence of a point y_0 is equal to the possibility of occurrence of x_0, where $x_0 = G^{-1}(y_0)$. Therefore, the possibility function of y can be obtained using Eq. (2.1) and appropriate transformations (Fig 2.1):

$$\mu_y(y) = \mu_x(G^{-1}(y)) \tag{2.1}$$

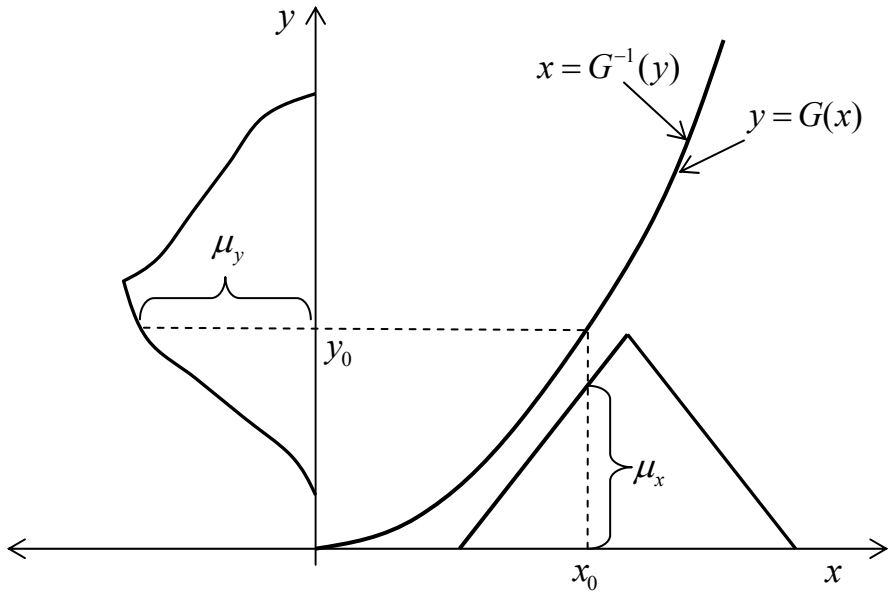

Figure 2.1: Transformation of Membership Function

According to possibility theory, the possibility of an event is equal to the maximum possibility of all the subsets of the event. The same applies in the transformation of the membership function. If there exists multiple values of x for a given y, then the possibility of that y is the maximum possibility of all the corresponding events of x. For example, if y_0 has two events x_{01} and x_{02}, which is generally the case when transforming based on $y = x^2$, then the possibility of y_0 is equal to the maximum possibility of the two individual events as shown in Eq. (2.2)

$$\mu_y(y_0) = \text{Max } \{ \mu_x(x_{01}), \mu_x(x_{02}) \} \tag{2.2}$$

If the uncertainties in the problem are quantified using fuzzy membership functions, these can be propagated through the structure to obtain the membership function of the response. Using the transformation technique described above, the bounds on the response at each level can be obtained without the use of optimization techniques if the response is available or approximated as a separable closed-form expression in terms of the uncertain variables.

2.1.1. Numerical Example

To illustrate the accuracy and the usage of transformation techniques to obtain the bounds on the response, consider a function with two fuzzy variables as shown in Eq. (2.3). The membership functions of x_1 and x_2 are given by Eq. (2.4) and Eq (2.5) respectively. Figures 2.2 and 2.3 show the membership functions of the fuzzy variables.

$$g(x_1, x_2) = x_1^2 + x_2^2 - 4x_1 + 4 \tag{2.3}$$

$$\mu_{x_1}(x_1) = \begin{cases} (4 - x_1) & 3 \le x_1 \le 4 \\ (x_1 - 1)/2 & 1 \le x_1 \le 3 \end{cases} \tag{2.4}$$

$$\mu_{x_2}(x_2) = \begin{cases} (1 - x_2) & 0 \le x_2 \le 1 \\ (x_2 - 1) & -1 \le x_2 \le 0 \end{cases} \tag{2.5}$$

$$y_1 = (x_1 - 2)^2, \; y_2 = {x_2}^2 \tag{2.6}$$

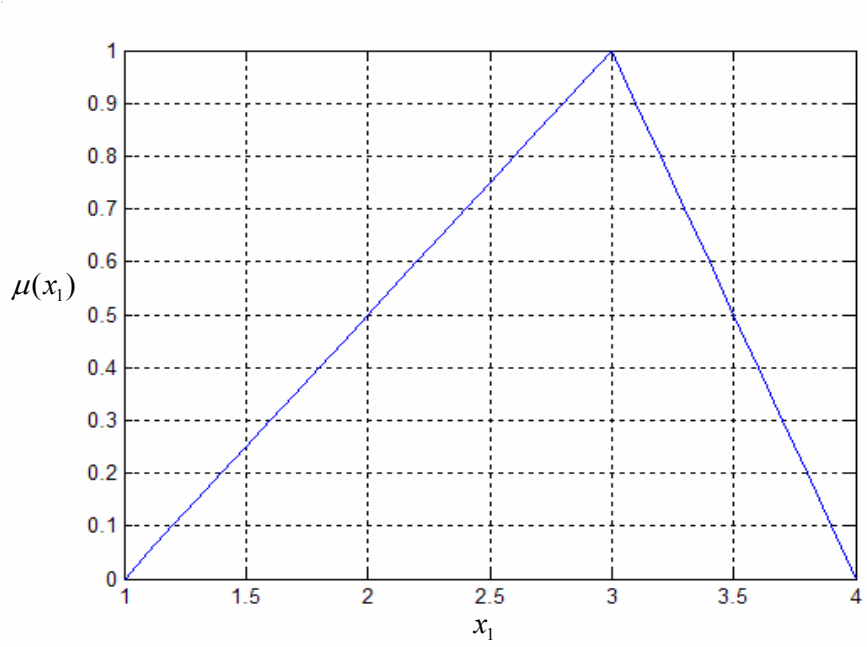

Figure 2.2: Membership Function of x_1

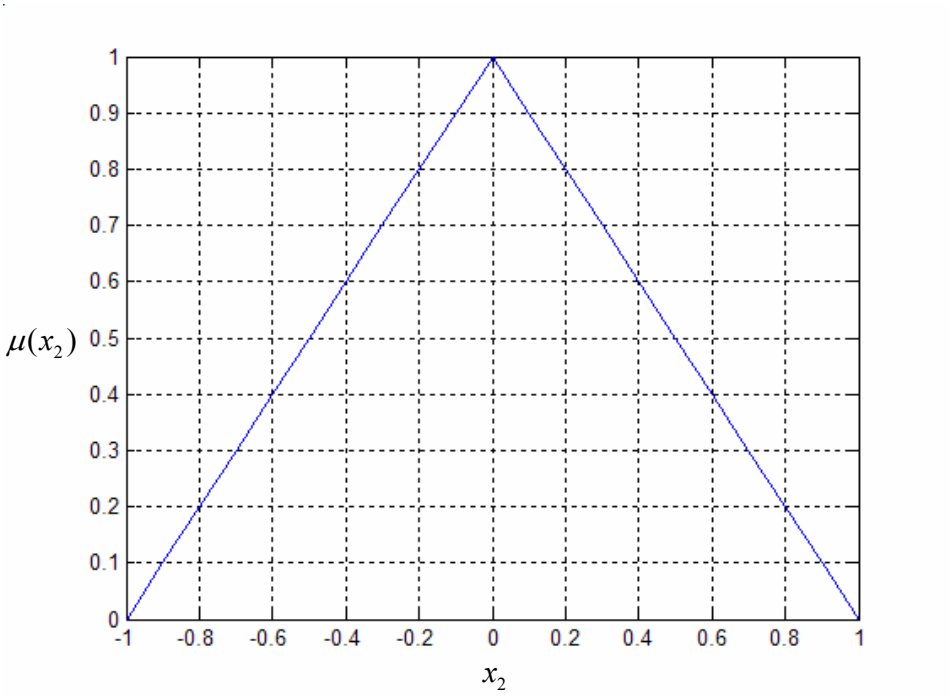

Figure 2.3: Membership Function of x_2

In this problem the minimum value of the response is at $x_1 = 2.0$ and $x_2 = 0.0$ which does not correspond to the vertices at any α-cut, as shown in figure 2.4. The membership function obtained by using the vertex method (fig. 2.5) fails to capture the minimum value of the response. This method calculates the minimum and maximum values of the response only at the lower and upper limits of the variables at each membership level. Therefore, it does not identify the minimum of the response which is located inside the design space.

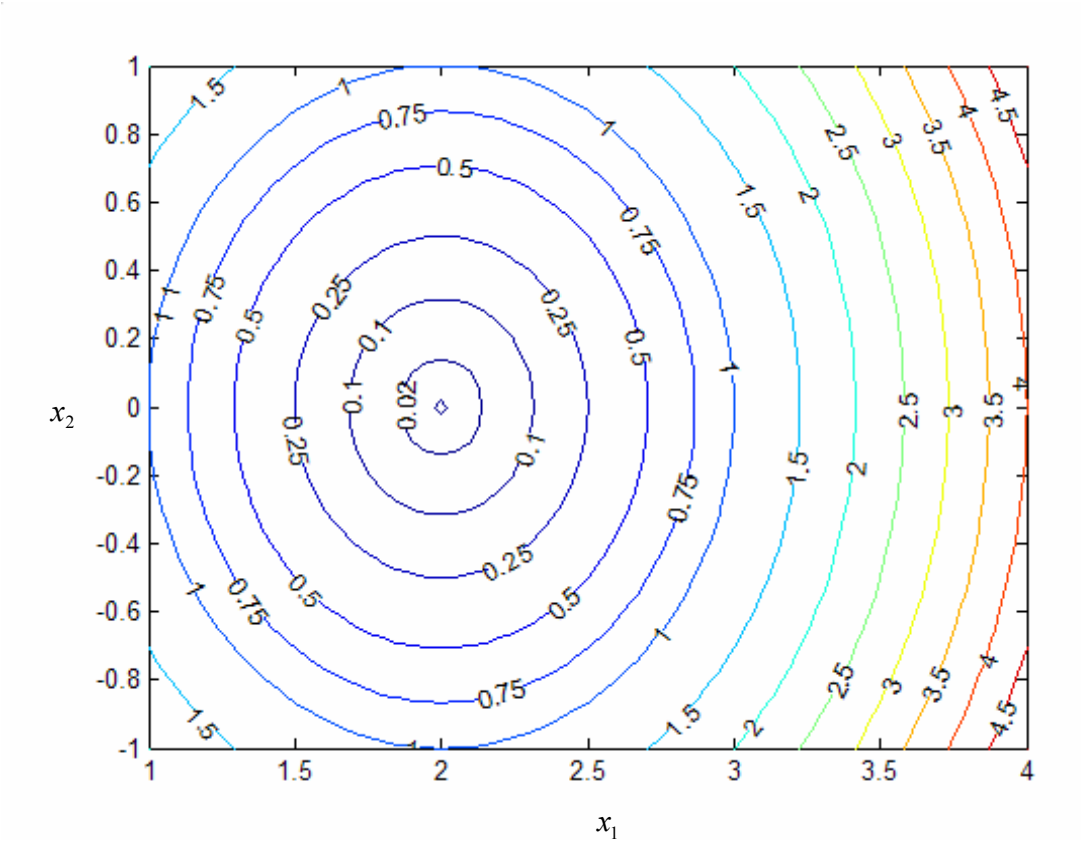

Figure 2.4: Contour Plot of the Function

The use of optimization techniques at each level estimates the extreme values within the interval accurately. Using transformation techniques, the membership function is also estimated accurately and is in good agreement with the membership function

obtained using optimization techniques as shown in figure 2.5. This method was also able to capture the extreme values within the interval. Once the closed-form expression is expressed as a linear combination in terms of intervening variables (Eq. 2.6), interval arithmetic can be used to estimate the response bounds. The drawback of using interval arithmetic for a closed-form expression is the problem with dependency [39]. If any variable appears more than once in an expression, it is treated as a different variable for each occurrence resulting in wider bounds. By using intervening variables, each variable appears only once in the expression resulting in accurate bounds on the response.

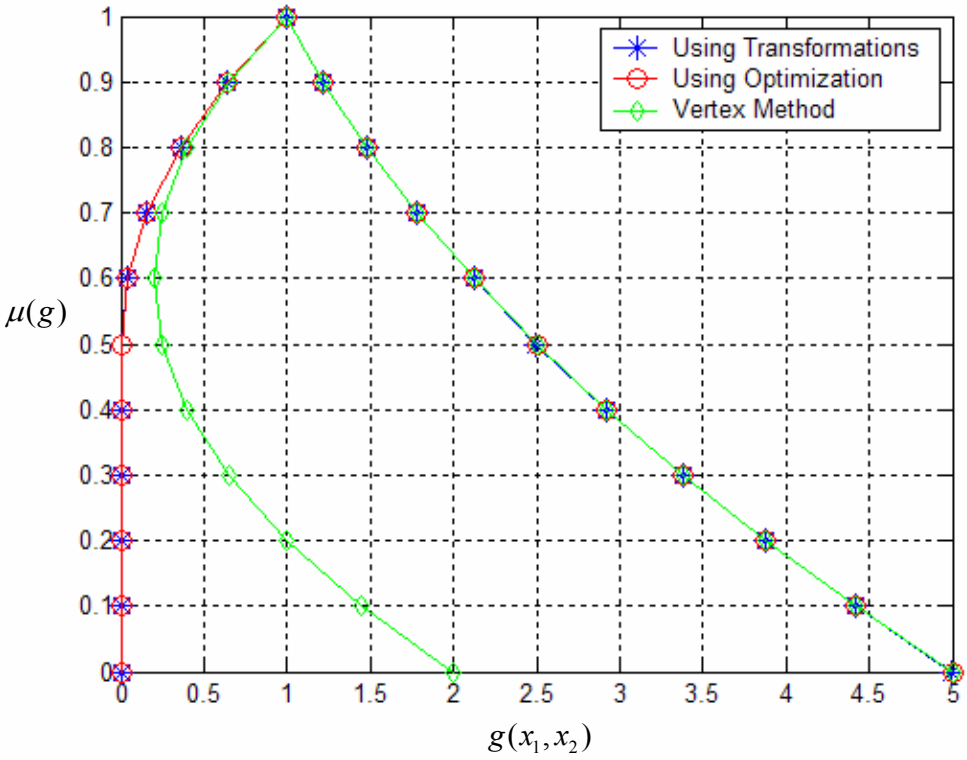

Figure 2.5: Comparison of Membership Function of Response

The use of transformations facilitates the determination of the minimum and maximum values of the fuzzy variables that correspond to the extreme values of the response at a particular level without the use of optimization techniques. Moreover, this

is an analytical procedure where there is little room for errors. So if the response is available as a separable closed-form expression, these transformations can be used to efficiently deal with problems having only fuzzy variables or both random and fuzzy variables to estimate the membership function of response or reliability accurately.

2.2. Membership Function of Reliability

Membership function of reliability represents bounds of reliability with varying possibility values based on the possibility information from the fuzzy variables. If the limit-state is available as a linear combination of the uncertain variables, then the estimation of the membership function of the reliability or failure probability can be determined using interval analysis. For a particular configuration of the fuzzy variables, Fast Fourier Transforms can be used to obtain the joint density function of the random variables, if a linear limit-state function is available. But a linear approximation often does not represent a nonlinear limit-state with required accuracy. Therefore, in this work, a second-order response surface model is used to approximate the limit-state function in terms of the uncertain variables (both random and fuzzy). The response surface model considered in this study is given by Eq. (2.7).

$$\tilde{g}(\boldsymbol{X}) = \beta_0 + \sum_{i=1}^{n} \beta_i x_i + \sum_{i=1}^{n} \beta_{ii} x_i^2 \tag{2.7}$$

where, $\boldsymbol{X} = (x_1, x_2, ..., x_n)^T$ is a vector of uncertain variables and β's are constants evaluated in the construction of the response surface model. This model can be transformed into a linear combination of intervening variables as shown in Eq. (2.8).

$$\tilde{g}(\mathbf{Z}) = z_1 + z_2 + ... + z_n + \beta_0 \tag{2.8}$$

where $z_i = \beta_i x_i + \beta_{ii} x_i^2$. Once the limit-state is available as a linear combination of uncertain variables, it is divided into two parts: one containing only random variables and the other containing the fuzzy variables. The part of the limit-state containing random variables is used to obtain the joint density function of these variables by performing the convolution using FFT. The remaining fuzzy variables in Eq. (2.8) are combined into a single membership function using an interval arithmetic algorithm. These two procedures would result in a joint PDF and a joint membership function. At each α-cut the minimum and maximum values of the fuzzy variables would act as linear horizontal shifts of the joint PDF, which would result in the membership function of reliability.

The details of the algorithm and its implementation are presented below:

1. The Most Probable failure Point (MPP) for the random variables is estimated using traditional approaches. During this process, the fuzzy variables are set to their values at maximum possibility.
2. Data points are sampled in the design space, around the estimated MPP, using a Latin hypercube sampling technique. The domain of interest is obtained by considering the bounds on the random variables to be two standard deviations on either side of the MPP and the minimum and maximum values of the fuzzy variables at the zero possibility level.
3. A truncated second-order response surface model, as shown in Eq. (2.7), is constructed with these design points. This surrogate model is divided into two parts, one containing the terms with random variables and the other containing fuzzy variables.

4. The joint PDF and the joint membership function are estimated using appropriate algorithms.
5. At each α-cut the minimum and the maximum values of the fuzzy variables are used to integrate the area under the joint PDF and obtain the membership function of reliability. Figure 2.6 illustrates the above-discussed methodology.

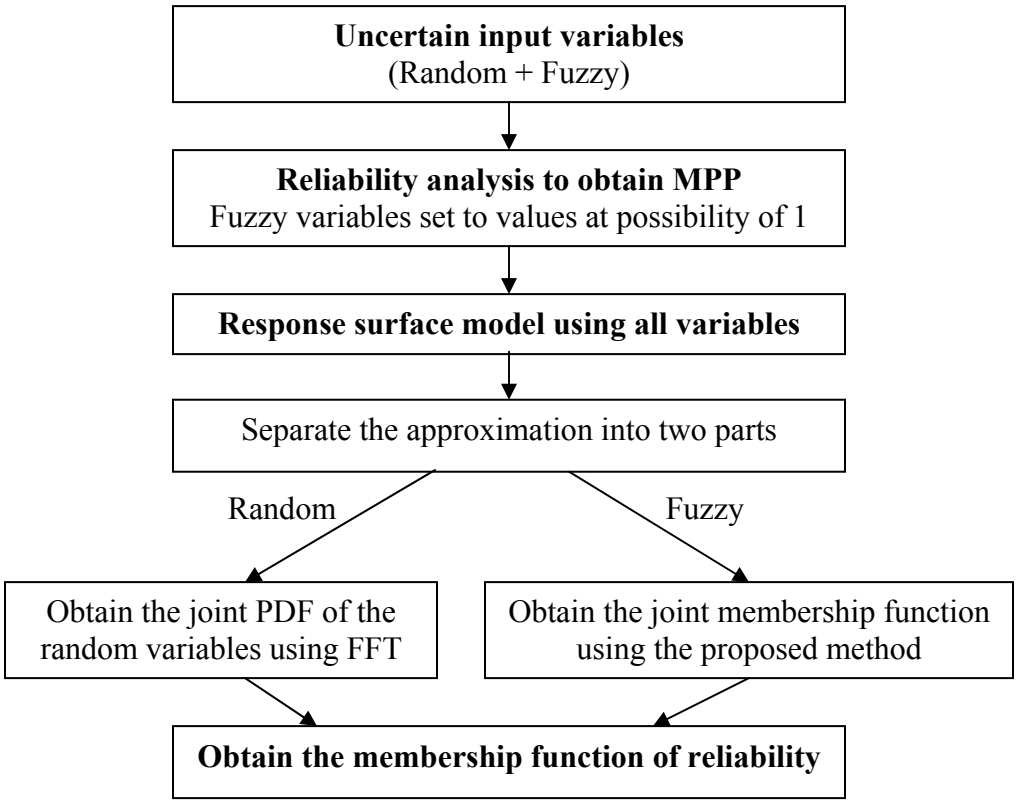

Figure 2.6: Algorithm for Estimating Membership Function of Reliability

One advantage of using FFT to solve the convolution is that the entire PDF of the performance function is obtained. The contributions of the fuzzy variables appear as a constant when performing the convolution leading to a linear shift in the PDF obtained. So, once the PDF and joint membership function are obtained, at each α-cut, the lower bound on the joint membership function is used to perform a linear shift in the PDF

obtained from the convolution. The lower bound on the failure probability is obtained by evaluating the area in the failure region of the resulting PDF. Similarly, the upper bound on the joint membership function is used to obtain the upper bound on the failure probability. Repeating this operation at several α-cuts results in the membership function of reliability.

The accuracy of the estimated membership function of reliability depends on the accuracy of the response surface model constructed around the MPP. In the proposed algorithm, the number of design points used for the approximate model is based on the fact that an accurate approximation can be obtained. Traditional Design of Experiments (DOE) sampling techniques [57-59] can also be used, as opposed to Latin Hypercube sampling. The disadvantage of using DOE is the exponential increase in the number of simulations needed with the number of uncertain variables. So for problems with a large number of variables, the number of simulations needed in the construction of the response surface model is very high. Using Latin Hypercube sampling, the number of simulations needed is independent of the number of uncertain variables.

2.3. Example Problems

Numerical examples are presented to demonstrate the accuracy and efficiency of the proposed methodology. The MPP is estimated and a second-order response surface model is constructed to represent the failure surface around this point. This methodology can be applied to any type of random variables or membership functions to result in an accurate estimation of the membership function of reliability. The results obtained using the proposed technique are compared with Monte Carlo simulation.

2.3.1. Closed-form Example

The limit-state considered for this problem is given in Eq. (2.9).

$$g(\boldsymbol{X}) = x_1^2 + 5x_1 + 2x_2^2 + 7x_2 + x_3^2 - 8x_3 + x_4^2 - 10x_4 - 200 \le 0 \tag{2.9}$$

where x_1 and x_2 are assumed to be normally distributed with a mean of 10.0 and a standard deviation of 2.0. The variables x_3 and x_4 are assumed to be fuzzy variables with their membership functions given by Eq. (2.10) and Eq. (2.11). Figure 2.7 shows the membership function of the fuzzy variables.

$$\mu_{x_3}(x_3) = \begin{cases} (x_3 - 5)/5 & 5 \le x_3 \le 10 \\ (x_3 - 15)/-5 & 10 \le x_3 \le 15 \end{cases} \tag{2.10}$$

$$\mu_{x_4}(x_4) = \begin{cases} (x_4 - 5)/5 & 5 \le x_4 \le 10 \\ (x_4 - 15)/-5 & 10 \le x_4 \le 15 \end{cases} \tag{2.11}$$

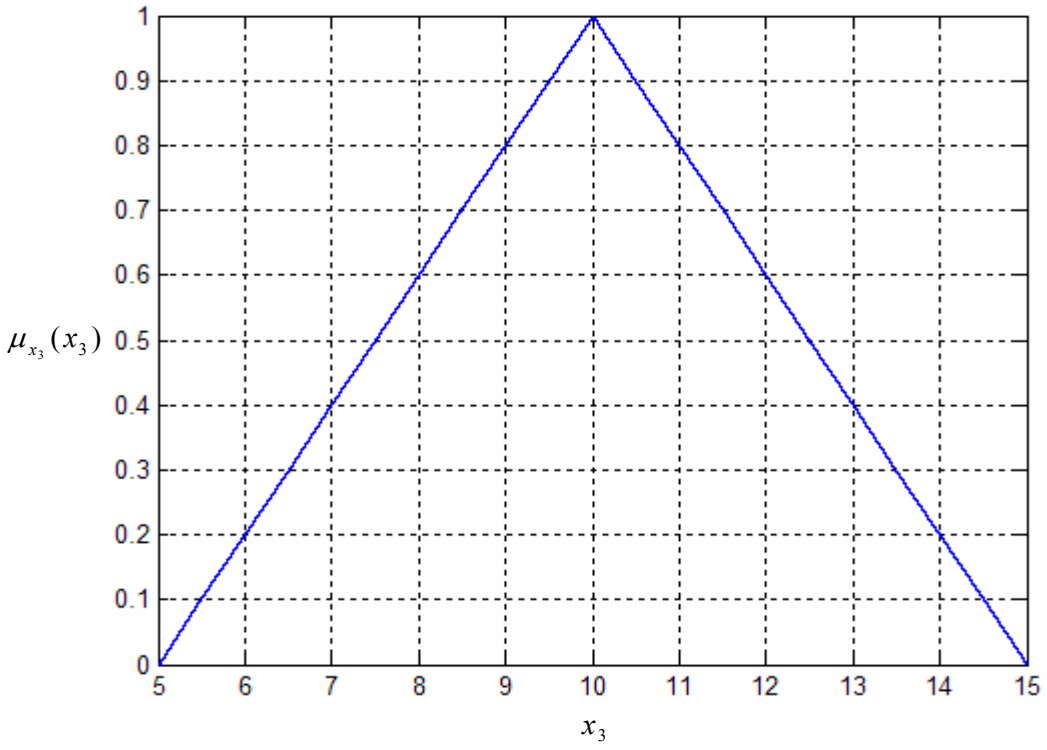

Figure 2.7: Membership Function of Fuzzy Variables

The limit-state function is divided into two parts, one with only the random variables and the other with the fuzzy variables as shown in Eq. (2.12).

$$g(\boldsymbol{X}) = g_R(x_1, x_2) + g_F(x_3, x_4) \tag{2.12}$$

where $g_R(x_1, x_2) = x_1^2 + 5x_1 + 2x_2^2 + 7x_2 - 200$ and $g_F(x_3, x_4) = x_4^2 - 8x_3 + x_4^2 - 10x_4$.

The joint density function is obtained by performing the convolution of the random variables using FFT based on $g_R(x_1, x_2)$. The joint membership function of $g_F(x_3, x_4)$ is obtained using transformations for the variables x_3 and x_4. Using this approach, the minimum and maximum values of the function $g_F(x_3, x_4)$ are obtained at each α-cut. These values are used to integrate the joint PDF and to obtain the bounds on reliability.

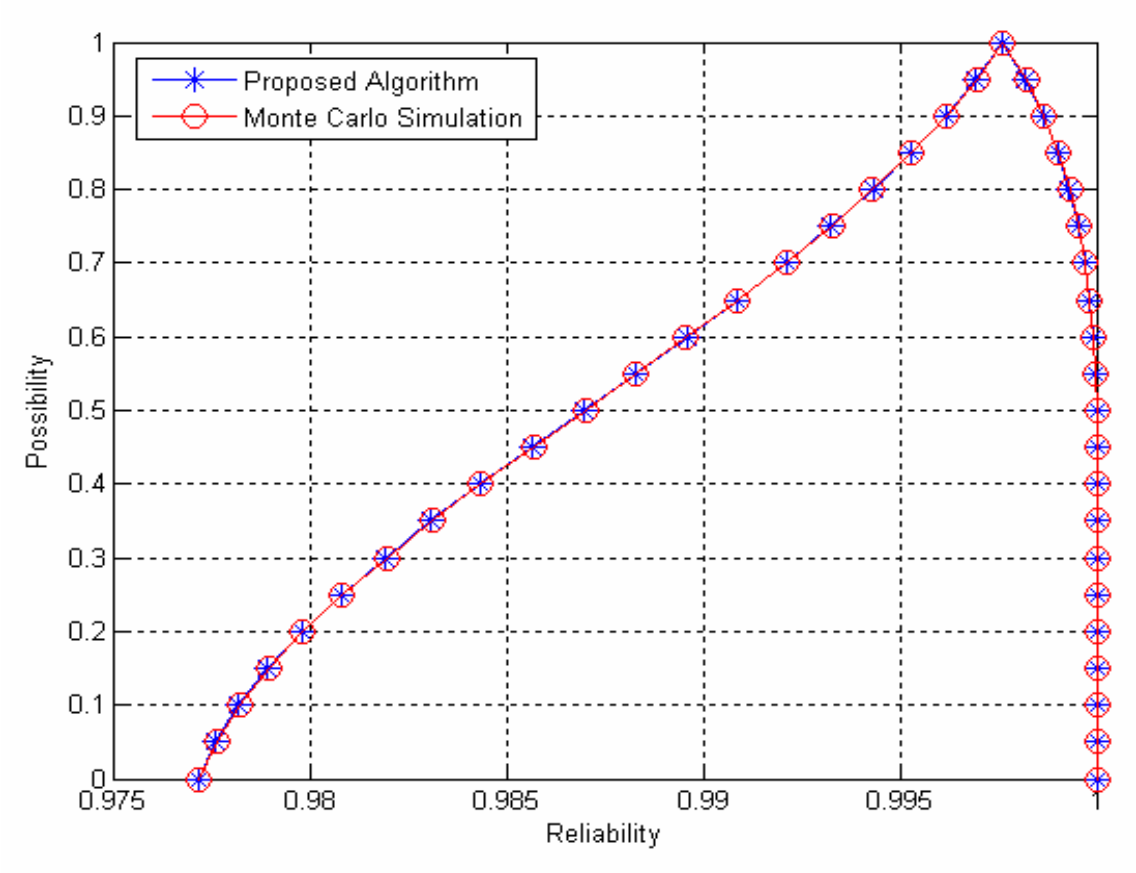

Figure 2.8: Membership Function of Reliability

Figure 2.8 shows the membership function of reliability estimated using the proposed methodology, as well as that obtained using traditional Monte Carlo simulation. The membership function obtained using the proposed methodology matches exactly with that obtained using the Monte Carlo simulation. One million sample points were used in Monte Carlo simulation at each α -cut. They matched exactly, because there were no approximations used in this example to model the limit-state function.

2.3.2. Ten Bar Truss

In this example, a ten bar truss, as shown in figure 2.9, was considered to estimate the membership function of its reliability. The criterion for failure was the maximum displacement at the tip of the structure to be less than 0.04826 m as shown in Eq. (2.13).

Displacement Limit-State $$g(\boldsymbol{X}) = \frac{D_{tip}(\boldsymbol{X})}{0.04826} - 1.0 \le 0 \qquad (2.13)$$

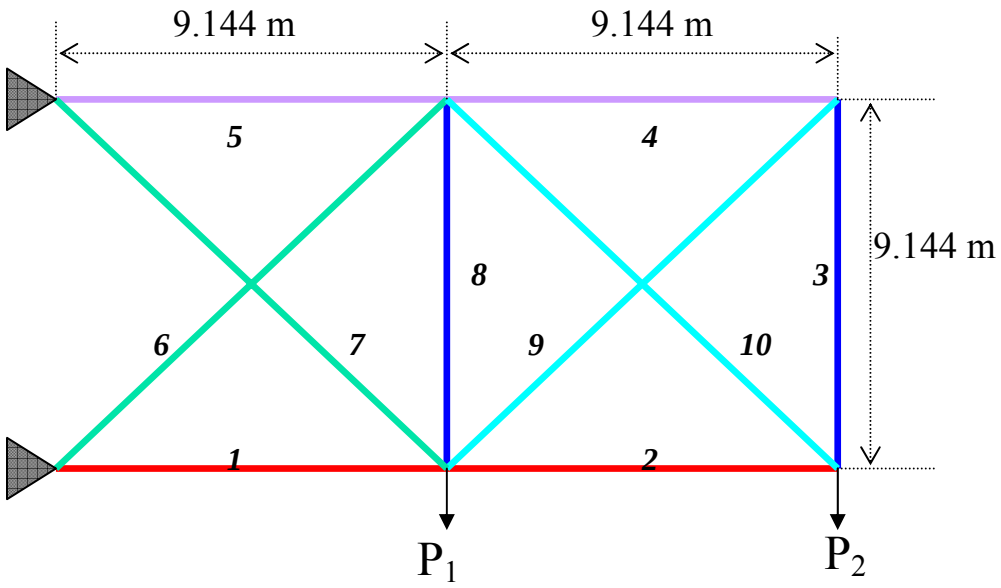

Figure 2.9: Ten-bar Truss

To demonstrate the applicability of the proposed method for multiple variables, five independent cross-sectional areas were considered. The cross-sectional areas of the

structure were physically linked as represented in Eq. (2.14). By linking the cross-sectional areas, the number of independent random variables was reduced to five. These random variables are assumed to be normally distributed with mean values of 0.0635 m^2 and a standard deviation of 0.00635 m^2.

$$A_1 = A_2 = x_1,\ A_4 = A_5 = x_2,\ A_3 = A_8 = x_3,\ A_6 = A_7 = x_4,\ A_9 = A_{10} = x_5 \tag{2.14}$$

The variations of the forces applied on the structure were modeled using triangular fuzzy membership functions given by Eq. (2.15) and (2.16). The Young's modulus is taken as 7.0E10 N/m^2.

$$\mu_{P_1}(P_1) = \begin{cases} (P_1 - 40.338)/4.482 & 40.338 \le P_1 \le 44.82 \\ (P_1 - 49.302)/-4.482 & 44.82 \le P_1 \le 49.302 \end{cases} \tag{2.15}$$

$$\mu_{P_2}(P_2) = \begin{cases} (P_2 - 40.338)/4.482 & 40.338 \le P_2 \le 44.82 \\ (P_2 - 49.302)/-4.482 & 44.82 \le P_2 \le 49.302 \end{cases} \tag{2.16}$$

The structural analysis was done in GENESIS [60], a commercial finite element analysis program. Since this example is a problem with an implicit limit-state function, the MPP was obtained for the limit-state with the fuzzy variables set to their values at the maximum possibility. Latin hypercube sampling technique was used to sample 50 design points around the MPP with the bounds on the random variables being 2 standard deviations on either side of the MPP. The bounds on the fuzzy variables were taken to be the minimum and maximum values at the zero possibility level. An accurate second-order response surface model was constructed with 50 sampled design points. This surrogate model was divided into two parts and the membership function of reliability was estimated.

Figure 2.10 shows the comparison of the membership function obtained by using the proposed methodology with that of Monte Carlo simulation. The maximum difference

in reliability was around 0.3% and was conservative. To show the difference between the proposed technique and Monte Carlo simulation, the membership function of the failure probability was plotted on a log scale as shown in Figure 2.11. Eighteen exact simulations were needed in obtaining the MPP. Therefore, a total of $18 + 50 = 68$ exact simulations were needed to obtain the membership function of reliability. At each level, 100,000 simulations were needed for convergence of Monte Carlo simulation. So a total of 2.1 million exact simulations were needed for Monte Carlo. This difference clearly shows the computational efficiency of the proposed methodology.

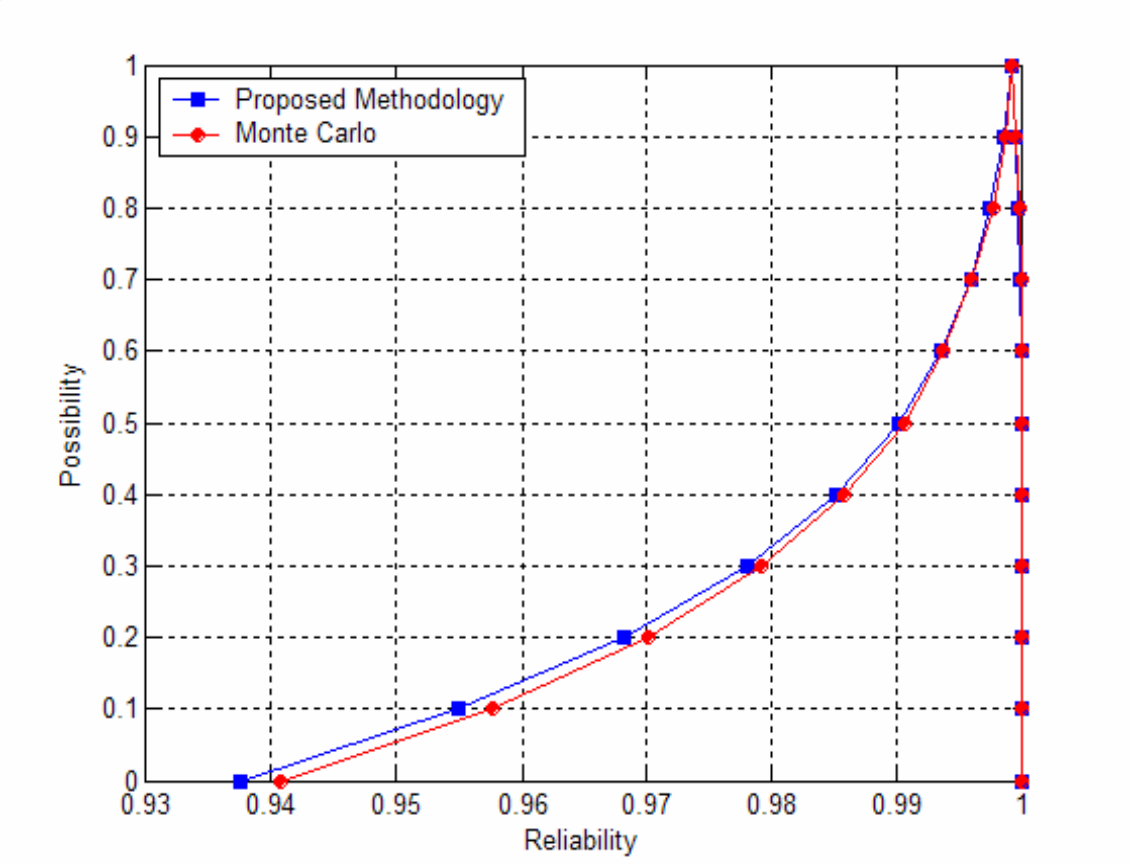

Figure 2.10: Membership Function of Reliability for the Ten-bar Truss

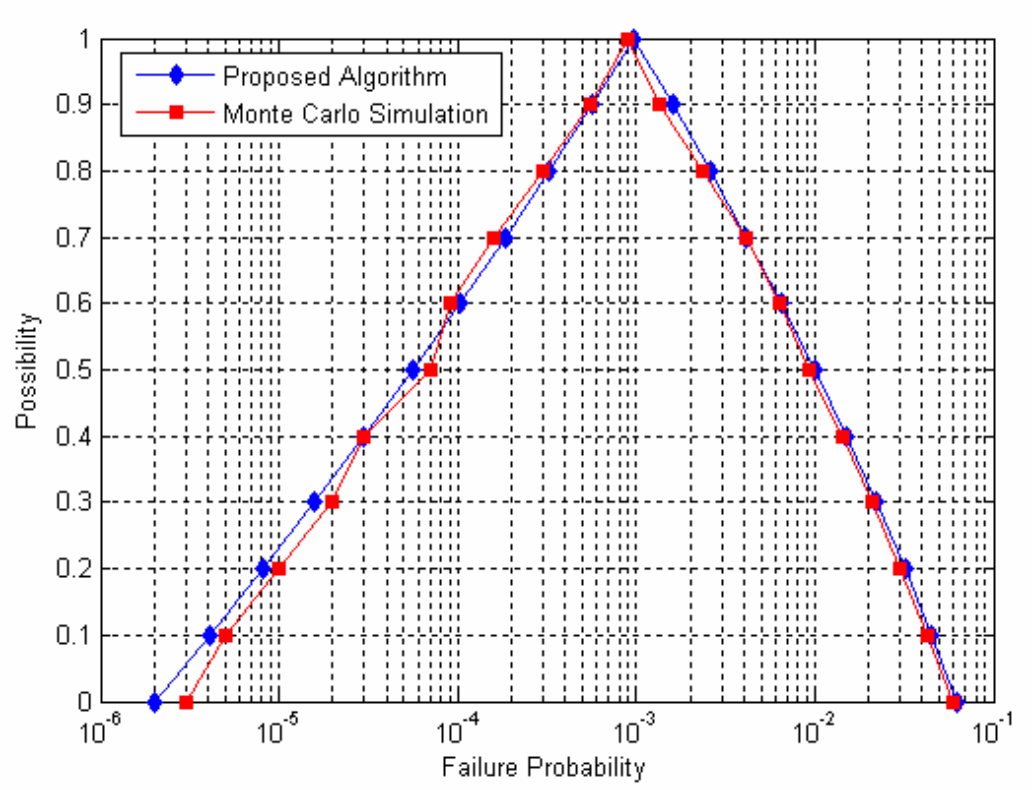

Figure 2.11: Membership Function of Failure Probability for the Ten-bar Truss

2.3.3. Wing Structure

A wing structure, as shown in Figure 2.12, is considered for estimating the bounds on the reliability at various confidence levels. The failure criterion considered was the fundamental natural frequency of the wing to be more than 1.52 Hz. (Eq. 2.17)

$$g(\boldsymbol{X}) = 1.52 - \omega_1(\boldsymbol{X}) \leq 0 \tag{2.17}$$

The thicknesses of the top and bottom skins were modeled as normally distributed random variables with mean values of 0.0381 m. All the spars were physically linked and the same is done with the ribs. The thicknesses of the spars and the ribs were also modeled as normally distributed random variables with mean values of 0.0127 m. Physical linking results in four random variables and the coefficient of variation is assumed to be 10% for all of these variables.

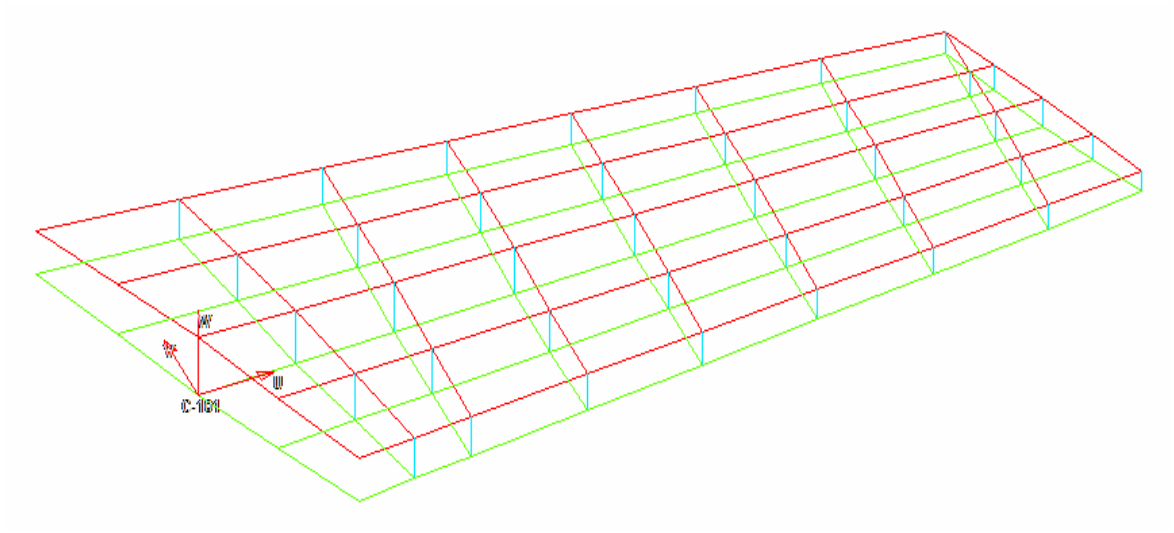

Figure 2.12: Finite Element Model of the Wing Structure

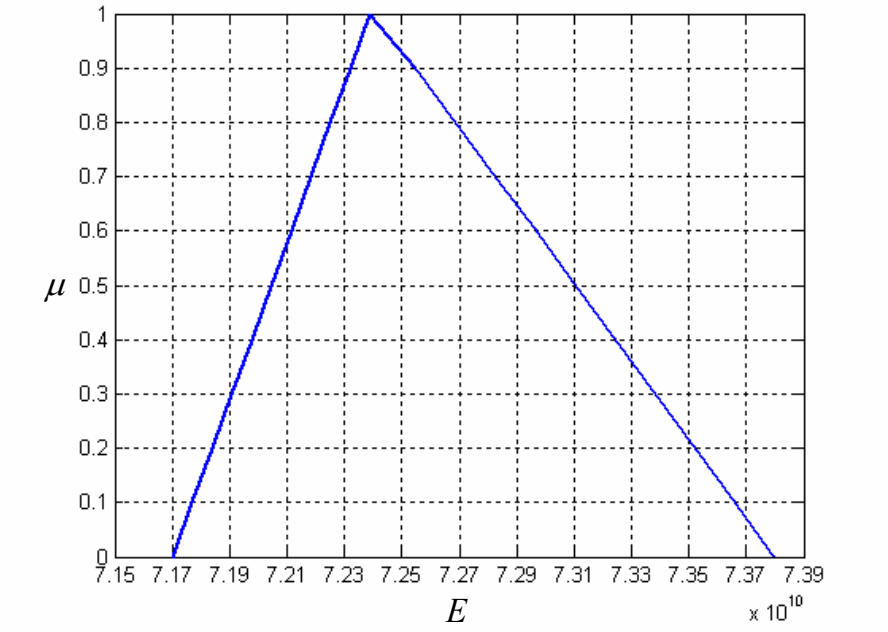

Figure 2.13: Membership Function of the Young's Moduli of the Skins

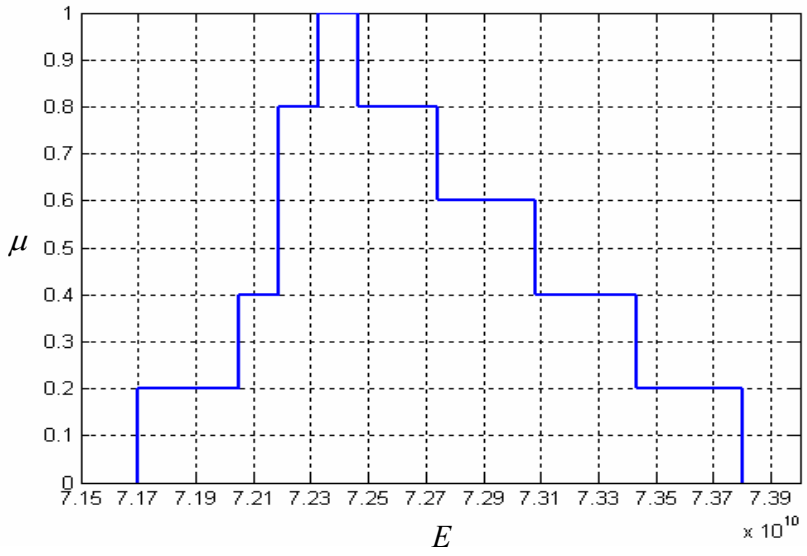

Figure 2.14: Membership Function of the Young's Moduli of Spars and Ribs

Figures 2.13 and 2.14 show the membership functions of the Young's moduli of the skins and the spars and ribs. Young's moduli of the top and bottom skins were modeled using triangular membership functions. The membership functions for the Young's moduli of the spars and ribs were constructed as step functions to model overlapping interval information from equally reliable sources. This was selected to demonstrate the versatility of the proposed method.

Since this is a problem with an implicit limit-state function, a reliability analysis is carried out with the fuzzy variables set to their values at maximum possibility. Then a response surface model is constructed around the most probable point obtained in the reliability analysis. This model is used in the estimation of the membership function of reliability. Figure 2.15 shows the comparison of the membership function estimated by the proposed technique with that of Monte Carlo simulation.

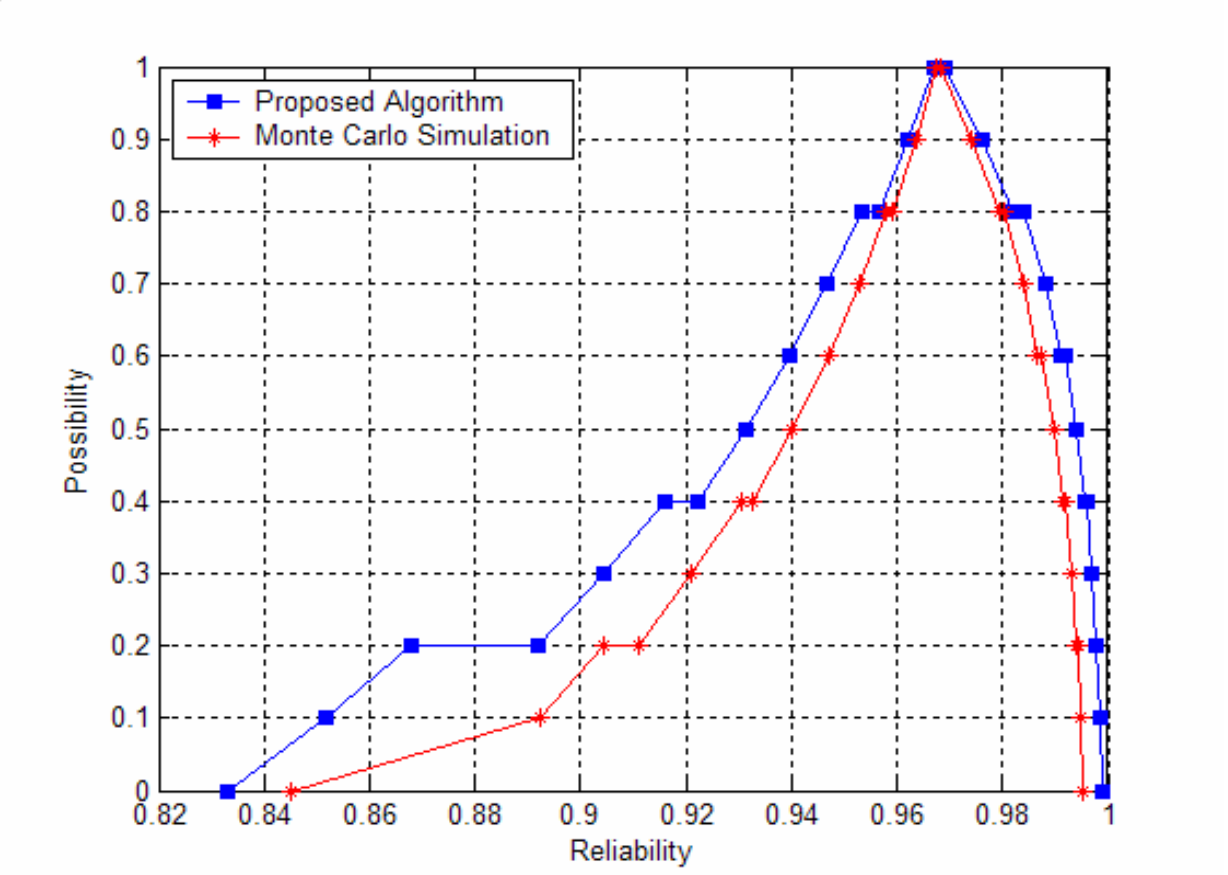

Figure 2.15: Comparison of the Membership Functions for the Wing Structure

The maximum percentage difference in the reliability estimated was around 5%. Twenty exact simulations were needed for estimating the most probable point. Moreover, 100 exact simulations were used in the construction of the response surface model around this point. So, a total of 120 simulations were needed in estimating the membership function as opposed to 100,000 simulations used for Monte Carlo simulation at each level.

The methods available in the literature efficiently deal with problems containing only random or nonrandom variables. Moreover, the computational cost associated is very high. The computational cost involved is minimal to use the proposed algorithm

when compared with Monte Carlo simulation. But the accuracy of the estimated membership function is greatly dependent on the accuracy of the response surface model constructed to represent the limit-state function. Once an accurate representation of the failure surface is obtained, using the proposed methodology, the membership function of the reliability of the structure can be estimated accurately.

Even though only one response surface was used in these examples to represent the entire failure surface, multiple response surface models can be used to represent different regions of the failure surface depending on its complexity. This provides additional flexibility to handle large scale highly non-linear problems that cannot be modeled using only one response surface. These details are provided in the following chapter.

3. STRUCTURAL SYSTEM RELIABILITY USING FAST FOURIER TRANSFORMS

The failure of a structural system is governed by multiple failure criteria, all of which have a potential to fail and are to be taken into consideration for the estimation of reliability of the system. In a multidisciplinary environment, where all the failure criteria are equally important, there is no methodology to convert the system reliability problem into a component reliability problem without the loss of critical information. These failure criteria are often correlated and the accuracy of the estimated structural failure probability highly depends on the ability to model the joint failure surface. Monte Carlo simulation can be used to estimate the reliability of the system, but the evaluation of limit-states often requires expensive Finite Element Analysis (FEA) or Computational Fluid Dynamics (CFD) simulation. So there is a need for accurate estimation of the reliability of the system without much computational effort.

In the reliability analysis of a system, there is an MPP for each limit-state criterion considered. Moreover, the intersection surfaces of these limit-states play an important role in the estimation of the system failure probability. In this work, the use of high quality function approximations for each of the limit-states and the joint failure surface are considered, to represent the failure region accurately. The approximations used to model the joint failure region should be valid to at least within the vicinity of the MPPs of all the limit-states. For highly nonlinear limit-state functions, modeling the entire failure region using a single approximation might be difficult. Therefore, a methodology is developed so that the convolution integral can be solved using several approximations, each of which accurately represent certain regions over the entire design

space. As the failure surface is represented accurately using several approximations the failure probability of a structural system can be estimated accurately.

3.1. Solving the Convolution Integral in Intervals

For solving the convolution integral using FFT, the function must be available as a closed-form and separable equation. As a single approximation cannot model a highly nonlinear joint failure region, a methodology was developed for solving the convolution integral based on several function approximations.

Let us suppose that the failure probability of the structural system is governed by two limit-state criteria, $g_1(x_1, x_2) \le 0$ and $g_2(x_1, x_2) \le 0$, where x_1 and x_2 are the random variables, as shown in Figure 3.1 (a). These limit-states intersect at a point where $x_1 = x_0$. The joint failure region comprises of the part of g_2 where $x_1 < x_0$ and the part of g_1 where $x_1 > x_0$. Based on this information, the convolution integral is divided into two different integrals, as shown in Eq. (3.1).

$$\iint_{\Omega} f_{\boldsymbol{X}}(\boldsymbol{X}) d\boldsymbol{X} = \int_{-\infty}^{x_0} \int_{-\infty}^{\infty} f_{\boldsymbol{X}}(\boldsymbol{X}) dx_2 dx_1 + \int_{x_0}^{\infty} \int_{-\infty}^{\infty} f_{\boldsymbol{X}}(\boldsymbol{X}) dx_2 dx_1 \tag{3.1}$$

The two integrals in Eq. (3.1) can be solved separately using the expression for the joint PDF in their respective ranges. The Probability Density Function (PDF) of x_1, when $x_1 < x_0$, is convoluted with the PDF of x_2, as shown in Figure 3.1 (b), based on the failure surface represented by g_2, to evaluate the first integral, since only g_2 represents the system failure surface. The PDF of x_1, when $x_1 > x_0$, is convoluted based on g_1, for

the second integral, as shown in Figure 3.1 (c). To enable the addition of the two individual PDFs, obtained from each of these integrals, the PDFs are padded with zeros in appropriate locations, for numerical implementation, and then combined. The sum of these PDFs results in the system PDF.

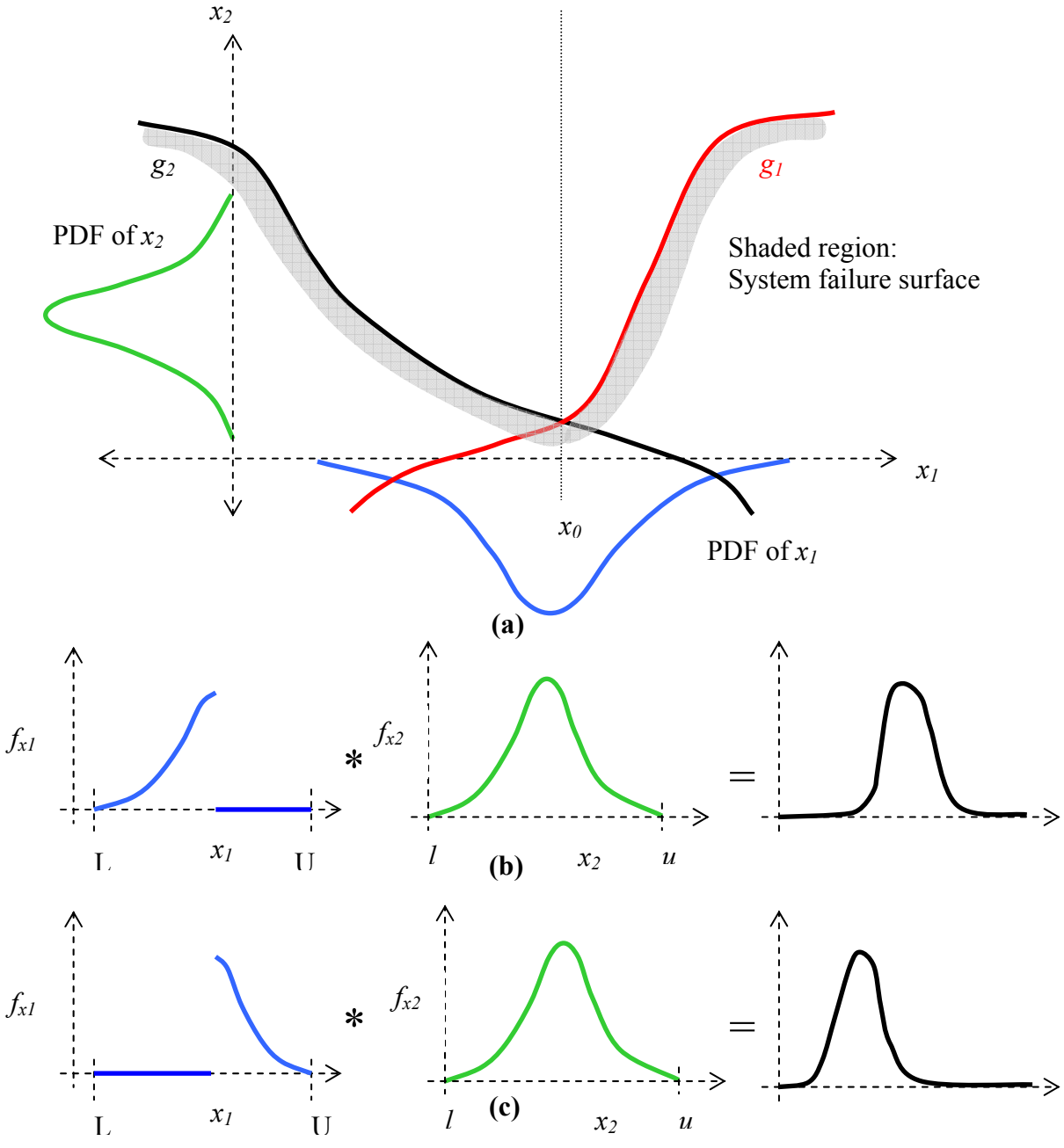

Figure 3.1: Convolution Based on More Than One Function

In a problem with more than two random variables, the intersection of the limit-states is not a point, but a surface (hyperplane). Therefore, obtaining the bounds of integration is not a trivial task. The probability density function of any of these variables cannot be split, as shown in Figure 3.1. Therefore, the entire design space is divided into several regions as explained below and the convolution integral is solved for each region separately. The convolution integral can then be written as the sum of integrals over all the regions as

$$\iiint_{\phi} f_x(\boldsymbol{X})d\boldsymbol{X} = \iiint_{\phi_1} f_x(\boldsymbol{X})d\boldsymbol{X} + \iiint_{\phi_2} f_x(\boldsymbol{X})d\boldsymbol{X} + ... \quad (3.2)$$

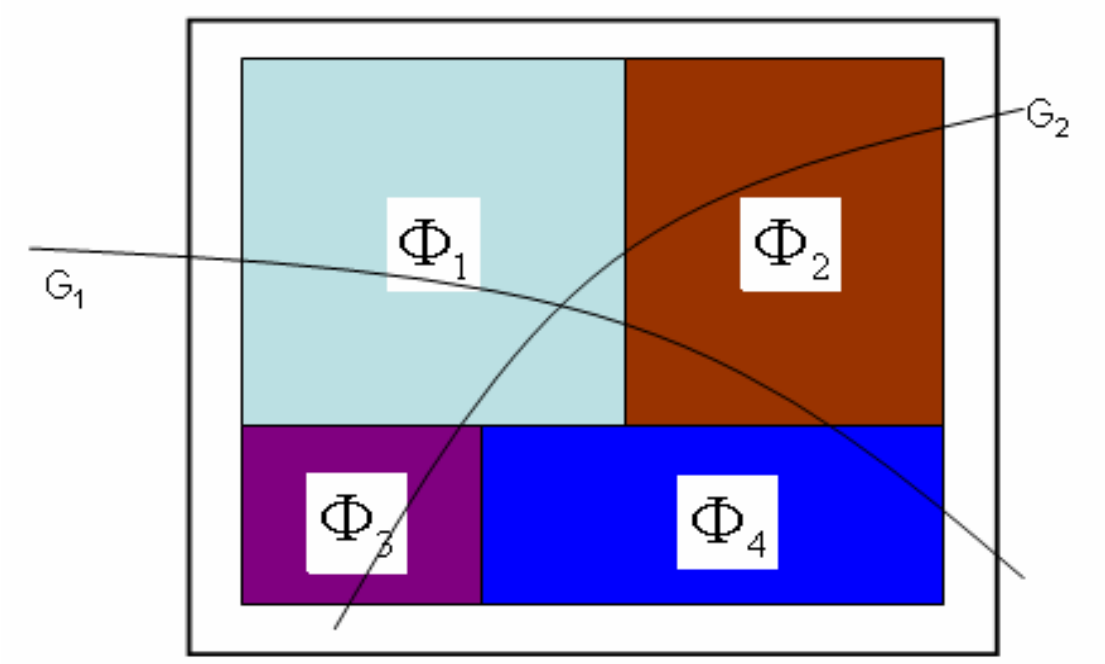

Figure 3.2: Solving the Convolution Integral in Intervals

As shown in Figure 3.2, the entire design space is divided into several regions such that the joint failure region can be modeled using approximations that are accurate within that region. The division of the design space is based on the accuracy of the approximations constructed. Initially only one approximation is constructed over the

entire design space to model the joint failure surface. The accuracy of the approximation is checked and if the required accuracy is met then the design space is not subdivided and the convolution integral is solved based on one approximation. In most problems, this is usually not the case as the joint failure surface is highly nonlinear. So the design space is split up into two divisions and an approximate model is constructed in each division. Based on their accuracy, the design space is subdivided. Once accurate approximations are constructed in each subdivision, the convolution integral is divided into several integrals, as shown in Eq. (3.2). Each of these integrals is then solved using FFT, based on the approximate model that is accurate within that region. Finally, all the probability density functions of the various models are added to result in the probability density function of the structural system. To enable this addition, the range of all the resulting PDFs should be the same. So for each original variable, the range of the PDF of the intervening variable before the convolution should be the same for all the approximate models. This is obtained by padding the PDFs with zeros at appropriate locations. The failure probability can be estimated by evaluating the area under this probability density function for all the values in the failure region. Using this method the convergence in failure probability can be verified by adding various regions (integrals) until the required accuracy is obtained.

To demonstrate the accuracy of the proposed technique, an example problem is presented here, where the failure of the system is governed by two limit-state functions as shown below (Eq. 3.3 and Eq. 3.4). The failure of the system is defined by the failure of each of the limit-states (parallel system). This type of failure was chosen to compare the estimated failure probability with that obtained using importance sampling. For a parallel

system, importance sampling technique can be used by sampling points from a distribution with the intersection point as the mean values.

$$g_1(x_1, x_2) = x_1^{\,2} - 8x_2 + 40 \geq 0 \tag{3.3}$$

$$g_2(x_1, x_2) = -16x_1 - x_2^{\,2} + 170 \geq 0 \tag{3.4}$$

where x_1 and x_2 are normally distributed random variables with mean values of 5.0 and standard deviation of 1.0. The intersection point of the above two functions is at $x_1 = 5.6203$ and $x_2 = 8.9485$. Based on this information the joint failure region is modeled and solved using the proposed technique. Figure 3.3 shows a comparison of the Cumulative Distribution Function (CDF) obtained using the proposed method and with that obtained by conventional Monte Carlo simulation. As there are no surrogate models involved, the CDFs match exactly.

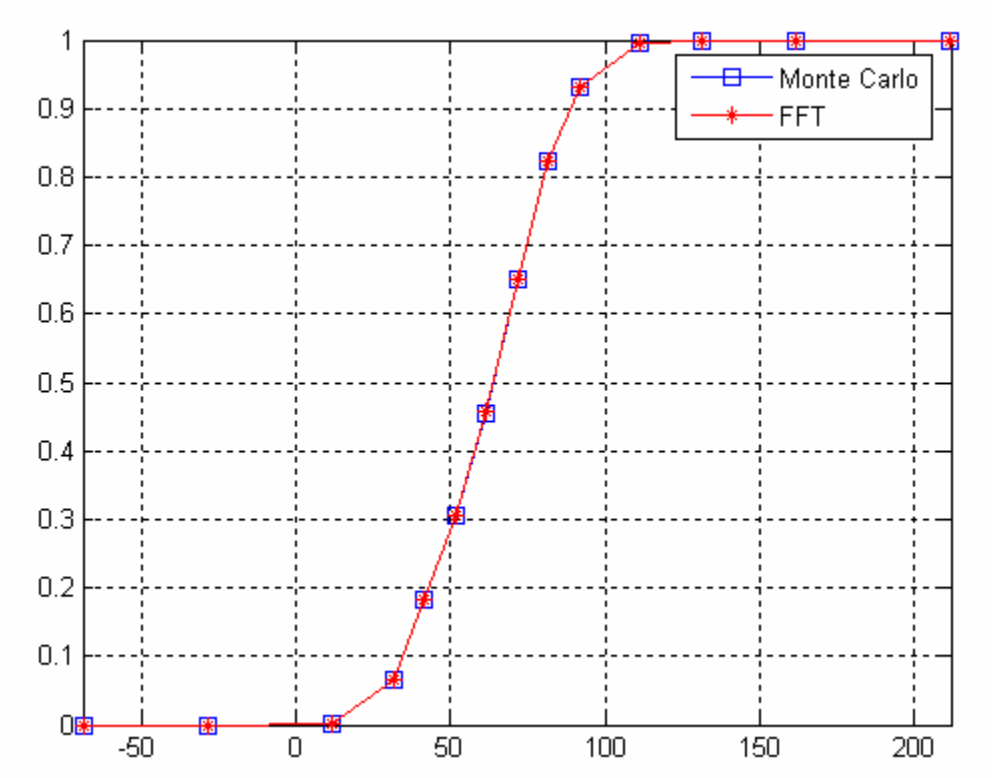

Figure 3.3: Comparison of Cumulative Distribution Function

Methodology	System P_f	% Difference	Number of Simulations
Monte Carlo	5.4E-6	-------	50,000,000
Importance Sampling	5.5E-6	1.85	1,000,000
Proposed Algorithm	5.36E-6	-0.74	27

Table 3.1: Comparison of Proposed Algorithm with Monte Carlo Simulation

Table 3.1 shows the comparison of the failure probabilities estimated using the proposed technique as well as Monte Carlo simulation. All the three techniques estimated the failure probability accurately within 2% difference. Because of the low order of failure probability, the number of simulations needed to estimate the failure probability using traditional Monte Carlo was 50 million. Even when using importance sampling, one million function evaluations were necessary to obtain convergence. The proposed technique needs only 27 function evaluations which were used in the evaluation of the intersection point. In the presence of implicit limit-state functions, there is an increase in the number of function evaluations using the proposed technique as the limit-states are to be approximated using multi-point approximations.

3.2. Proposed Methodology

For modeling the joint failure region using an approximation, the limit-state functions should be available in closed-form so that the points on the joint failure region can be sampled. In the case of an implicit function, several local approximations can be constructed with design points around the MPP for each limit-state function and then blended into a Multi-Point Approximation (MPA). As the accuracy of the MPA is based

on the accuracy of the local approximations, Two-point Adaptive Nonlinear Approximations (TANA2) are used as local approximations to construct the MPA for each limit-state function. TANA2 can capture the information of the limit-state function around the vicinity of the points used, and MPA can retain this information for each of the failure surfaces without increasing the computational effort. Since each of the limit-state functions are modeled using high quality approximations, these approximations can be used as closed-form expressions for sampling the points on the joint failure surface.

Reliability analysis methods begin with the prediction of the most probable failure point. This can be efficiently estimated using the algorithm presented by Wang and Grandhi [9]. This algorithm uses TANA2 approximations in the search procedure to reduce computational cost. This method is efficient for highly nonlinear problems with a large number of random variables. Once the MPPs are obtained for each of the limit-states, a Latin hypercube sampling technique is used to obtain the design points around each MPP. Local approximations are constructed with points that are sampled to within two standard deviations of either side of the MPP for each of the limit-state functions. Based on these local approximations, an MPA is constructed for each of the limit-state functions. Using these MPAs, several points are sampled on the joint failure region to construct response surface models. The design space is sub-divided into regions based on the accuracy of the response surface models. The convolution integral is then solved in intervals to obtain the failure probability of the structural system.

The maximum contribution to the failure probability is around the MPP of each of the limit-states. The probability density decreases away from the MPP of the limit-states. So for accurately estimating the reliability, one has to model the joint failure surface

accurately at least around each of the MPPs. In this work, two standard deviations on either side of each MPP were considered to sample points for modeling the MPAs. In most cases, this design space effectively captures the contribution to the failure probability of the system. If improved accuracy is needed, then the design space for the construction of the MPAs can be expanded to three or four standard deviations around each MPP.

3.2.1. Estimation of System Failure Probability

1. Estimate the MPP of each of the limit-state functions using local approximations.
2. Design points are sampled within the vicinity of each MPP using a Latin hypercube sampling technique. The bounds on the random variables are taken to be two standard deviations on either side of each MPP.
3. Several local TANA2 approximations are constructed for the set of design points sampled around each MPP. These local TANA2 approximations are blended into a multi-point approximation, which captures the behavior of the limit-state function around the MPP. Using this same procedure, an MPA is constructed for each of the limit-state functions.
4. Points are sampled on the joint failure surface using surrogate representations for each of the limit-states. Multiple response surface models are constructed using these sampled points on the joint failure surface. Based on the accuracy (R^2 value was used in this research) of the response surface models, the design space is sub-divided into regions and one model is constructed for each region.

5. The convolution integral is solved using FFT, based on the response surface models, to estimate the probability of failure of the structural system. Figure 3.4 illustrates the methodology discussed above.

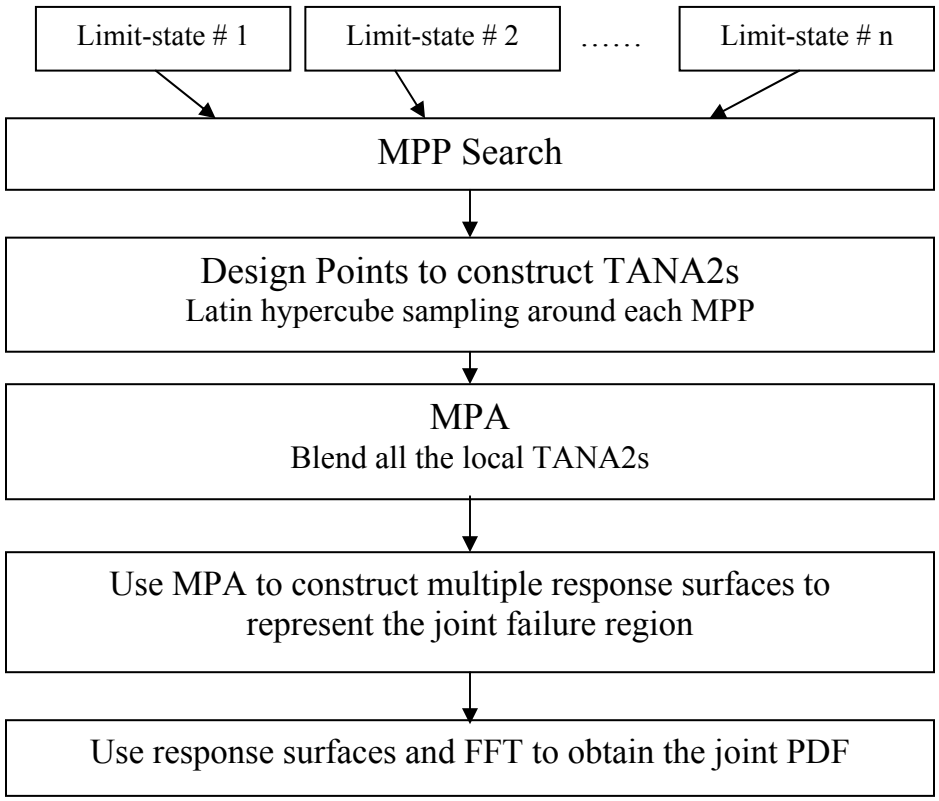

Figure 3.4: Algorithm Details for System Reliability Estimation

The accuracy in the estimation of the failure probability greatly depends on the accuracy of the approximations constructed. Therefore, all the TANA2s that are used in the construction of the MPAs for the limit-state functions should be accurate. The information of two design points is used in the construction of a TANA2 approximation. So, for any design point, TANA2s were constructed with the design points in the immediate vicinity of that point. The use of this strategy leads to the construction of accurate TANA2 approximations thereby reducing the error involved with the MPA. The

accuracy of the MPA can be checked by randomly sampling points in the design space and comparing with the function value of the exact limit-state. Once accurate MPAs are constructed for each of the limit-states, the criterion for system failure is considered while sampling points on the joint failure surface using these MPAs. For multiple limit-states, this criterion can be the union or intersections of the individual failure surfaces. In these cases, optimization techniques can be employed to obtain the points on the joint failure surface by using the surrogate representations of the limit-state functions.

For multiple limit-states, optimization problems can be formulated and solved to obtain a point on the joint failure surface. For example, consider three limit-state functions as shown in figure 3.5. The failure of the system is defined as the failure of either of the limit-state functions i.e. $g_1(\boldsymbol{X}) \geq 0$ or $g_2(\boldsymbol{X}) \geq 0$ $g_3(\boldsymbol{X}) \geq 0$. So based on this failure criteria, three optimization problems can be formulated to obtain three points on the joint failure surface. These optimization problems are given by Eqs. (3.5) – (3.7).

$$\text{Minimize } d = (\boldsymbol{X} - \boldsymbol{X}_i) \bullet (\boldsymbol{X} - \boldsymbol{X}_i)$$

$$\text{subject to } g_1(\boldsymbol{X}) = 0,\ g_2(\boldsymbol{X}) \leq 0, g_3(\boldsymbol{X}) \leq 0 \tag{3.5}$$

$$\text{Minimize } d = (\boldsymbol{X} - \boldsymbol{X}_i) \bullet (\boldsymbol{X} - \boldsymbol{X}_i)$$

$$\text{subject to } g_1(\boldsymbol{X}) \leq 0,\ g_2(\boldsymbol{X}) = 0, g_3(\boldsymbol{X}) \leq 0 \tag{3.6}$$

$$\text{Minimize } d = (\boldsymbol{X} - \boldsymbol{X}_i) \bullet (\boldsymbol{X} - \boldsymbol{X}_i)$$

$$\text{subject to } g_1(\boldsymbol{X}) \leq 0,\ g_2(\boldsymbol{X}) \leq 0, g_3(\boldsymbol{X}) = 0 \tag{3.7}$$

where $\bullet$ denotes the dot product and $d = (\boldsymbol{X} - \boldsymbol{X}_i) \bullet (\boldsymbol{X} - \boldsymbol{X}_i)$ is the distance between any point $\boldsymbol{X}$ to the initial point $\boldsymbol{X}_i$. The difference between each of the above three optimization problems is the constraints. These constraints are dependent on the definition of the failure of the system. The solution of each of the optimization problems yields one point on the joint failure surface as shown in figure 3.5. By considering several initial points, $\boldsymbol{X}_i$, points on the joint failure surface can be obtained which can be used to approximate this surface using response surface models. As accurate MPAs are used in these optimization problems, the computational cost is minimal.

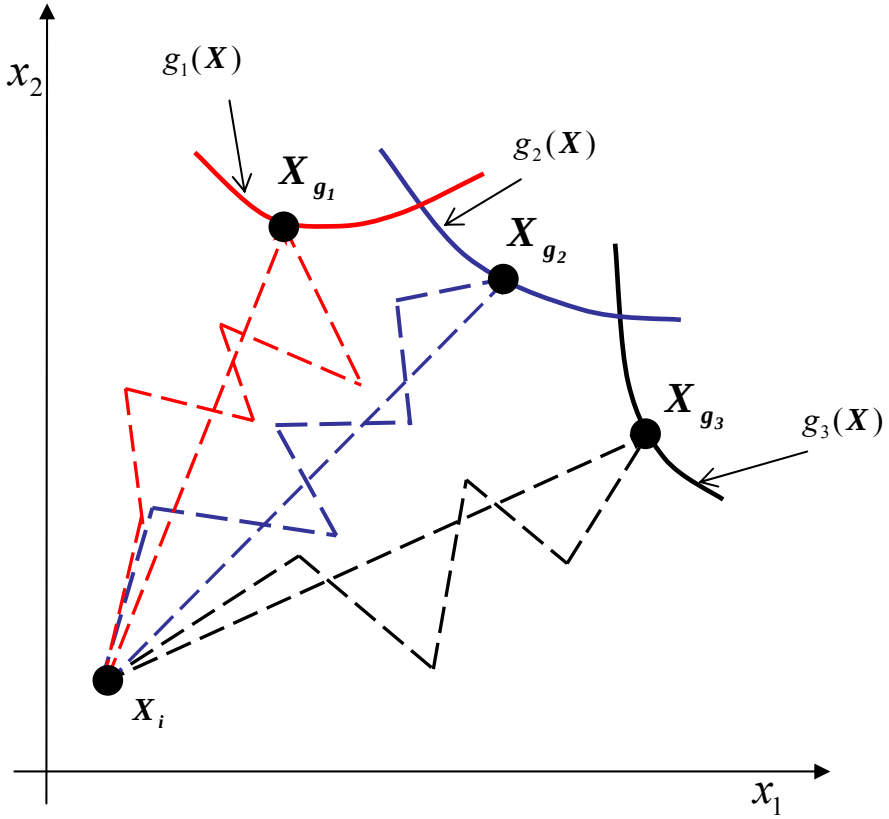

Figure 3.5: Estimating Points on the Joint Failure Surface using Optimization

Once points on the joint failure surface are obtained, these points can be used to construct accurate response surface models. R^2 criterion was chosen to check the accuracy of the response surface model constructed. Using the sampled points on the

joint failure surface, one response surface model is constructed initially. The accuracy of this modeled is checked and if the R^2 value is acceptable then the design space is not subdivided and the convolution integral is solved based on that one approximation. Usually this is not the case as the joint failure surface is highly nonlinear. The design space is divided into half and an approximate model is constructed in each subdivision. Based on the accuracy of the models, the design space is subdivided. This procedure is repeated until all the approximate models achieve the required degree of accuracy. The design space was divided so that the R^2 value was always greater than 0.99 for all of the response surfaces. A high order of accuracy was maintained for the response surface models so that the error associated in the representation of the joint failure surface is minimal. Moreover, because of this high accuracy of the response surface models, the error associated with not satisfying the transition conditions at the boundaries of the subregions is very less.

3.3. Numerical Examples and Discussion

Numerical examples are presented to show the applicability of the proposed method. This methodology can be applied to problems with multiple non-normal random variables and implicit or explicit limit-state functions, providing an accurate estimation of the failure probability of the system. The final failure probability estimated by using the above-mentioned method is compared with the results obtained from Monte Carlo simulations.

3.3.1. Cantilever Beam

A cantilever beam, as shown in Figure 3.6, is subjected to a tip load of 444.82 N. Two failure criteria for the structure were considered: (i) the displacement at the tip of the beam should be less than 0.002 m, as shown in Eq. (3.8), and (ii) the stress in the beam should be less than 34 MPa, as shown in Eq. (3.9).

Displacement Limit-State $$g_1(\boldsymbol{X}) = \frac{4PL^3}{Ebh^3} - 0.002 \le 0 \tag{3.8}$$

Stress Limit-State $$g_2(\boldsymbol{X}) = \frac{12PL}{bh^2} - 34*10^6 \le 0 \tag{3.9}$$

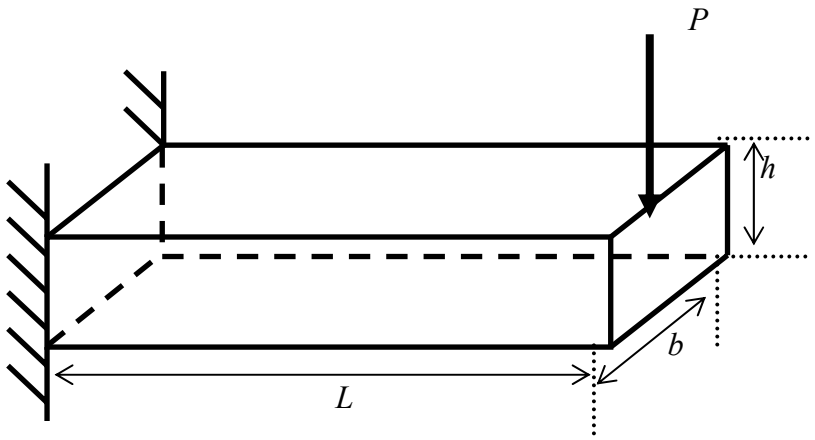

Figure 3.6: Cantilever Beam

where L, b, h are the length, width, and height of the beam, which are taken as random variables. The length of the beam was assumed to be normally distributed with a mean value of 0.762 m and standard deviation of 0.0762 m. The width and height of the beam were both assumed to be normally distributed with mean values of 0.0635 m and standard deviations of 0.00635 m.

As the limit-state functions are available as closed-form expressions in terms of the random variables, there was no need for constructing approximations of each of the limit-state functions. Using these closed-form expressions, several points were sampled on the joint failure region. These sampled points were used in the construction of multiple response surface models to represent the joint failure region. The domains for the response surface models are given in Table 3.2. The design space was then divided into smaller domains such that the response surface model captures the joint failure region accurately within that domain. The convolution integral was then solved over the entire design space to obtain the failure probability of the system.

Response Surfaces	**Interval for** b	**Interval for** h	**Interval for** L
1	[0.0254, 0.0457]	[0.0254, 0.0635]	[0.381, 1.143]
2	[0.0254, 0.0457]	[0.0635, 0.1016]	[0.381, 1.143]
3	[0.0457, 0.0635]	[0.0254, 0.0635]	[0.381, 1.143]
4	[0.0457, 0.0635]	[0.0635, 0.1016]	[0.381, 1.143]
5	[0.0635, 0.1016]	[0.0254, 0.1016]	[0.381, 1.143]

Table 3.2: Domains for the Response Surface Models for the Cantilever Beam

Methodology	**System Failure Probability**	**% Difference**
Monte Carlo Simulation	0.0091	----------
RSM + FFT	0.0093	2.19
First-order Series Bounds	0.0089 to 0.0111	-2.19 to 21.98

Table 3.3: System Reliability Results for a Cantilever Beam

Table 3.3 illustrates the accuracy of the methodology in predicting the failure probability of the system. The difference in the failure probability estimated by the proposed methodology compared to that of Monte Carlo simulation was around 2.19%. One million evaluations of the limit-state functions were used in the estimation of the failure probability using Monte Carlo. The first-order bounds capture the estimated failure probability as each of the individual failure probabilities were estimated accurately. The lower bound was estimated with a difference of 2.19% but was not conservative. The upper bound was very inaccurate with a difference of over 20 %.

3.3.2. Ten-bar Truss Structure

A ten-bar truss structure, as shown in Figure 2.9, is considered in this example to calculate the system failure probability. Two failure criteria were considered for the estimation of failure probability of the system. One criterion was the displacement limit and the other was the stress limit. The maximum displacement at the tip of the structure should be less than 0.04826 m, and the stresses developed in element number 1 (critical element) should be less than 72 MPa, as shown in Eq. (3.10) and Eq. (3.11), respectively.

Displacement Limit-State $$g_1(\boldsymbol{X}) = \frac{D_{tip}(\boldsymbol{X})}{0.04826} - 1.0 \le 0 \tag{3.10}$$

Stress Limit-State $$g_2(\boldsymbol{X}) = \frac{\sigma_1(\boldsymbol{X})}{72 * 10^6} - 1.0 \le 0 \tag{3.11}$$

To demonstrate the applicability of the proposed method for multiple variables, five cross-sectional areas were considered. The cross-sectional areas of the structure were physically linked, as represented in Eq. (3.12). By linking the cross-sectional areas, the number of independent random variables was reduced to five.

$$A_1 = A_2 = x_1,\ A_4 = A_5 = x_2,\ A_3 = A_8 = x_3,\ A_6 = A_7 = x_4,\ A_9 = A_{10} = x_5 \tag{3.12}$$

The random variables are normally distributed with mean values of 0.0635 m^2 and a standard deviation of 0.00635 m^2. The Young's modulus is taken as 7.0E10 N/m^2 and the forces applied are $P_1 = P_2 = 44.482$ kN.

The structural analysis was done in GENESIS [60]. Since this example is a problem with implicit limit-state functions, the MPPs were obtained for each of the limit-states. Latin hypercube sampling technique was used to sample ten design points around the MPP of each limit-state. Local approximations were constructed using eleven points (ten design points and the MPP of that limit-state) and combined into a multi-point approximation. The MPAs obtained were used as closed-form expressions of the limit-state functions to sample points on the joint failure region. Using these points on the joint failure region, five accurate response surface models were constructed to span over the entire design space and used to solve the multidimensional convolution integral. The number of response surfaces required depends on the R^2 value of each of the models. When improved accuracy is desired, each of the regions is further subdivided until the required R^2 value is obtained.

Methodology	System Failure Probability	% Difference
Monte Carlo Simulation	0.00741	----------
MPA + FFT	0.00758	2.29
First-order Series Bounds	0.00669 to 0.00718	-9.72 to -3.11

Table 3.4: Comparison of Results for a Ten-bar Truss

A comparison of the failure probabilities obtained using the proposed methodology and Monte Carlo simulation is shown in Table 3.4. The estimated failure probability was comparable to Monte Carlo with a difference of 2.29%. One million exact finite element simulations were needed to obtain convergence of the Monte Carlo simulation. Eighteen exact simulations were needed in the search for the MPP of each of the limit-state functions and ten additional design points were sampled around each MPP. So the total number of exact simulations used to obtain the system failure probability using the proposed methodology was $2(18+10)=56$, as opposed to one million using Monte Carlo simulation. The estimated failure probability was not within the FORM bounds because the individual failure probabilities estimated using FORM were not accurate.

3.3.3. Torpedo Structure

The finite element model of the torpedo structure used for the analysis is shown in Figure 3.7. The structure is modeled using 1176 quadrilateral and 48 triangular shell elements between 1202 nodes. The structure is also comprised of longitudinal and radial stiffeners that provide additional structural integrity. The overall length of the structure is 2.60 m with a diameter of 0.32 m. The thickness of the shell is taken as 0.0635 m and the width and breadth of the stiffeners is 0.01 m and 0.015 m. To represent the mass of the various subsystems in the structure, concentrated masses are added at the nodes. The structure is divided into four sections and the values of the concentrated masses in each section are modeled as random variables with a lognormal distribution and mean value of 1.9231 kg. The Young's modulus and density are modeled, as shown in Figure 3.8. The modulus of elasticity and density are normally distributed with means

of 7E10 N/m^2 and 2780 kg/m^3, respectively. The coefficient of variation for all the random variables was taken to be 10%. Figure 3.8 shows the random variables considered in the analysis.

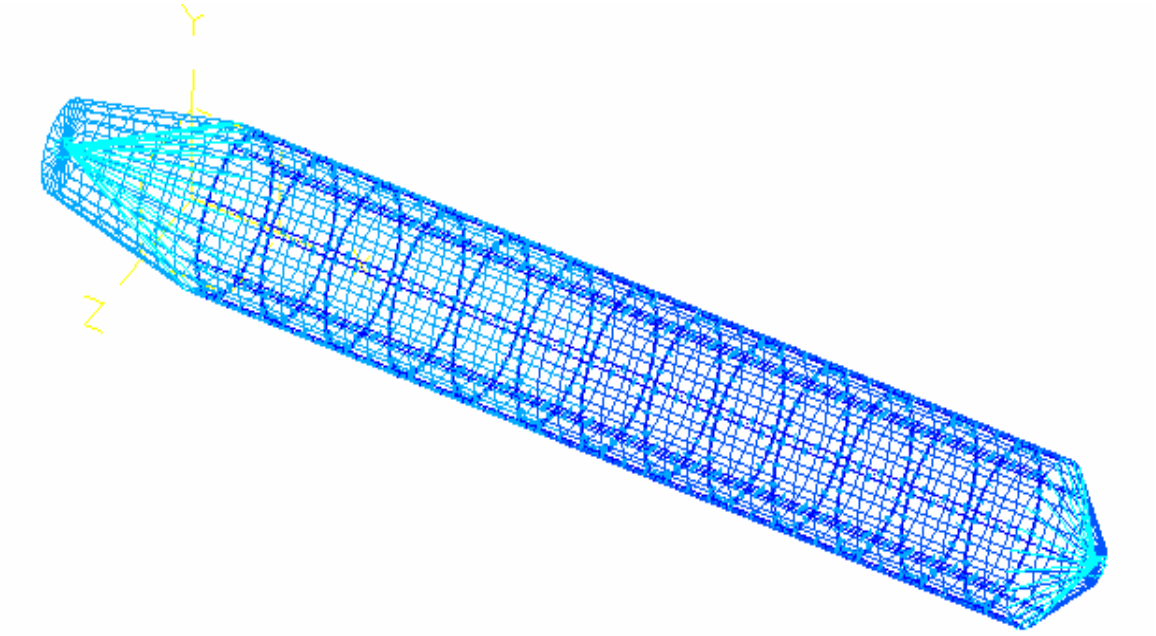

Figure 3.7: Finite Element Model of a Torpedo Structure

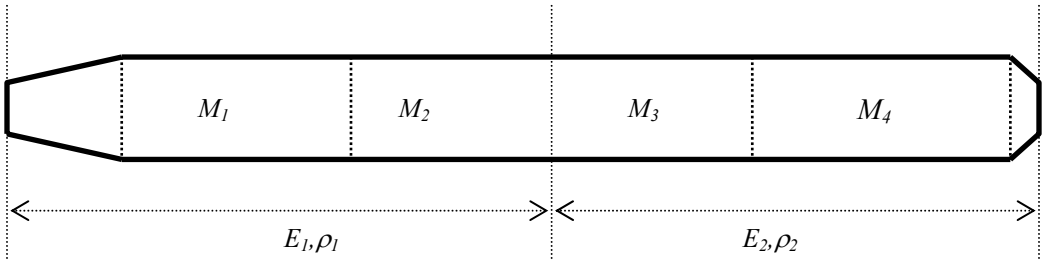

Figure 3.8: Description of the Random Variables

Two failure criteria are considered for the calculation of failure probability of the system. One criterion, shown in Eq. (3.13), is that the fundamental natural frequency of

the structure should be greater than 19 Hz. The other criterion, given by Eq. (3.14), is the maximum strain to be less than the yield strain of the material.

Frequency Limit-State $$g_1(\boldsymbol{X}) = \frac{\omega_1(\boldsymbol{X})}{19.0} - 1.0 \geq 0 \tag{3.13}$$

Strain Limit-State $$g_2(\boldsymbol{X}) = \frac{\varepsilon_{158}(\boldsymbol{X})}{0.00147} - 1.0 \leq 0 \tag{3.14}$$

The structural analysis was performed using GENESIS and the MPP of each of the limit-states was estimated. As the Young's modulus of element 158 is the only variable that affects the strain limit-state function, a reciprocal approximation was used in place of an MPA for the strain limit-state function. An MPA was constructed for the frequency limit-state by sampling points around the MPP. These approximations were then used to sample points on the joint failure region that are used in the construction of accurate response surface models, in multiple regions.

Methodology	System failure probability	% Difference
Monte Carlo Simulation	0.00398	----------
MPA + FFT	0.00413	3.76
First-order Series Bounds	0.00351 to 0.00397	-11.81 to -0.25

Table 3.5: Comparison of Results for a Torpedo Structure

Table 3.5 shows the comparison of the resulting probability of failure of the system using the proposed method and exact Monte Carlo simulation. Using the proposed methodology, the system failure probability was estimated to be 0.00413. The difference in the estimated failure probability when compared with Monte Carlo was about 3.76%,

which is conservative. One million exact simulations were needed to obtain convergence. Eighteen exact simulations were needed in the MPP search for each of the limit-state functions and ten design points were taken around the MPP for the frequency limit-state function for the construction of the MPA. No design points were sampled for the strain limit-state, because for the strain limit-state a reciprocal approximation at the MPP was able to capture the response. So, a total of $2(18)+10=46$ exact simulations were needed in the estimation of the failure probability as opposed to two million simulations (one million for each limit-state) using Monte Carlo. The first-order series bounds were obtained to be 0.00351 to 0.00397. The upper bound estimated the failure probability very accurately, but was not conservative. However, the estimation of the lower bound was highly inaccurate. Without any knowledge of the accuracy, these bounds would result in improper decisions.

3.3.4. Composite Model of a Torpedo Structure

The methodology for estimating the reliability of a structural system is applied for the composite model of a light weight torpedo. This example is selected to demonstrate the method using 16 random variables and 11 limit-states. The finite element model is as shown in Fig. 3.9. The shell is made of a honeycomb core with fiber-reinforced laminates to form the top and bottom plates. The composition of the shell is as shown in Fig. 3.10. The difference between the metallic model (fig 3.7) and the composite model (fig 3.9) is the lack of stiffeners in the composite model. The stiffeners in the longitudinal and radial direction, which provide structural strength, were not modeled to see whether the composite structure could achieve the same performance characteristics as a metallic lightweight torpedo without these stiffeners. The composite model was optimized to have

the same performance characteristics as that of the metallic model. The obtained optimum configuration was considered as the candidate design for the reliability analysis.

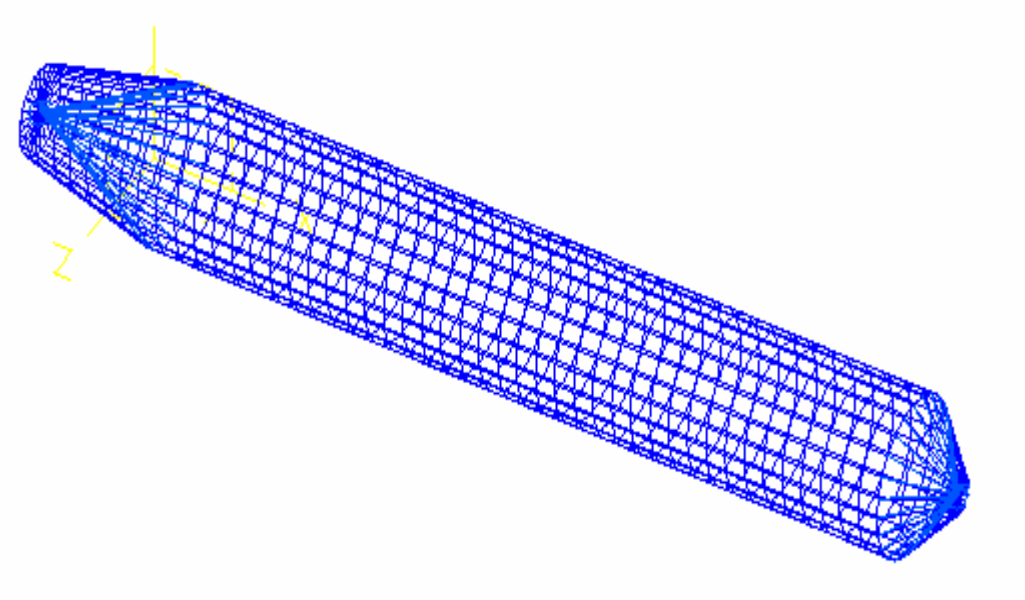

Figure 3.9: Finite Element Model of a Torpedo Hull

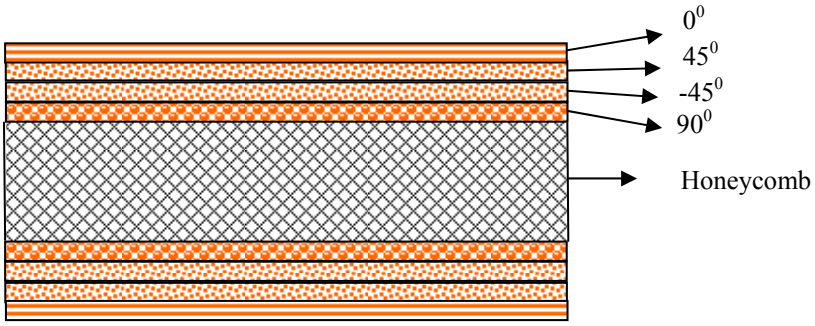

Figure 3.10: Torpedo Shell – Composite Layout

Eleven failure criteria were considered in the calculation of failure probability. One criterion is that the fundamental natural frequency has to be greater than 20.0 Hz. The criterion on the buckling of the structure is that of the critical buckling load factor should not be less than 1.0. The maximum principal strain in each layer of the element

should be more than -0.0065, which results in nine criteria, one for each layer. These criteria are given in Eqs. (3.15)- (3.17).

Frequency Limit-State $$g_1(\boldsymbol{X}) = \frac{\omega_1(\boldsymbol{X})}{20.0} - 1.0 \geq 0 \tag{3.15}$$

Buckling Limit-State $$g_2(\boldsymbol{X}) = \frac{P_{cr}(\boldsymbol{X})}{1.0} - 1.0 \geq 0 \tag{3.16}$$

Strain Limit-State $$g_i(\boldsymbol{X}) = \frac{\varepsilon_i(\boldsymbol{X})}{-0.0065} - 1.0 \leq 0\,,\ i = 3...11 \tag{3.17}$$

where ω_1 is the fundamental natural frequency, P_{cr} is the critical buckling load factor and ε_i are the strains in each layer.

A total of 16 random variables were considered in this problem. The thickness of the laminate in a particular orientation direction and the thickness of the honeycomb were assumed to be log-normally distributed with a coefficient of variation of 5%. The longitudinal and transverse moduli and the density of the laminate were modeled with a normal distribution and a variation of 5%. The structure is divided into four sections and the values of the concentrated masses in each section are modeled as random variables with a lognormal distribution with a 10% coefficient of variation. The mean values, the coefficient of variation and the type of distribution of the 16 random variables are given in Table 3.6.

Random Variable	Distribution	Mean	Coefficient of Variation
Top Plate Laminate Thickness 0^0 orientation	Lognormal	0.0012 m	5%
Top Plate Laminate Thickness 45^0 orientation	Lognormal	0.0008 m	5%
Top Plate Laminate Thickness -45^0 orientation	Lognormal	0.0008 m	5%
Top Plate Laminate Thickness 90^0 orientation	Lognormal	0.0004 m	5%
Honeycomb Thickness	Lognormal	0.0306 m	5%
Bottom Plate Laminate Thickness 90^0 orientation	Lognormal	0.0004 m	5%
Bottom Plate Laminate Thickness -45^0 orientation	Lognormal	0.0008 m	5%
Bottom Plate Laminate Thickness 45^0 orientation	Lognormal	0.0008 m	5%
Bottom Plate Laminate Thickness 0^0 orientation	Lognormal	0.0012 m	5%
Concentrated Mass, M_1	Lognormal	1.9231 kg	10%
Concentrated Mass, M_2	Lognormal	1.9231 kg	10%
Concentrated Mass, M_3	Lognormal	1.9231 kg	10%
Concentrated Mass, M_4	Lognormal	1.9231 kg	10%
Longitudinal Young's Modulus, E_1	Normal	1.4E10 N/m^2	5%
Longitudinal Young's Modulus, E_2	Normal	9.0E09 N/m^2	5%
Density of Laminates, ρ_1	Normal	1600 kg/m^3	5%

Table 3.6: Random Variables – Composite Model of a Torpedo Structure

Methodology	System failure probability	% Difference
Monte Carlo Simulation	0.00214	----------
MPA + FFT	0.00224	4.67
First-order Series Bounds	0.00123 to 0.00205	-42.52 to -4.21

Table 3.7: Results of the Composite Model of a Torpedo Structure

Table 3.7 shows the comparison of the failure probability values obtained using the proposed methodology and Monte Carlo simulation. The system failure probability was estimated to be 0.00224 with a difference of 4.67%. The first-order series bounds using FORM were obtained as 0.00123-0.00205. The upper bound was close to the estimated reliability value, but was not conservative; whereas, the lower bound was highly inaccurate. The proposed methodology needed 1412 exact simulations, which include the simulations required for calculating the gradients needed for the analysis. For each of the limit-states, 500,000 random points were needed to obtain convergence using Monte Carlo for each of the limit-states. This clearly shows the computational efficiency of the proposed system reliability estimation method.

The use of MPA enables the representation of implicit limit-state functions in a closed-form expression in terms of the random variables. Since information at more than one point is used in the construction of the MPA, it is accurate over a larger region compared to one and two-point approximations. Once the n-dimensional joint failure region is approximated, the convolution integral can be solved using the FFT technique. The FFT technique uses a robust algorithm to solve for the convolution integral accurately and efficiently to result in a reliable estimate of the probability of failure of the structural system. Moreover, the correlation between the various limit-states is taken into account by the accurate estimation of the joint failure region.

The accuracy of the proposed methodology depends on the accuracy of the MPA constructed for each of the limit-state criteria because the points on the joint failure region are sampled based on these MPA. So care should be taken in the construction of

MPAs for each of the limit-state functions. The use of accurate local TANA2 approximations leads to an accurate MPA.

The difference between a series and a parallel system is in the definition of the joint failure region. Based on the definition of failure, MPAs are to be constructed in the region of interest. For a parallel system, MPAs can be constructed around the closest intersection point that has the maximum likelihood of failure. Once accurate MPAs are obtained, design points are sampled on the joint failure region and the system reliability is estimated. Therefore, the proposed methodology can be easily applied to any type of system by modeling the appropriate joint failure region accurately.

In most structural problems, information is available to model some uncertain variables with a PDF while some variables have limited information. The following two chapters deal with the estimation of bounds on system reliability when some variables are random and others are nonrandom in nature. Chapter 4 deals with the extension of this algorithm for handling interval variables while the algorithm for handling random and fuzzy variables and multiple failure modes is presented in chapter 5.

4. BOUNDS ON STRUCTURAL SYSTEM RELIABILITY

If all the uncertain parameters are defined as random variables, then the reliability of a structural system can be estimated accurately by using the algorithm presented in the previous chapter. But when the knowledge about some of the variables is limited to lower and upper bounds, the entire range of these bounds should be explored while estimating the bounds on the reliability. The computational cost involved in estimating these bounds increases tremendously because a single reliability analysis, which is a computationally expensive procedure, is performed multiple times for each configuration of the interval variables. To reduce the computational cost involved, transformation of intervals is used along with high quality function approximations for each of the limit-states and the joint failure surface. The use of transformation techniques facilitates the estimation of the interval configurations that correspond to the bounds on system reliability. Once the configurations are estimated, the system reliability at each configuration can be estimated accurately using the algorithm presented earlier.

4.1. Transformation of Interval Variables

In the presence of mixed uncertain parameters, the joint failure surface, which is highly nonlinear, is dependent on the configuration of the interval variables. The entire domain of the interval variables is to be explored to determine the configuration of the interval variables that correspond to the minimum and maximum values of the reliability. The contribution of the interval variables to each of the convolution integrals can be obtained by using transformation techniques.

Consider a response is given by $Y(x_1, x_2) = x_1^2 + x_2^2 - 4x_1 + 4$ where $x_1 = [1,4]$ and $x_2 = [-1,1]$ are interval variables. The response equation can be expressed as a linear combination given by $Y(z_1, z_2) = z_1 + z_2$ where $z_1 = (x_1 - 2)^2$ and $z_2 = x_2^2$. Based on these relations, the bounds of the original variables are transformed to obtain the bounds of the intervening variables. The bounds of the intervening variables are $z_1 = [0,4]$ and $z_2 = [0,1]$. Now as the response is a linear combination of the intervening variables, the bounds on the response are the summation of the lower and upper bounds of the intervening variables resulting in the range of $Y = [0,5]$. The solution obtained by applying interval arithmetic on the original equation is $Y = [2,5]$. This is because the minimum value of the response occurs when $x_1 = 2$ and $x_2 = 0$ which are within the bounds. The problems associated with the dependency is eliminated as each variable appears only once in the response leading to accurate estimation of the bounds.

4.2. Algorithm for Estimating System Reliability Bounds

In the presence of both random and interval variables, every configuration of the interval variables has an unknown probability. To estimate this probability, the new joint failure region needs to be modeled accurately at each configuration of the interval variables. For modeling this joint failure region using an approximation, the limit-state functions should be available in closed-form so that the points on the joint failure surface can be sampled. In the case of an implicit function, several local TANA2 approximations can be constructed, with sample points around the Most Probable Point (MPP) for each limit-state function, and blended into a Multi-Point Approximation (MPA). The MPP of

each of the limit-state functions is estimated by setting the interval variables to their central values. The domain around this MPP is approximated using an MPA. The bounds on the random variables are taken to be two standard deviations on either side of the MPP while the lower and upper bounds were considered for the interval variables. Once an accurate MPA is constructed for each of the limit-state functions, there is no need for running exact simulations as the MPAs capture the behavior of the limit-states accurately in this domain. These MPAs along with Fast Fourier Transforms (FFT) are used for estimating the bounds on the reliability of the system.

The details of the algorithm and its implementation are presented below:

1. Estimate the MPP of each of the limit-state functions with the interval variables at their central values. The MPP is obtained by using the modified HL-RF (Hasofer Lind – Rackwitz Fiessler) algorithm with TANA2 approximate models.
2. Design points are sampled within the vicinity of each MPP using a Latin hypercube sampling technique. All the uncertain variables (random + interval) are used during this sampling. The bounds on the random variables are taken to be two standard deviations on either side of each MPP. The lower and upper limits are used as the bounds in the sampling for the interval variables.
3. Multiple local TANA2 approximations are constructed using the set of design points sampled. These local TANA2 approximations are blended into a multi-point approximation. Since all the interval variables are included in the design points sampled, the MPA constructed captures the behavior of the limit-state for the whole range of the intervals. Using the same procedure, an MPA is constructed for each of the limit-state functions.

4. Points are sampled on the joint failure surface using these surrogate representations of each of the limit-states. Multiple response surface models are then constructed using these sampled points. In order to obtain an accurate representation of the joint failure surface, the design space is sub-divided based on the accuracy of the response surface models as described in section 3.2.
5. Based on the response surface models constructed, the convolution integral is divided into several regions found in step 4 spanning the entire design space. Each of these integrals is evaluated separately.
6. Each response surface is divided into two parts, one containing the terms with random variables and the other containing interval variables. The part of the interval variables is used to determine the contribution of the interval variables to the particular integral by applying necessary transformations. The part with the random variables is convoluted using FFT to obtain the joint PDF. The contribution of the interval variables acts as a linear shift in the PDF obtained.
7. Once the joint PDFs and interval variable contributions for all the integrals are evaluated, the minimum and maximum values of the intervals are used to combine and integrate the joint PDF to obtain the bounds on the system reliability. Figure 4.1 illustrates the methodology discussed above.

For nonlinear responses, the contribution of the interval variables that correspond to the extreme values of the reliability is estimated using transformations. These contributions appear as a constant when performing the convolution using fast Fourier transforms leading to a linear shift in the PDF obtained from the convolution. In this methodology, the contribution of the intervals to the reliability are evaluated separately

and used in the failure probability calculation. So even if it seems like the interval values appear more than once during the failure probability calculation, there is no overestimation of the bounds as interval arithmetic is not implemented in the estimation of the bounds. Only the contributions of the interval variables to the reliability are used.

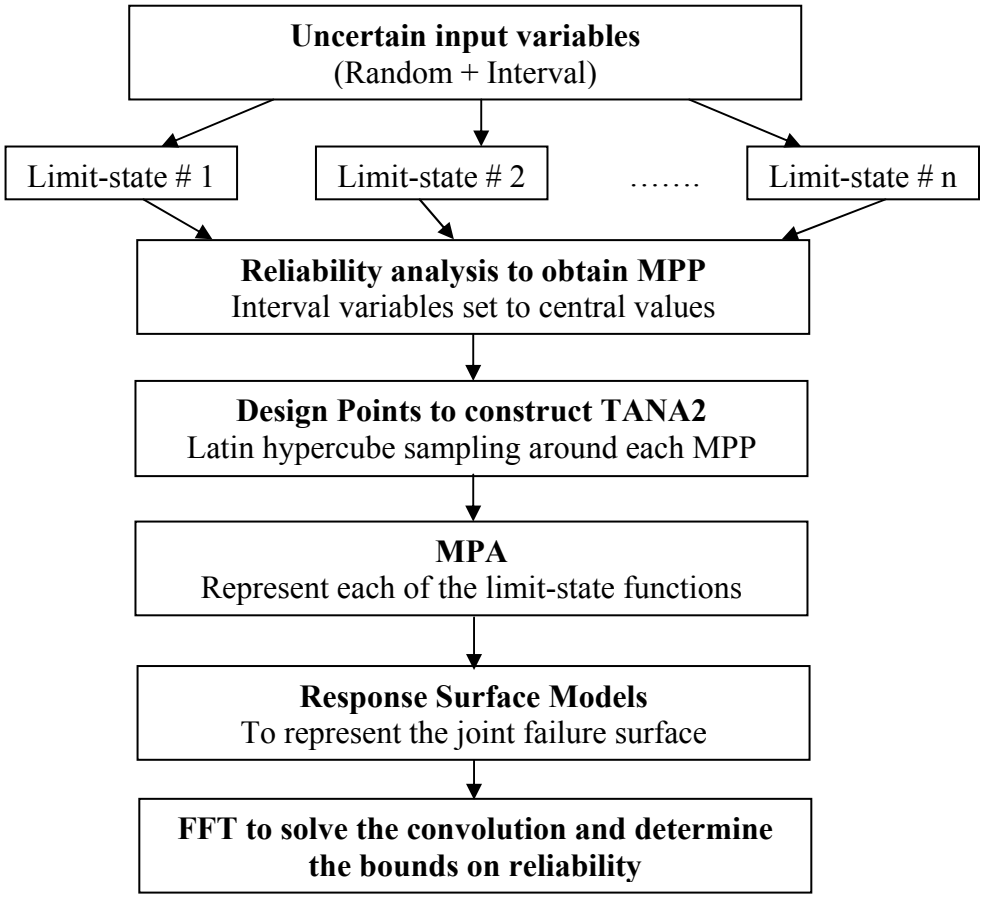

Figure 4.1: Methodology for Estimating System Reliability Bounds

4.3. Numerical Examples

4.3.1. Cantilever Beam

A cantilever beam, as shown in figure 3.6 is subjected to a tip load, *P*. Two failure criteria were considered: (i) the displacement at the tip of the beam should be less than 0.002 m, as shown in Eq. (4.1), and (ii) the stress in the beam should be less than 34 MPa, as shown in Eq. (4.2).

Displacement Limit-state $$g_1(\boldsymbol{X}) = \frac{4PL^3}{Ebh^3} - 0.002 \leq 0 \tag{4.1}$$

Stress Limit-state $$g_2(\boldsymbol{X}) = \frac{12PL}{bh^2} - 34 * 10^6 \leq 0 \tag{4.2}$$

where *L*, *b*, *h* are the length, width and height of the beam which are taken as random variables. The length of the beam was assumed to be normally distributed with a mean value of 0.762 m and standard deviation of 0.0762 m. The width and height of the beam were both assumed to be normally distributed with mean values of 0.0635 m and standard deviations of 0.00635 m. The point load, *P*, acting on the tip of the beam was assumed to be between the interval of [355.856, 533.784] N.

As the limit-state functions are available as closed-form expressions in terms of the uncertain variables, there was no need for constructing approximations of each of the limit-state functions. The closed-form expressions of the limit-state functions are used for sampling points on the joint failure region. These sampled points were used in the construction of multiple response surface models to represent the joint failure region. The design space was divided into smaller domains so that the response surface model captures the joint failure region accurately within that domain. As there is only one

interval variable in this problem, the configurations of the load that yields the bounds on the reliability are obtained using transformation techniques. These configurations were used to solve the convolution integral over the entire design space to obtain bounds on the system failure probability.

Methodology	**Failure probability bounds**	**% Difference**	
		Lower limit	Upper limit
Monte Carlo	[0.00227, 0.02598]	---	---
Proposed algorithm	[0.00228, 0.02704]	0.44	4.08

Table 4.1: Failure Probability Bounds of the Cantilever Beam

Table 4.1 illustrates the accuracy of the methodology in predicting the failure probability of the system. The bounds obtained by the proposed methodology were conservative with a difference of around 4%. For each configuration of load, one million evaluations of the limit-state functions were used in the estimation of the failure probability using conventional Monte Carlo simulation.

4.3.2. Wing Structure

A wing structure, as shown in Figure 4.2, is considered to estimate the bounds on the failure probability. Two failure criteria of the system are considered. The displacement at the tip of the wing when subject to aerodynamic loading to be less than 0.04 m (Eq. 4.3) and the fundamental natural frequency of the wing to be more than 1.52 Hz. (Eq. 4.4)

$$g_1(\boldsymbol{X}) = D_{tip}(\boldsymbol{X}) - 0.04 \leq 0 \tag{4.3}$$

$$g_2(\boldsymbol{X}) = 1.52 - \omega_1(\boldsymbol{X}) \leq 0 \tag{4.4}$$

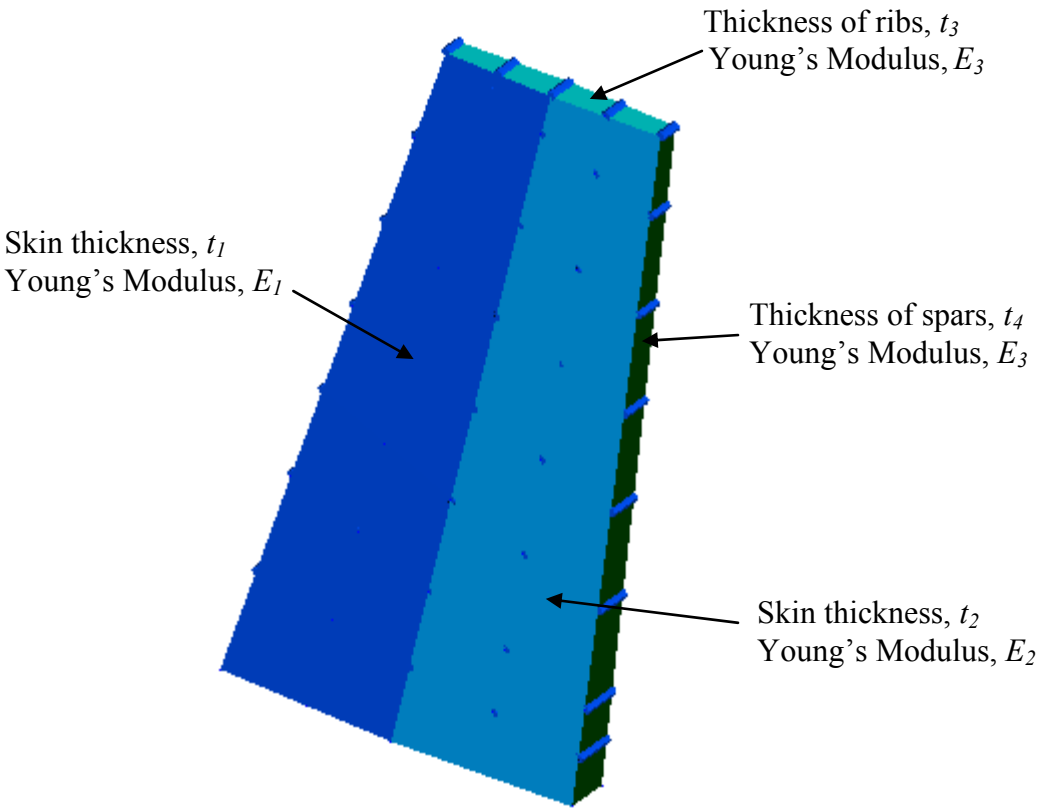

Figure 4.2: Wing Structure

The thicknesses of the first two span-wise skins are physically linked to have the same value, which is modeled as a normal distribution with a mean of 0.0381 m. The same is done with the other two span-wise skins. All of the spars are linked to have the same thickness and the same is done with the ribs. These are also modeled as normally distributed random variables with a mean of 0.0127 m. Physical linking results in four random variables and the coefficient of variation is assumed to be 10% for all of these variables. The Young's moduli of the two physically linked skins are modeled as interval variables. Moreover, the Young's modulus of the spars and ribs is also modeled as an

interval variable. These variables were considered to be in the interval of [7.17E10, 7.31E10] N/m^2.

Methodology	**Failure probability bounds**	**% Difference**	
		Lower limit	Upper limit
Monte Carlo	[0.00132, 0.04522]	---	---
Proposed algorithm	[0.00125, 0.04692]	-5.30	3.76

Table 4.2: Failure Probability Bounds of the Wing Structure

Table 4.2 shows the comparison of the reliability estimated using the proposed methodology and Monte Carlo simulation. As this is a problem with implicit limit-state functions, multi-point approximations were constructed for each of the limit-states which were used as closed-form expressions in estimating the bounds on the reliability. A total of 31 exact function evaluations were needed in the estimation of both the MPPs. 25 design points were used in the construction of each of the MPAs. The bounds obtained by using the proposed technique were conservative with a difference of around 5% on the lower bound and 4% on the upper bound. The proposed methodology required only $2(25)+31=81$ exact simulations as opposed to 1.2 million simulations for Monte Carlo.

4.3.3. Turbine Blade

The methodology of estimating the bounds on system reliability was applied to a twisted turbine blade with a 45-deg twist angle. The finite element model is shown in Figure 4.3. The blade is modeled using 80 quadrilateral plate elements between 99 nodes. All the degrees of freedom along the hub are fixed. This blade is subjected to a uniform pressure loading.

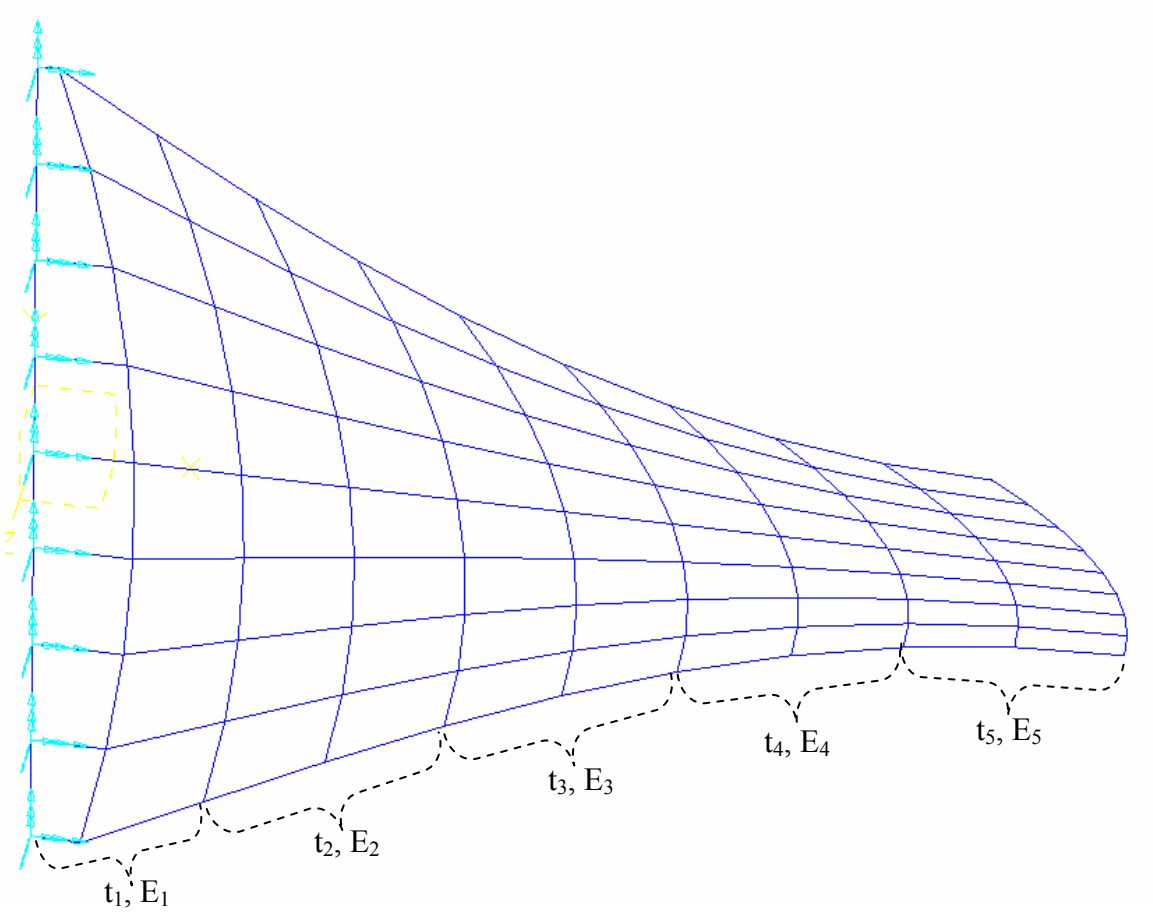

Figure 4.3: Finite element model of the turbine blade

The thicknesses and the moduli of elasticity were considered as uncertain parameters, but with physical linking only 10 independent uncertain variables were considered. Every two sets of the chordwise elements are assumed to have the same thickness and same Young's modulus. The five Young's moduli are modeled as normally distributed random variables with a mean value of 20E10 N/m^2 and a coefficient of variation of 10%. The thickness of the blade decreases from the hub to the tip. These

thicknesses are modeled as interval variables with the lower and upper bounds as shown in Table 4.3.

Interval Variable	Lower Bound	Upper Bound
Thickness, t_1	0.00838 m	0.00939 m
Thickness, t_2	0.00825 m	0.00927 m
Thickness, t_3	0.00812 m	0.00914 m
Thickness, t_4	0.00800 m	0.00902 m
Thickness, t_5	0.00787 m	0.00889 m

Table 4.3: Intervals of the Thickness Distribution of the Turbine Blade

Two different failure modes are considered. One limit-state is that the displacement at the tip in the direction perpendicular to the plate should be less than 0.000635 m. Another limit-state is that the fundamental natural frequency should be greater than 1850 Hz. These criteria are shown in Eqs. (4.5) and Eq. (4.6)

$$g_1(\boldsymbol{X}) = D_{tip}(\boldsymbol{X}) - 0.000635 \leq 0 \tag{4.5}$$

$$g_2(\boldsymbol{X}) = 1850 - \omega_1(\boldsymbol{X}) \leq 0 \tag{4.6}$$

The MPPs of each of the limit-states are estimated, and Latin Hypercube sampling technique was used to sample 25 design points around these MPPs. Local TANA2 approximations were constructed with these 26 design points (25 design points + MPP of that limit-state) and combined into a multi-point approximation. These MPAs were used as closed-form expressions of the limit-states to obtain points on the joint failure surface. These points were used in the construction of accurate response surface models based on which the bounds on the system failure probability are obtained.

A comparison of the bounds on the system failure probability obtained using the proposed algorithm and traditional Monte Carlo simulation is shown in Table 4.4. The bounds obtained by using the proposed technique were comparable with those obtained by Monte Carlo simulation. The proposed methodology needed a total of 590 exact simulations, which include the simulations required for calculating the gradients needed in the construction of the MPAs. At each configuration of the interval variables, Monte Carlo simulation needed 1 million simulations to obtain convergence. This clearly shows the computational efficiency of the proposed methodology.

Methodology	**Failure probability bounds**	**% Difference**	
		Lower limit	Upper limit
Monte Carlo Simulation	[0.000028, 0.1127]	---	---
Proposed algorithm	[0.000025, 0.1204]	-10.71	6.83

Table 4.4: Failure Probability Bounds for the Turbine Blade Example

Due to the vagueness in the available information, all of the uncertain parameters in a problem cannot be assumed to be random in nature. When dealing with a combination of random and interval variables, the computational cost for estimating the bounds on system reliability increases exponentially. To reduce the computational cost without a loss of accuracy, a methodology that uses transformations for interval variables along with the system reliability estimation algorithm is presented to efficiently deal with mixed variables problems.

The technique of transforming interval variables can be used to accurately estimate the configurations that correspond to the bounds of system reliability. This technique yields the same results as the expensive optimization method to obtain the

extreme values for non-linear functions. Since innovative transformation techniques based on the interval variables is used in this research, there is no overestimation in the bounds even if it seems like the interval variables appear more than once in the estimation of the reliability bounds.

5. MEMBERSHIP FUNCTION OF SYSTEM RELIABILITY

When dealing with a combination of probability distributions and fuzzy membership functions, the computational cost involved in estimating the membership function of reliability increases exponentially because multiple reliability analysis are needed. Moreover, when multiple failure modes are involved, the joint failure region is dependent on the configuration of the fuzzy variables at various possibility levels. For accurate estimation of the membership function of the system reliability, the configuration of the fuzzy variables that correspond to the extreme values of reliability as well as the system reliability are to be estimated accurately. In this work, the transformation techniques for membership functions as well as the system reliability algorithm presented previously are combined to estimate the membership function of system reliability accurately.

5.1. Proposed Algorithm

The details of the proposed algorithm and its implementation are presented below.

1. The MPP is estimated for each of the limit-state functions. During this process, the fuzzy variables are set to their values that have maximum possibility.
2. Design points are sampled within the vicinity of each MPP using a Latin hypercube sampling technique. The bounds on the random variables are taken to be two standard deviations on either side of each MPP. Fuzzy variables are then set to their bounds at zero possibility level.

3. Multiple local TANA2 approximations are constructed for the set of design points sampled around each MPP. These local TANA2 approximations are blended into a multi-point approximation, which captures the behavior of the limit-state function around the MPP. Using the same procedure, an MPA is constructed for each of the limit-state functions.
4. Points are sampled on the joint failure surface using these surrogate representations of each of the limit-states. Multiple response surface models are constructed using these sampled points as illustrated in section 3.2. In order to improve the accuracy of each of the response surface models, the design space is sub-divided until the regression sum of squares value of the approximations in each sub-division are acceptable.
5. Each response surface is divided into two parts, one containing the terms with random variables and the other containing fuzzy variables. The part with the random variables is convoluted using FFT to obtain the joint PDF and the part with the fuzzy variables is used to obtain the joint membership function by applying the necessary transformations.
6. At each α-cut the minimum and the maximum values of the joint membership functions are used to combine and integrate the area under the joint PDF and obtain the membership function of reliability. Figure 5.1 illustrates the methodology discussed above.

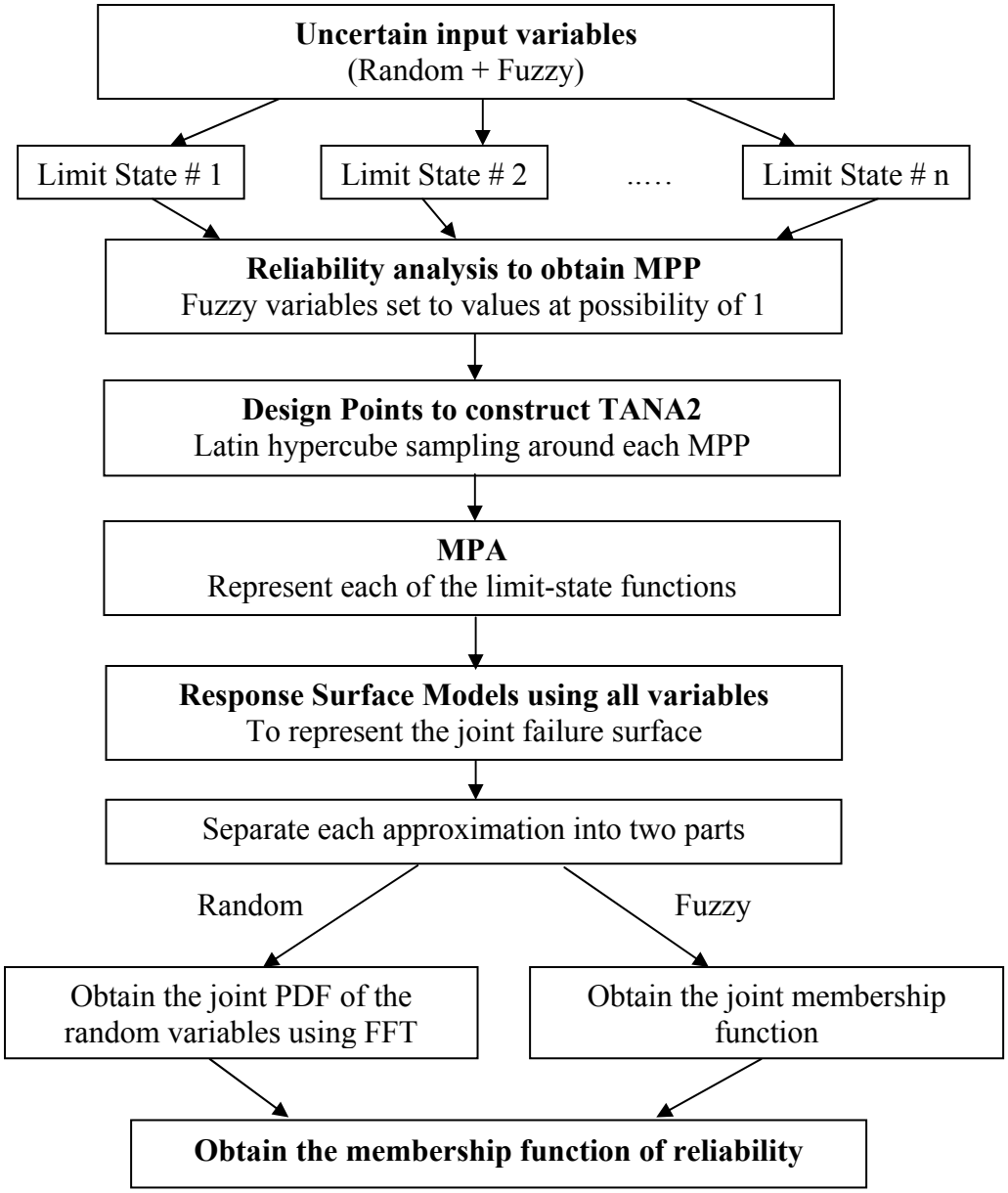

Figure 5.1: Proposed Algorithm Details

5.2. Numerical Examples and Discussion

5.2.1. Simply Supported Beam

A simply supported beam, as shown in Figure 5.2, is subjected to a central point load of 444.82 N. The two failure criteria for the structure are: (i) the displacement at the midspan of the beam should be less than 0.001 m, as shown in Eq. (5.1), and (ii) max. stress in the beam should be less than 19.86 MPa, as shown in Eq. (5.2).

Displacement Limit-State $$g_1(\boldsymbol{X}) = \frac{PL^3}{4Ebh^3} - 0.001 \le 0 \tag{5.1}$$

Stress Limit-State $$g_2(\boldsymbol{X}) = \frac{3PL}{2bh^2} - 19.86 * 10^6 \le 0 \tag{5.2}$$

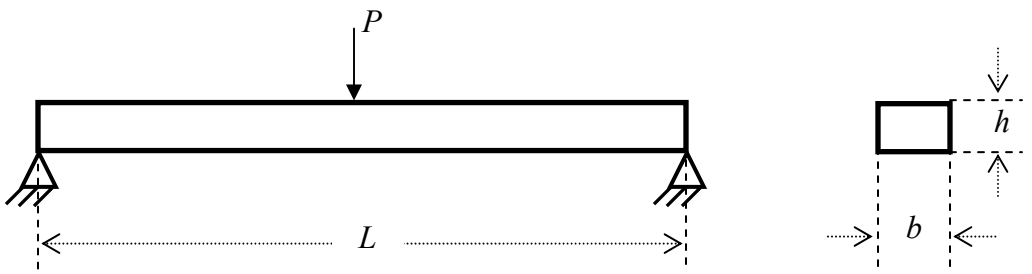

Figure 5.2: Simply Supported Beam

where L, b, h are the length, width and height of the beam. The width and height of the beam were both assumed to be normally distributed random variables with mean values of 0.0635 m and standard deviations of 0.00635 m. The length of the beam was modeled as a fuzzy variable with the membership function given by Eq. (5.3). Figure 5.3 shows the membership function of the fuzzy variable. The modulus of elasticity of the beam was taken to be 68.9 GPa.

$$\mu_L(L) = \begin{cases} (L - 0.635)/0.127 & 0.635 \le L \le 0.762 \\ (L - 0.889)/-0.127 & 0.762 \le L \le 0.889 \end{cases} \tag{5.3}$$

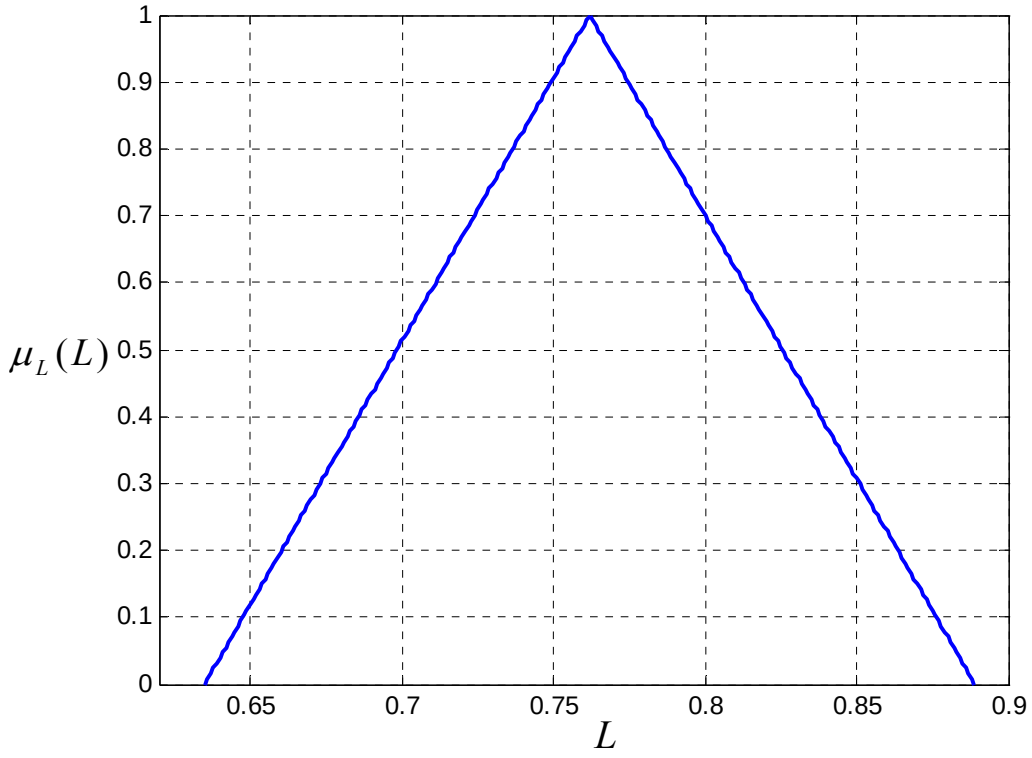

Figure 5.3: Membership Function of Fuzzy variable

As the limit-state functions are available as closed-form expressions in terms of the random variables, there was no need for constructing approximations of each of the limit-state functions. Using these closed-form expressions, several points were sampled on the joint failure region. These sampled points were used in the construction of multiple response surface models to represent the joint failure region. The design space was divided into smaller domains such that the response surface model captures the joint failure region accurately within that domain. Each of the response surface models were then linearized in terms of the intervening variables and divided into two parts. The part with the random variables was used for convolution to obtain the joint PDF and the part

with the fuzzy variable was used for transforming the membership function of the original variable into that of the intervening variable. Due to the presence of only one fuzzy variable in the problem, the joint membership function of the fuzzy variables is nothing but the membership function of the fuzzy intervening variable. At each α-cut, the bounds of the fuzzy intervening variable were used to combine the joint PDFs, obtained from each response surface, to result in the system PDF which is integrated in the failure region to obtain the membership function of system reliability.

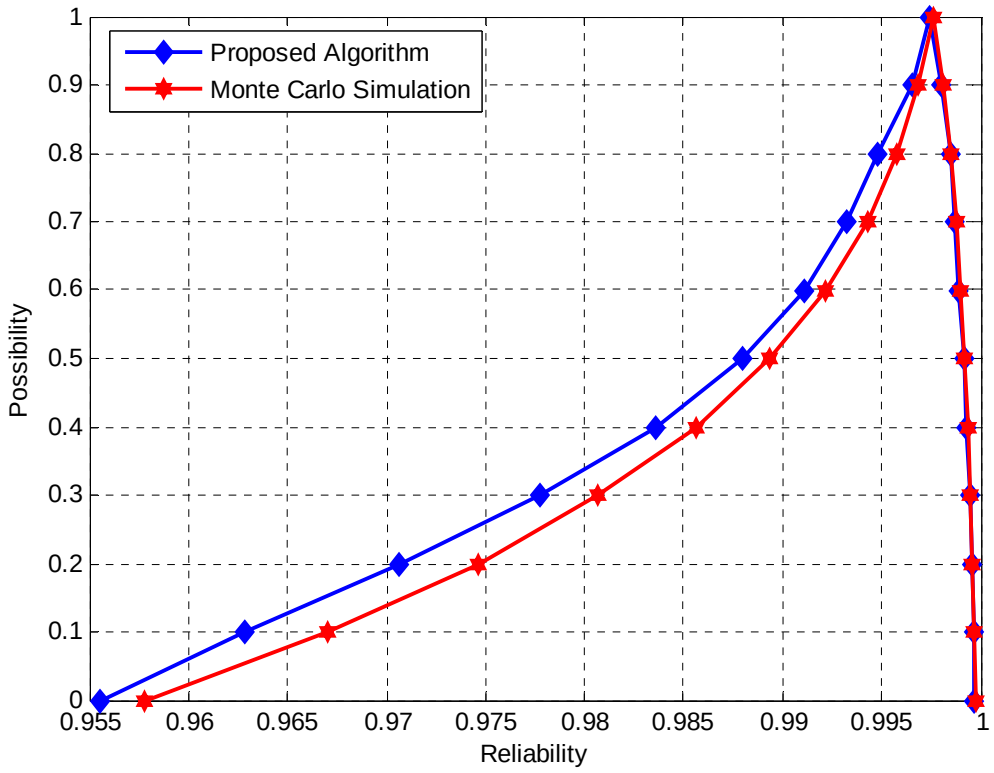

Figure 5.4: Membership Function of Reliability for the Simply Supported Beam

Figure 5.4 shows the membership function of reliability estimated using the proposed methodology, as well as that obtained using traditional Monte Carlo simulation. To illustrate the difference in the failure probability, the membership function of failure probability was compared by plotting the failure probability using a log scale as shown in figure 5.5. The maximum difference in reliability was around 0.25% and was

conservative. At each level, one million function evaluations were needed for convergence of the Monte Carlo simulation.

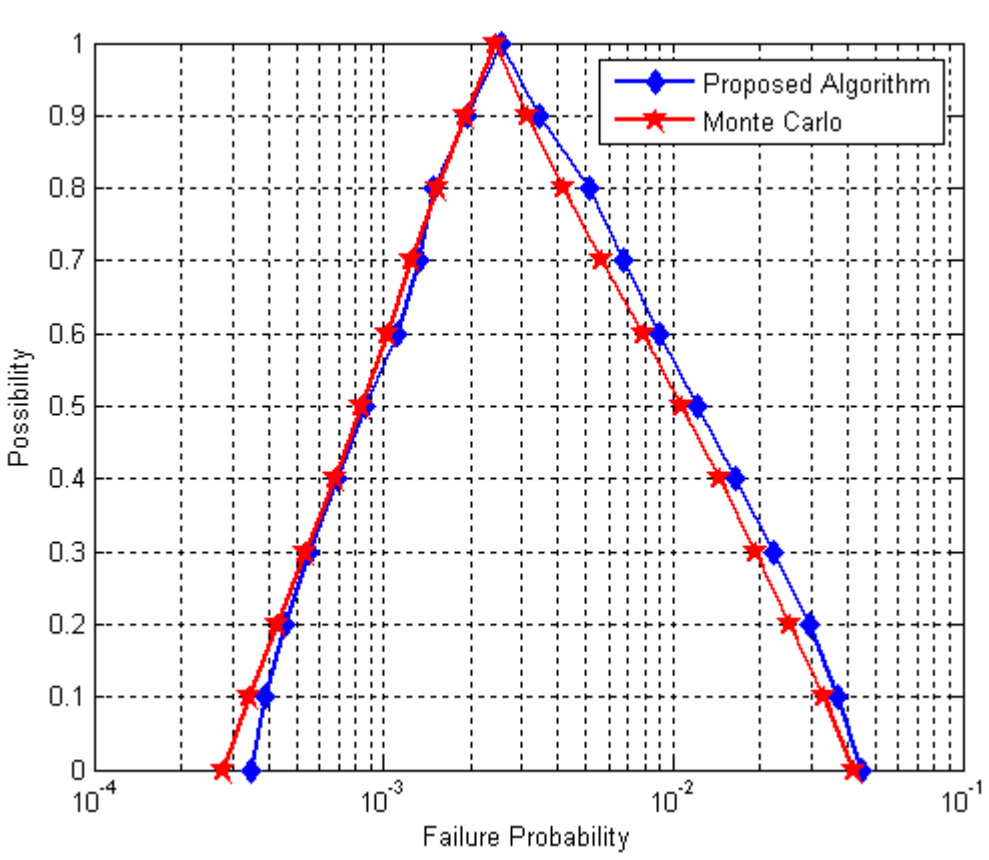

Figure 5.5: Comparison of Failure Probability for the Simply Supported Beam

5.2.2. Wing Structure

The methodology was applied to a wing structure, as shown in figure 2.12, to obtain the membership function of system reliability. The displacement at the tip of the wing when subject to aerodynamic loading to be less than 0.04 m (Eq. 5.4) and the fundamental natural frequency of the wing to be more than 1.52 Hz. (Eq. 5.5) are the criteria considered for the failure of the system.

$$g_1(\boldsymbol{X}) = D_{tip}(\boldsymbol{X}) - 0.04 \leq 0 \tag{5.4}$$

$$g_2(\boldsymbol{X}) = 1.52 - \omega_1(\boldsymbol{X}) \leq 0 \tag{5.5}$$

The Young's moduli of the top and bottom skins were modeled as normally distributed random variables with mean values of 7.24E10 N/m^2. All the spars were physically linked and the same is done with the ribs. The Young's moduli of the spars and the ribs were also modeled as normally distributed random variables with mean value of 7.24E10 N/m^2. Physical linking results in three random variables and the coefficient of variation is assumed to be 10% for all of these variables. The thicknesses of the top and bottom skins (Eq. 5.6) as well as the thickness of the spars and ribs (Eq. 5.7) are modeled using triangular fuzzy membership functions. A total of six uncertain variables, three random variables and three fuzzy variables, were considered in this problem.

$$\mu_{t_1}(t_1) = \begin{cases} (t_1 - 0.0331)/0.0005 & 0.0331 \leq L \leq 0.0381 \\ (t_1 - 0.0432/-0.0005 & 0.0381 \leq L \leq 0.0432 \end{cases} \tag{5.6}$$

$$\mu_{t_3}(t_3) = \begin{cases} (t_3 - 0.0076)/0.0005 & 0.0076 \leq L \leq 0.0127 \\ (t_3 - 0.0178/-0.0005 & 0.0127 \leq L \leq 0.0178 \end{cases} \tag{5.7}$$

As this is a problem with implicit limit-state functions, multi-point approximations were constructed for each of the limit-states which were used as closed-form expressions in estimating the bounds on the reliability. The bounds obtained by using the proposed technique are comparable with those obtained by Monte Carlo simulation. The use of accurate MPAs for the limit-states facilitates the accurate estimation of the system reliability bounds at each α-cut without increasing the computational cost. Figures 5.6 and 5.7 show the comparison between the membership function obtained using the proposed algorithm and the one obtained using the Monte Carlo simulation.

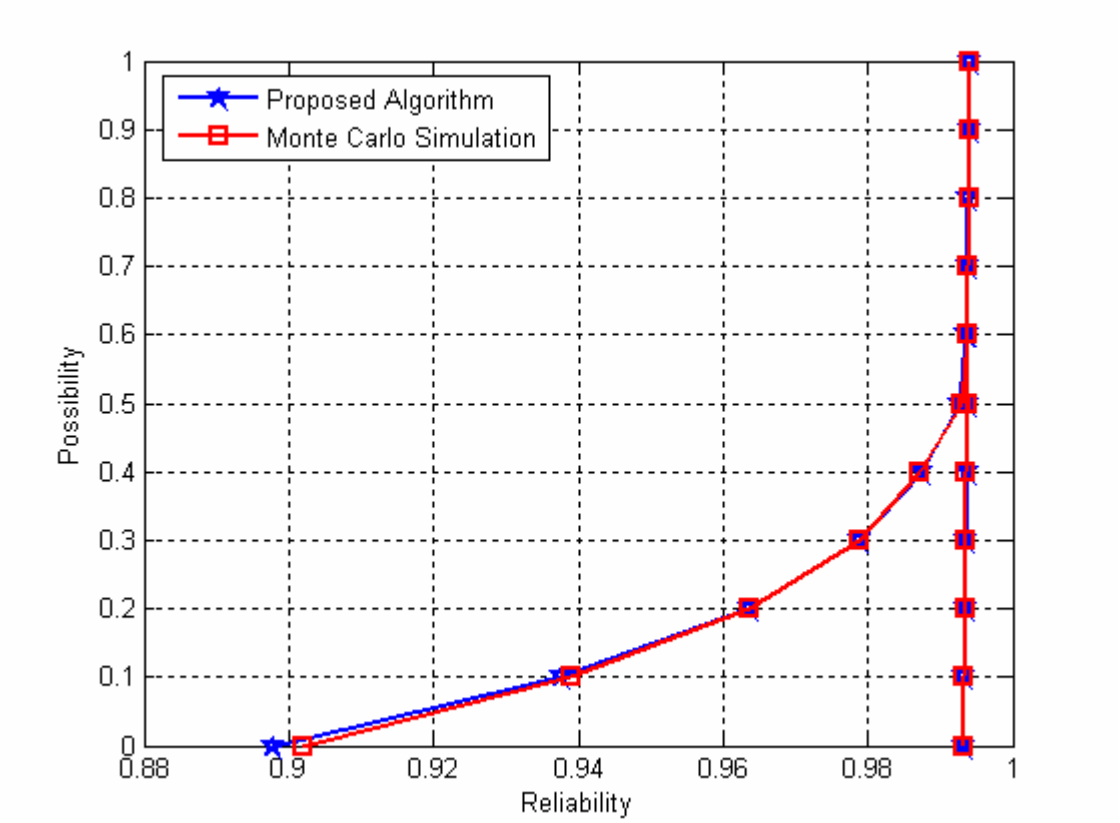

Figure 5.6: Comparison of the Reliability Estimation of the Wing Structure

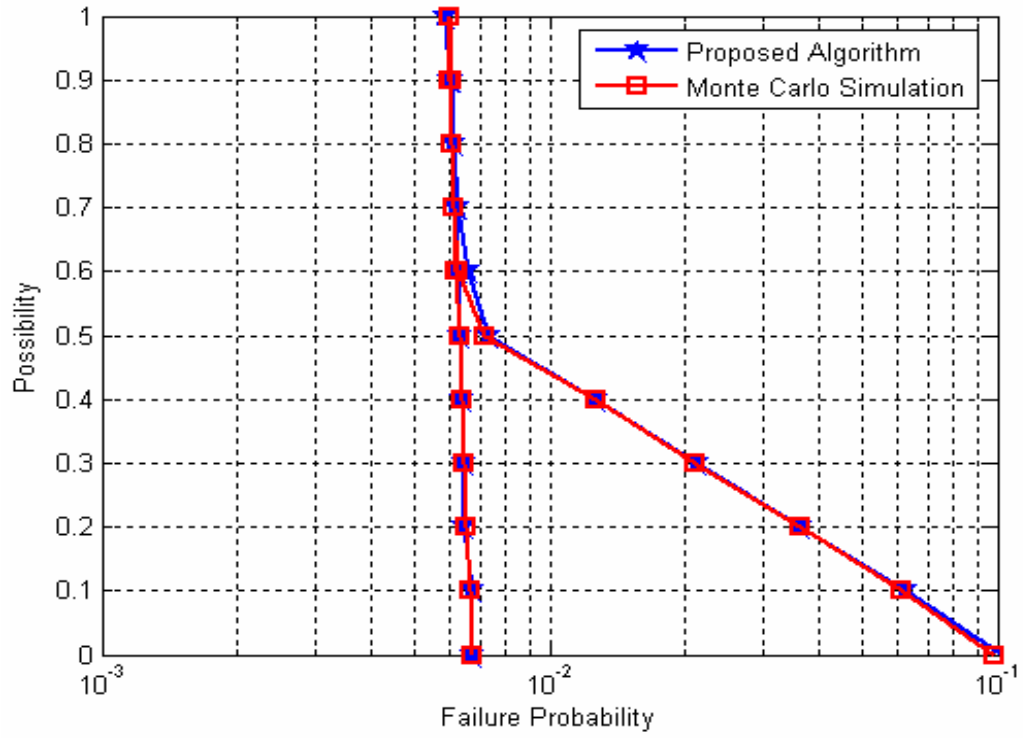

Figure 5.7: Comparison of the Failure Probability of the Wing Structure

5.2.3. Turbine Blade

The methodology of estimating the membership function of system reliability was applied to a twisted turbine blade with a 45-deg twist angle. The finite element model is shown in Figure 4.3. The blade is modeled using 80 quadrilateral plate elements between 99 nodes. All the degrees of freedom along the hub are fixed. This blade is subjected to a uniform pressure loading.

The thicknesses and the moduli of elasticity were considered as uncertain parameters, but with physical linking only 10 independent uncertain variables were considered. Every two sets of the chordwise elements are assumed to have the same thickness and same Young's modulus. The five Young's moduli are modeled as normally distributed random variables with a mean value of 20E10 N/m^2 and a coefficient of variation of 10%. The thickness of the blade decreases from the hub to the tip. These thicknesses are modeled using triangular fuzzy membership functions given by the equations below (Eq. 5.8-5.12).

$$\mu_{t_1}(t_1) = \begin{cases} (t_1 - 0.00838)/0.000508 & 0.00838 \le t_1 \le 0.00889 \\ (t_1 - 0.00939)/-0.000508 & 0.00889 \le t_1 \le 0.00939 \end{cases} \quad (5.8)$$

$$\mu_{t_2}(t_2) = \begin{cases} (t_2 - 0.00825)/0.000508 & 0.00825 \le t_2 \le 0.00876 \\ (t_2 - 0.00927)/-0.000508 & 0.00876 \le t_2 \le 0.00927 \end{cases} \quad (5.9)$$

$$\mu_{t_3}(t_3) = \begin{cases} (t_3 - 0.00812)/0.000508 & 0.00812 \le t_3 \le 0.00863 \\ (t_3 - 0.00914)/-0.000508 & 0.00863 \le t_3 \le 0.00914 \end{cases} \quad (5.10)$$

$$\mu_{t_4}(t_4) = \begin{cases} (t_4 - 0.00800)/0.000508 & 0.00800 \le t_4 \le 0.00851 \\ (t_4 - 0.00902)/-0.000508 & 0.00851 \le t_4 \le 0.00902 \end{cases} \quad (5.11)$$

$$\mu_{t_5}(t_5) = \begin{cases} (t_5 - 0.00787)/0.000508 & 0.00787 \le t_5 \le 0.00838 \\ (t_5 - 0.00889)/-0.000508 & 0.00838 \le t_5 \le 0.00889 \end{cases} \quad (5.12)$$

Two different failure modes are considered. One limit-state is that the displacement at the tip in the direction perpendicular to the blade should be less than 0.000635 m. Another limit-state is that the fundamental natural frequency should be greater than 1850 Hz. These criteria are shown in Eqs. (5.13) and Eq. (5.14)

$$g_1(\boldsymbol{X}) = D_{tip}(\boldsymbol{X}) - 0.00635 \le 0 \quad (5.13)$$

$$g_2(\boldsymbol{X}) = 1850 - \omega_1(\boldsymbol{X}) \le 0 \quad (5.14)$$

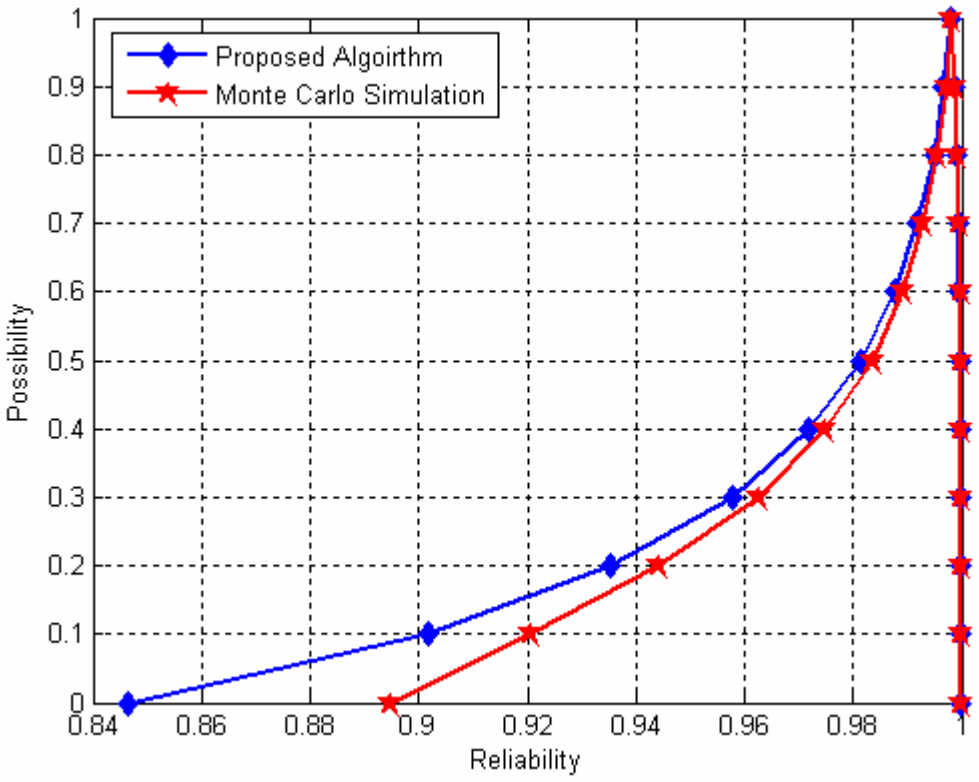

Figure 5.8: Membership Function of Reliability for the Turbine Blade

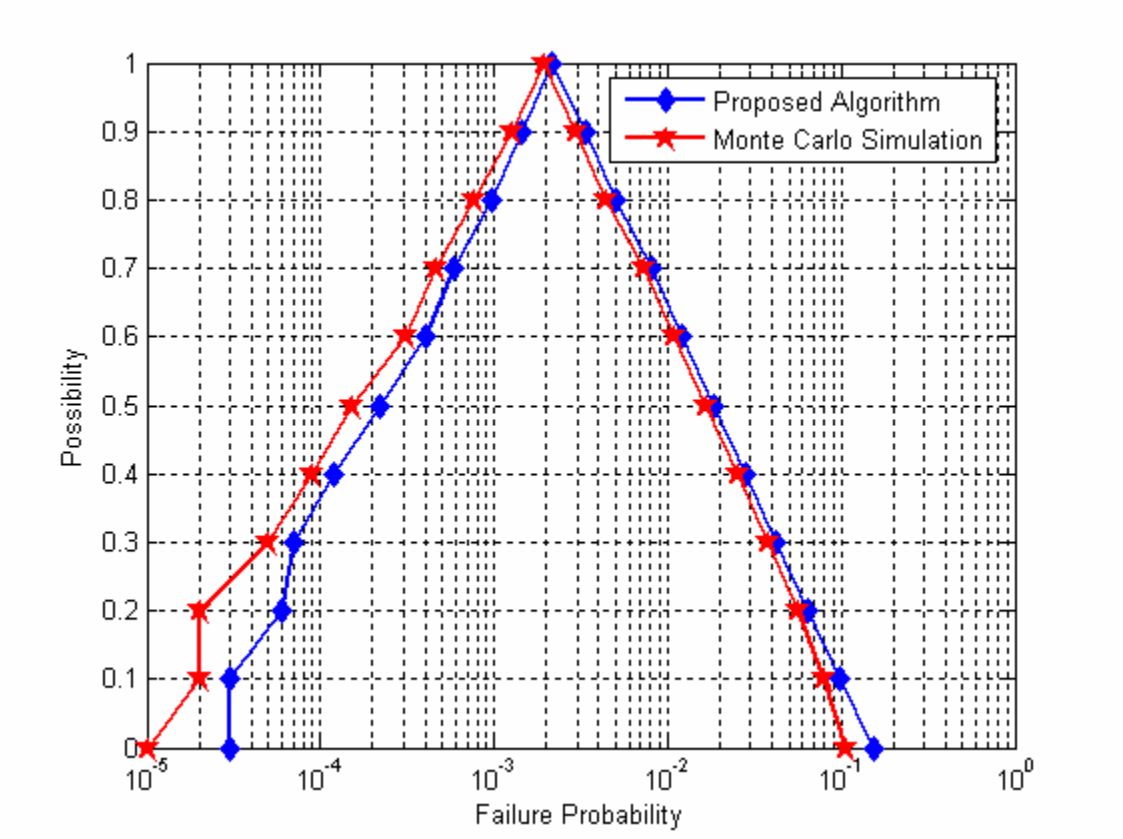

Figure 5.9: Membership Function of Failure Probability for the Turbine Blade

Figure 5.8 shows a comparison of the membership function of system reliability obtained using the proposed algorithm and conventional Monte Carlo simulation. To show the difference between the proposed technique and Monte Carlo simulation, the membership function of the failure probability was plotted on a log scale as shown in fig. 5.9. The MPPs of each of the limit-states are estimated, and Latin Hypercube sampling technique was used to sample design points around these MPPs for the construction of MPAs. These MPAs were used as closed-form expressions of the limit-states to obtain points on the joint failure surface. The proposed methodology needed a total of 590 exact simulations, which include the simulations required for calculating the gradients needed in the construction of the MPAs. At each configuration of the fuzzy variables, Monte

Carlo simulation needed 1 million simulations to obtain convergence. This clearly shows the computational efficiency of the proposed methodology.

The use of transformation techniques for membership functions leads to the estimation of the contribution of the fuzzy variables to the convolution integral accurately. These techniques coupled with the system reliability algorithm facilitate the improvement in the computational efficiency of the proposed algorithm.

6. OPTIMIZATION WITH SYSTEM RELIABILITY CONSTRAINT

The advantage of using a system reliability constraint as opposed to one reliability constraint for each failure mode is demonstrated by considering the composite model of the lightweight torpedo as an example. Different types of system reliability constraints are investigated in this work. An optimization problem was formulated to obtain a minimum weight composite structure that has the same characteristics as a metallic torpedo. Since there are numerous uncertainties associated with composites, a robust design was obtained by using reliability-based optimization techniques. A system reliability constraint is used in the probabilistic optimization rather than individual constraints on each of the failure modes. The algorithm presented earlier was used in determining the system reliability accurately during the optimization process. Results from the system level design constraint are compared with the results from the individual reliability constraints.

6.1. Reliability-Based Optimization with System Reliability Constraint

Traditionally, the optimization problem with reliability constraints is formulated using either safety index or failure probability constraints. But in the presence of multiple limit-states, all the limit-states can be taken into consideration for estimating and constraining their reliability. If the reliability of the structure is estimated based on all the failure modes, i.e. system reliability, then only one reliability constraint can be used in the optimization routine as opposed to multiple constraints.

A general optimization problem with system reliability can be defined as

Minimize $f(\boldsymbol{X}, \boldsymbol{B})$

subject to $P_{system}[g_i(\boldsymbol{X}, \boldsymbol{B}) < 0] \leq p_{system}$, $i = 1....n$ (6.1)

$b_j^L \leq b_j \leq b_j^U$, $j = 1...m$

where $\boldsymbol{X}$ represents the random variables, $\boldsymbol{B}$ represents the design variables, n is the number of limit states.

This system-reliability constrained optimization problem cannot be formulated in terms of a safety index. This is because the whole failure surface should be modeled accurately for a precise estimate of the system reliability, rather than just the MPP.

An advantage of using a system reliability formulation is that the system reliability estimation algorithm takes into account the definition of the failure of the structure. Based on whether it is a series or parallel system, the joint failure surface can be modeled and the failure probability can be imposed as constraint. Moreover, in the presence of an intersection region of the limit-states in the design space of the joint probability density function of the random variables, the system reliability formulation captures this intersection region accurately, leading to a better reliability estimate. Even if there is no intersection region and the system failure probability is the combination of the individual failure probabilities, the optimizer has the freedom of satisfying this combination rather that each individual constraint resulting in a better design. Therefore, an optimization problem formulated using a system reliability constraint yields a more robust optimal design than one obtained by using individual safety index or failure probability constraints.

6.2. Results and Discussion

A robust design must satisfy constraints such as weight, performance, cost, etc., as well as the reliability of the design due to the uncertainties in the system. To demonstrate the advantage of using a system reliability constraint in the design process rather than using failure probability or safety index constraints for each of the limit-states, the reliability-based optimization problem was formulated and solved with each of these constraints examined in three different cases.

The objective of the optimization problem was to minimize the total weight of the torpedo structure. The design variables were taken as the thicknesses of the laminates in the three orientation directions considered, i.e., 0^0, $\pm 45^0$, and 90^0, along with the thickness of the honeycomb core. These variables were also modeled as normally-distributed random variables with a coefficient of variation of 5%. The mean values of these variables were taken as the design variables in the optimization problem. In addition to these random variables, the material properties of the composite laminate, i.e., the moduli of elasticity in the longitudinal and transverse directions along with the density of the laminates were also modeled as random variables with a normal distribution. The coefficient of variation for these variables was also taken to be 5%.

Two deterministic constraints were used to ensure that the performance of the composite model matches that of the metallic model of the lightweight torpedo. These deterministic constraints are given in Eq. (6.2) and Eq.(6.3)

Fundamental Natural Frequency $\omega_1 \geq 22.0 Hz$ (6.2)

Buckling Load Factor (at 1000 m) $P_{cr} \geq 1.0$ (6.3)

In addition to these deterministic constraints, the structure was constrained to attain a prescribed reliability level of $P_f \leq 0.001$. The failure criteria for determining the reliability was that the fundamental natural frequency must be greater than 22.0 Hz and the buckling load factor must be greater than 1.0. Three different optimization problems were solved with the three different reliability constraints. In the first case, the failure probability of the system was constrained to be less than 0.001. In the second case, the failure probability of each of the limit-state functions was constrained to be less than 0.001. In the final case, the constraints were applied on the safety index of each of the limit-state functions. A failure probability of 0.001 corresponds to a safety index value of 3.09. So in this case, the safety index of each of the limit-states was constrained to be greater than 3.09. The optimization formulation for each of these cases is given below in (6.4) - (6.6).

$$\begin{aligned} &\text{Minimize } W(\boldsymbol{X}) \\ &\text{subject to } P_f\left[\omega_1 < 22.0 \cup P_{cr} < 1.0\right] \leq 0.001 \\ &\qquad \omega_1 \geq 22.0 Hz\,,\ P_{cr} \geq 1.0 \end{aligned} \tag{6.4}$$

$$\begin{aligned} &\text{Minimize } W(\boldsymbol{X}) \\ &\text{subject to } P_f\left[\omega_1 < 22.0\right] \leq 0.001\,,\ P_f\left[P_{cr} < 1.0\right] \leq 0.001 \\ &\qquad \omega_1 \geq 22.0 Hz\,,\ P_{cr} \geq 1.0 \end{aligned} \tag{6.5}$$

$$\begin{aligned} &\text{Minimize } W(\boldsymbol{X}) \\ &\text{subject to } \beta_1\left[\omega_1 \geq 22.0\right] \geq 3.09\,,\ \beta_2\left[P_{cr} \geq 1.0\right] \geq 3.09 \\ &\qquad \omega_1 \geq 22.0 Hz\,,\ P_{cr} \geq 1.0 \end{aligned} \tag{6.6}$$

The target failure probability on each of the component reliabilities was chosen to be the same as the system reliability. This is due to the lack of information on how to divide the system level requirement to the individual component level requirement.

The above three optimization problems were solved by the Design Optimization Tool (DOT) using the modified method of feasible directions algorithm. The structural analysis was performed using GENESIS. The failure probability of the system was estimated using the algorithm presented in chapter 3. The failure probabilities of each limit-state were calculated using the algorithm presented by Penmetsa and Grandhi [16]. The safety indices of the limit-states were estimated using the methodology presented by Wang and Grandhi [9]. A stacking sequence of $[0_{t1}/\pm45_{t2}/90_{t3}]_s$ was considered for this study. In all three cases, the starting point of the probabilistic optimization routine was the optimal solution from the deterministic optimization.

		Deterministic Optimum	With System P_f	With Individual P_f	With Individual β
Objective	Weight (kg)	224.27	229.20	228.67	227.98
Design Variables – Thickness (m)	0^0	0.0012	0.00143	0.00141	0.00144
	45^0	0.0008	0.00089	0.00087	0.00090
	90^0	0.0004	0.00062	0.00061	0.00045
	Honeycomb	0.0306	0.03067	0.03067	0.03065
Constraints	Frequency (Hz)	22.40	24.18	23.98	23.93
	Buckling Factor	1.1181	1.21	1.20	1.19
	Reliability	System P_f=0.53	System P_f=0.0007	P_{f1}=0.001, P_{f2}=0.00005 *System P_f=0.00105*	β_1=3.11, β_2=3.63 *System P_f=0.0014*

Table 6.1: Comparison of Reliability-Based Optimization Results

Table 6.1 shows a comparison of the optimum results obtained by the three different cases mentioned above. When compared to the deterministic optimization results, the weight of the structure obtained by probabilistic optimization was higher because the failure probability of the structure at the deterministic optimum was very high. This was because the optimizer tried to satisfy the constraint on the failure probability by increasing the thicknesses of the laminates. The increase in the thickness of the laminates increased the fundamental natural frequency and buckling load factor of the structure, thereby decreasing the failure probability. The system failure probability at the optimum design obtained was 0.0007, as opposed to 0.53 at the deterministic optimum. In the case of failure probability constraints on each limit-state, the weight of the obtained design was less than the weight obtained with a system reliability constraint, as can be seen from Table 6.1. But the system failure probability at the optimum was 0.00105, which violated the system reliability constraint. When the optimization problem was solved using safety index constraints, it produced an even lighter design, but the system failure probability was 0.0014. The calculation of the safety index did not take into account the nonlinearity of the failure surface, thereby resulting in an inaccurate estimation of the failure probability.

In the system reliability formulation, the failure surface was modeled accurately, which resulted in an accurate estimate of the failure probability. These results indicate that the optimization problems with individual failure probability or safety index constraints can produce lighter designs but cannot meet the design requirement of the system reliability. Moreover, by using the system reliability constraint, the definition of the structural failure (series or parallel) can be taken into account.

7. SUMMARY AND FUTURE DIRECTIONS

This work mainly focuses on two aspects of uncertainty quantification. One is to deal with mixed variable problems where some variables are quantified with probability distribution, while others are either interval or fuzzy membership functions. The other aspect is to propagate the uncertainties through structural systems with multiple correlated failure criteria. While dealing with these types of problems, the computational cost involved increases tremendously. This is due to the increase in non-random variables and the number of failure modes for the structure. So, to reduce the computational cost without losing much accuracy, function approximations are used to model the limit-state functions, as well as the failure surface.

Once the failure surface is available or approximated as a closed-form expression, the use of Fast Fourier Transforms (FFT) to solve the convolution integral efficiently has been demonstrated in the literature. Some of the approximation concepts used in this work are presented in the appendix. These high quality approximations are constructed around the MPP of the limit-state functions, thereby capturing their behavior around the MPP. Moreover, these approximations require only the computation of the first-order gradients to capture the nonlinearity of the limit-state functions.

In chapter 2, a methodology was presented for problems with a single failure mode and both random and fuzzy variables to result in an estimate of the membership function of reliability. Transformation techniques for fuzzy membership functions are introduced and these techniques are used along with FFT. The use of transformations facilitates the determination of the minimum and maximum values of the fuzzy variables that correspond to the extreme values of the response at a particular possibility level

without the use of optimization techniques. This is demonstrated with a numerical example where the extreme values of the response are within the region of interest. In the case of mixed variables, this configuration of the fuzzy variables can be used in estimating the bounds on the reliability at that level. Numerical examples were presented to show the accuracy of this methodology for mixed variable problems.

An algorithm for efficiently dealing with multiple correlated failure modes was presented in chapter 3. In the literature, the convolution integral was solved using FFT based on the failure region being represented by a single function. As the joint failure region in the case of structural systems is highly nonlinear, representing this region accurately with a single function can be complex. So a methodology was developed to solve the convolution using FFT based on multiple functions over several disjoint regions spanning the whole design space. The use of Multi-Point Approximations (MPA) enabled the accurate representation of the limit-states which can be used to obtain points on the joint failure surface. Response surface models were used to represent the failure region as a closed-form expression. The accuracy of the estimated failure probability of the system highly depends on the approximations used to model the failure surface. Therefore, the design space was divided until all the response surface models were accurate.

This technique for estimating the reliability of a structural system was extended for problems with random as well as interval variables. In the presence of interval variables, each configuration of these variables has an unknown probability. Moreover, for each configuration, an entirely new joint failure region is to be estimated. By the inclusion of interval variables in the construction of the MPA for the limit-states, the computational cost was greatly reduced. These techniques were applied to problems with

a large number of non-normal variables and multiple failure criteria. The numerical examples presented show the accuracy and applicability of these techniques.

For dealing with a combination of random and fuzzy variables in problems with multiple failure modes, the algorithm for estimating the system reliability is combined with transformation techniques for membership function. This technique can be used to solve a general uncertain analysis program where the variables could be modeled as using fuzzy membership functions or intervals or random variables. This methodology is capable of handling a wide range of random variable distributions and multiple failure criteria. It also has the capability of handling both series as well as parallel systems by modeling the joint failure surface accordingly.

A brief introduction of reliability based optimization is presented. By including additional constraints on the reliability of the structure, the obtained final design is not only optimal but also reliable. These reliability constraints can be placed on the reliability of each component or on the reliability of the system as a whole. The advantages of using a system reliability constraint as opposed to one reliability constraint for each failure mode is demonstrated by performing the optimization of the composite model of a lightweight torpedo. The results indicate that an optimization problem formulated with a system reliability constraint yields a better design that one formulated with individual failure probability or safety index constraints.

The use of high fidelity approximations to model implicit limit-state functions as well as the joint failure surface facilitates the reduction in the computational cost without losing accuracy. Fast Fourier transforms based reliability estimation technique has been developed to estimate the reliability based on multiple failure modes. Moreover,

transformation techniques for nonrandom variables are introduced and used to efficiently deal with mixed variables problems. These methodologies are the first of their kind and can be used to efficiently deal with a general uncertainty analysis problem with multiple failure modes as well as mixed forms of uncertainties.

Future Directions

In this dissertation, function approximations were used to estimate the reliability in problems with multiple forms of uncertainty as well as multiple failure modes. The accuracy of the reliability estimates is highly dependent on the quality of the approximations constructed. One area of further research is the development of a methodology to obtain the confidence intervals on these reliability estimates. This is a challenging task as the effect of the accuracy of the approximations used on the reliability estimates is to be studied. Moreover, the focus of these methodologies was on uncorrelated random variables. However, further research can be carried out for dealing with correlated uncertain variables where the random and non-random variables are correlated.

Another area of research would be system reliability estimation when the uncertain quantities are expressed as random fields as opposed to random variables. Component reliability can be estimated using existing stochastic finite element methods. But new techniques are to be developed for propagating random fields through structures with multiple failure modes.

APPENDIX A: APPROXIMATIONS

Reliability analysis is a computationally expensive iterative procedure. The problem for solving the multidimensional convolution integral can be transformed into a safety index problem. This requires optimization to find the point on the failure surface that is closest to the origin in the standard normal space. As this is an optimization problem, difficulty arises in obtaining convergence for highly nonlinear response functions and large scale structural problems. The computational expense involved in reliability analysis of an implicit response can be greatly reduced with the use of approximations. These approximations use the information about the behavior of the response at a limited number of points and establish a closed-form relation between the response and the input variables. Based on the validity of the approximation and the number of design points used in constructing the approximate model, they can be classified as local approximations and global approximations.

A.1. Local Approximations

Local approximations are those which use information at one or two points in the design space. As a limited amount of information is used in constructing these models, the validity of these approximations is restricted to the design space around the points used in the process. Most of the local approximations are constructed by using a first-order Taylor series expansion about a point where the function and gradient information are available. For example, a linear approximation is a first-order Taylor series expansion in terms of the design variables, x_i. Due to the truncation error associated with the first-

order Taylor series, the validity of these approximations is limited to the close vicinity of the expansion point. To improve the accuracy of these approximations, intervening variables can be used. A reciprocal approximation is obtained by expanding the first-order Taylor series in terms of intervening variable, $y_i = 1/x_i$. As can be seen here, the nonlinearity associated with the variables is fixed to be -1. The usage of this fixed nonlinearity restricts the capability of the model to adapt to different types of responses. This led to the development of approximations with adaptive intervening variables. These approximations calculate the nonlinearity indices of the intervening variables by using the information at two design points. One point is used as an expansion point for the Taylor series and the other is the comparison point based on which the nonlinearity indices are calculated.

A.1.1. Two-point Adaptive Nonlinear Approximation (TANA) [61]

This approximation is a first-order Taylor series expansion in terms of the intervening variables, $y_i = x_i^r$, as shown in Eq. (A.1).

$$\tilde{g}(\boldsymbol{X}) = g(\boldsymbol{X}_2) + \frac{1}{r}\sum_{i=1}^{n} x_{i,2}^{1-r}\frac{\partial g(\boldsymbol{X}_2)}{\partial x_i}(x_i^r - x_{i,2}^r) \tag{A.1}$$

where $\boldsymbol{X}_2$ is the expansion point. The nonlinearity index, r, is estimated by matching the function value at the comparison point, $\boldsymbol{X}_1$, with that of the approximate model. This model has increased flexibility than one point approximations for representing the response accurately. But the nonlinearity index is same for all the variables, which might not be the case for many structural problems. Moreover, only the information about the function value at the comparison point is used in the construction of this model.

Therefore, using the gradient information at the comparison point, this approximation can be improved to obtain a different nonlinearity index for each variable.

A.1.2. Improved Two-point Adaptive Nonlinear Approximation (TANA2) [62]

TANA2 is a second-order Taylor series expansion in terms of the intervening variables

$$y_i = x_i^{p_i} \qquad i = 1,2,\ldots,n \tag{A.2}$$

where the exponents p_i represent the nonlinear indices and are different for each variable, y_i is the intervening variable, and x_i is the physical variable. The approximation is expanded about $\boldsymbol{X}_2$ and is given by Eq. (A.3).

$$\tilde{g}(\boldsymbol{X}) = g(\boldsymbol{X}_2) + \sum_{i=1}^{n} \frac{\partial g(\boldsymbol{X}_2)}{\partial x_i} \frac{x_{i,2}^{1-p_i}}{p_i} (x_i^{p_i} - x_{i,2}^{p_i}) + \frac{1}{2}\varepsilon \sum_{i=1}^{n} (x_i^{p_i} - x_{i,2}^{p_i})^2 \tag{A.3}$$

This equation is a second-order Taylor series expansion in terms of the intervening variables, in which the Hessian matrix has only diagonal elements of the same value ε. Therefore, this approximation does not need the calculation of second-order derivatives. The error from the approximate Hessian matrix is partially corrected by adjusting the nonlinearity index p_i. In contrast to the true quadratic approximation, this approximation is closer to the actual function for highly nonlinear problems due to its adaptability.

Eq. (A.3) has $n+1$ unknown constants, so $n+1$ equations are required. By differentiating Eq. (A.3), n equations are obtained by matching the derivatives available at the comparison point $\boldsymbol{X}_1$:

$$\frac{\partial g(\boldsymbol{X}_1)}{\partial x_i} = \left(\frac{x_{i,1}}{x_{i,2}}\right)^{p_i-1} \frac{\partial g(\boldsymbol{X}_2)}{\partial x_i} + \varepsilon(x_i^{p_i} - x_{i,2}^{p_i}) x_{i,1}^{p_i-1} p_i \qquad i = 1,2,\ldots,n \tag{A.4}$$

Another equation is obtained by matching the exact and approximate function values with the comparison point X_1:

$$g(\boldsymbol{X}_1) = g(\boldsymbol{X}_2) + \sum_{i=1}^{n} \frac{\partial g(\boldsymbol{X}_2)}{\partial x_i} \frac{x_{i,2}^{1-p_i}}{p_i} (x_{i,1}^{p_i} - x_{i,2}^{p_i}) + \frac{1}{2}\varepsilon \sum_{i=1}^{n} (x_{i,1}^{p_i} - x_{i,2}^{p_i})^2 \tag{A.5}$$

The $n+1$ unknown constants are solved simultaneously using the $n+1$ equations given by Eq. (A.4) and Eq. (A.5). In this method, the exact function and derivative values are equal to the approximate function and its derivative, respectively, at the comparison and expansion points. So the approximate model generated is more accurate than the one-point approximations.

A.2. Global Approximations

Global approximations use the information at several design points spanning the whole design space. Due to the use of information at more design points they are accurate over a larger design space than local approximations. In this section, a brief review of the two global approximations used in this study is discussed.

A.2.1. Multi-point Approximation (MPA) based on Local Approximations [63]

The multi-point approximation can be regarded as the connection of many local approximations. With function and sensitivity information already available at a series of points, one local approximation is built at each point. All local approximations are then integrated into a multi-point approximation by the use of a weighting function. The

weighting functions are selected such that the approximation reproduces function and gradient information at the known data points.

If the function $F(\boldsymbol{X})$ and gradient $\frac{\partial F(\boldsymbol{X})}{\partial x}$ information is available at $\boldsymbol{X}_k = (x_{1,k}, x_{2,k}, ..., x_{n,k})^T$, $k = 1, 2, ..., K$, where K is the number of local approximations, then the multi-point approximation can be written in terms of the local approximations as,

$$\widetilde{F}(\boldsymbol{X}) = \sum_{k=1}^{K} W_k(\boldsymbol{X}) \widetilde{F}_k(\boldsymbol{X}) \tag{A.6}$$

where W_k is a weighting function

$$W_k(\boldsymbol{X}) = \frac{\phi_k(\boldsymbol{X})}{\sum_{j=1}^{K} \phi_j(\boldsymbol{X})} \tag{A.7}$$

and $\widetilde{F}_k(\boldsymbol{X})$ is a local approximation. $W_k(\boldsymbol{X})$ adjusts the contribution of $\widetilde{F}_k(\boldsymbol{X})$ to $\widetilde{F}(\boldsymbol{X})$ in Eq. (A.6). The weighting function, $W_k(\boldsymbol{X})$ has its maximum of 1 at $\boldsymbol{X}_k$ and vanishes when $\boldsymbol{X}_k$ is very far from $\boldsymbol{X}$.

Several blending functions, $\phi_k(\boldsymbol{X})$, can be used to make the MPA reproduce the exact function and gradient values at the data points where the local approximation was built. There are at least three blending functions that could meet this requirement. They are

$$\phi_k(\boldsymbol{X}) = \frac{1}{Exp(h_k) - 1} \tag{A.8}$$

$$\phi_k(\boldsymbol{X}) = \frac{1}{\log(h_k + 1)} \tag{A.9}$$

and $$\phi_k(\boldsymbol{X}) = \frac{1}{h_k} \tag{A.10}$$

where $h_k = (\sum_{i=1}^{n} (x_i - x_{i,k})^2)^m$ (A.11)

where m is a positive integer. Additionally, it is recommended, from computational consideration, that the design space be normalized as $x_i \in [0,1]$ to measure the weighting function.

With each of Eqs. (A.8-A.10), the weighting function of Eq. (A.7) has the properties

$W_k(\boldsymbol{X}_j)=\delta_{kj}$ (A.12)

$0 \le W_k(\boldsymbol{X}_j) \le 1$

$$Lim_{x_i \to \pm\infty} W_k(\boldsymbol{X}) = \frac{1}{K} \tag{A.13}$$

$$\sum_{k=1}^{K} W_k(\boldsymbol{X}) = 1 \tag{A.14}$$

The weighting function varies between 0 and 1, and the summation of all weighting functions is 1. The following properties can be shown for each blending function given in Eqs. (A.8-A.10).

$$\frac{\partial W_k(\boldsymbol{X}_j)}{\partial x_i} = 0 \tag{A.15}$$

Differentiating Eq. (A.6).

$$\frac{\partial \widetilde{F}(\boldsymbol{X})}{\partial x_i} = \sum_{k=1}^{K} [\frac{\partial W_k(\boldsymbol{X})}{\partial x_i} \widetilde{F}_k(\boldsymbol{X}) + W_k(\boldsymbol{X}) \frac{\partial \widetilde{F}_k(\boldsymbol{X})}{\partial x_i}],\ i=1,2, \dots, n \tag{A.16}$$

From Eqs. (A.6), (A.12), (A.15) and (A.16), the following are obtained as

$$\widetilde{F}(\boldsymbol{X}_j) = \widetilde{F}_j(\boldsymbol{X}_j) = F(\boldsymbol{X}_j),\ j = 1, 2, \dots, K \tag{A.17}$$

$$\frac{\partial \widetilde{F}(\boldsymbol{X}_j)}{\partial x_i} = \frac{\partial \widetilde{F}_j(\boldsymbol{X}_j)}{\partial x_i} = \frac{\partial F(\boldsymbol{X}_j)}{\partial x_i},\ i=1, 2, \dots, n;\ j=1, 2, \dots, K \tag{A.18}$$

Equations (A.17) and (A.18) show that the multi-point approximation has the same zero-order and first-order information as the original function at the data points.

$$Lim_{x_i \to \pm\infty} \widetilde{F}(\boldsymbol{X}) = \frac{1}{K}\sum_{k=1}^{K} \widetilde{F}_k(\boldsymbol{X})$$

The MPA is an average value of all the local approximation estimations when a design point is far from every data point.

Reliability analysis involves iterations, which require implicit function evaluations and gradient evaluations that are expensive and come from finite element simulation. Therefore, the use of approximations helps reduce the cost involved in each analysis without sacrificing the accuracy of the results. Multi-point function approximations are suitable for reliability analysis as the behavior of the response is accurately represented in the design space. The accuracy of the MPA is dependent on the local approximations used. TANA2 captures the information of the response accurately around the expansion and comparison points. Therefore, this approximation discussed-above is used as the local approximation in the construction of the MPAs.

A.2.2. Response Surface Methodology [64]

In this methodology, a polynomial equation is considered to represent the dependency of the input variables on the structural response as shown in Eq. (A.19).

$$\widetilde{g}(\boldsymbol{X}) = \beta_0 + \sum_{i=1}^{n} \beta_i x_i + \sum_{i=1}^{n} \beta_{ii} x_i^2 + \sum_{i=1}^{n}\sum_{j=i}^{n} \beta_{ij} x_i x_j + ... \qquad \text{(A.19)}$$

where, $\boldsymbol{X} = (x_1, x_2, ..., x_n)^T$ is a vector of the input variables in the problem and all the β's are constants evaluated in the construction of the response surface model. The number of design points needed to construct the model must be more than the number of

unknown coefficients. These unknowns are estimated using the method of least squares which minimizes the sum of square errors between the predictions from the model and the actual values at the data points. Adding additional terms to the model in Eq. (A.19), increases the number of unknown coefficients which increases the number of design points needed to construct the model. This becomes computationally expensive for a large number of variables.

To add more nonlinearity into the model, intervening variables can be used [65]. A response surface model with intervening variables is as shown in Eq. (A.20)

$$\tilde{g}(\boldsymbol{X}) = \beta_0 + \sum_{i=1}^{n} \beta_i x_i^{p_i} + \sum_{i=1}^{n} \beta_{ii} x_i^{2p_i} + \sum_{i=1}^{n} \sum_{j=i}^{n} \beta_{ij} x_i^{p_i} x_j^{p_j} + \ldots\ldots\ldots \quad \text{(A.20)}$$

where p's are the nonlinearity indices of each of the input variables. These indices are estimated while solving for the unknown coefficients in the model. An optimal configuration of these indices can be obtained by minimizing the sum of error squares.

In this work, response surface models were used to obtain closed-form expressions between the uncertain variables and the response. These closed-form expressions were used in conjunction with fast Fourier transforms to solve the convolution integral. To employ this methodology for solving the convolution, the closed-form expressions must be separable. Moreover, these closed-form expressions must be expressed as a linear combination of intervening variables. So a second-order response surface model without interaction terms was used. If this model failed to capture the variation in the response, then a second-order model with intervening variables is used. These models are shown in Eq. (A.21) and (Eq. A.22) respectively.

$$\tilde{g}(\boldsymbol{X}) = \beta_0 + \sum_{i=1}^{n} \beta_i x_i + \sum_{i=1}^{n} \beta_{ii} x_i^2 \tag{A.21}$$

$$\tilde{g}(\boldsymbol{X}) = \beta_0 + \sum_{i=1}^{n} \beta_i x_i^{p_i} + \sum_{i=1}^{n} \beta_{ii} x_i^{2p_i} \tag{A.22}$$

As the failure surface is modeled using response surfaces, the accuracy of the models constructed should be checked. One of the statistical criteria used to evaluate this accuracy is the R^2 criterion. R^2 accounts for the amount of variation in the response explained by the set of inputs in the response surface model. It is defined as

$$R^2 = \frac{SSR}{SST} = \frac{\sum_{i=1}^{n} \hat{y}^2}{\sum_{i=1}^{n} y^2} \tag{A.23}$$

where SSR is the Sum of Squares of Regression and SST is the Sum of Squares Total, $\hat{y}_i$ are the values predicted by the surrogate model and y_i are the exact values of the response used for constructing the model. An R^2 value of 1.0 indicates that all the variability of the response is explained by the response surface model, and an R^2 value of 0 indicates that none of the variability is explained by the response surface model. Therefore, a higher values of R^2 are preferred.

BIBLIOGRAPHY

1. Metropolis, N., and Ulam, S., "The Monte Carlo Method," *Journal of the American Statistical Association*, Vol. 44, 1949, pp. 335-341.
2. Coddington, P.D., "Analysis of Random Number Generators using Monte Carlo Simulation," *International Journal of Modern Physics*, Vol. C 5, 1994, pp. 547-562.
3. Morokoff, W. J., Caflisch, R. E., "Quasi-Monte Carlo Integration," *Journal of Computational Physics*, Vol. 122, No. 2, 1995, pp. 218-230.
4. Hasofer, A. M, and Lind, N. C., "Exact and Invariant Second -Moment Code Format," *Journal of the Engineering Mechanics Division*, ASCE, 100(EM), 1974, pp.111-121.
5. Wu, Y.-T., Millwater, H. R., and Cruse, T. A., "Advanced Probabilistic Structural Analysis Methods for Implicit Performance Functions," *AIAA Journal*, Vol. 28, No. 9, 1990, pp.1663-1669.
6. Breitung, K., "Asymptotic Approximations for Multinormal Integrals," *Journal of the Engineering Mechanics Division*, ASCE, Vol.110, No.3, 1984, pp.357-366.
7. Tvedt, L., "Distribution of Quadratic Forms in Normal Space-Application to Structural Reliability," *Journal of the Engineering Mechanics Division*, ASCE, Vol.116, 1990, pp. 1183-1197.
8. Tvedt, L., "Two Second Order Approximations to the Failure Probability," *Section on Structural Reliability*, A/S vertas Research, Hovik, Norway, 1984.
9. Wang, L. P., and Grandhi, R. V., "Safety Index Calculation Using Intervening Variables for Structural Reliability Analysis," *Computers and Structures*, Vol. 59(6), 1996, pp. 1139-1148.

10. Grandhi, R. V. and Wang, L. P., "Higher -Order Failure Probability Calculation Using Nonlinear Approximations," *Computer Methods in Applied Mechanics and Engineering*, Vol. 168, Issue 1-4, 1999, pp.185-206.
11. Bucher, C. G., and Bourgund, U., "A Fast Efficient Response Surface Approach for Structural Reliability Problems", *Structural Safety*, Vol. 7(1), 1990, pp. 57-66.
12. Rackwitz, R., and Fiessler, B., "Structural reliability under combined load sequences", *Computers and structures*, Vol.9, 1978, pp. 489-494.
13. Cia, G.Q., and Elishakoff, I., "Refined Second-Order Reliability Analysis," *Structural Safety*, Vol. 14(4), 1994, pp. 267-276.
14. Papadrakakis, M., Papadopoulos, V., and Lagaros, D. N., "Structural Reliability Analysis of Elastic-plastic Structures using Neural Networks and Monte Carlo Simulation," *Computer Methods in Applied Mechanics and Engineering*, Vol. 136, 1996, pp. 145-163.
15. Sakamoto, J., Mori, Y., and Sekioka, T., "Probability Analysis Method using Fast Fourier Transform and its Application," *Structural Safety*, Vol.19 (1), 1997, pp.21-36.
16. Penmetsa, R.C., Grandhi, R.V., "Adaptation of Fast Fourier Transforms to Estimate Structural Failure Probability," *Journal of Finite Element Analysis and Design*, Vol. 39 (5-6), 2003, pp. 473-485.
17. Benjamin, R. J., and Cornell, C. A., *Probability, Statistics and Decision for Civil Engineers*, McGraw-Hill, 1970.
18. Lin, Y. K., *Probabilistic Theory of Structural Dynamics*, Krieger Publishing Company, 1976.

19. Melchers R.E., *Structural Reliability; Analysis and Prediction*, Ellis Horwood, 1987, pp. 140-149.
20. Cornell, C.A., "Bounds on the Reliability of Structural Systems," *Journal of Structures ASCE*, Vol. 93(1), February 1967, pp 171-200.
21. Bennett, R.M., Ang, A.H-S., *Investigation of Methods for Structural System Reliability,* Structural Research Series No. 510, University of Illinois, Urbana, 1983.
22. Ditlevsen, O., "Narrow Reliability Bounds for Structural System," *Journal of Structural Mechanics*, Vol.7 (1), 1979, pp. 453-472.
23. Feng, Y., "A Method for Computing Structural System Reliability with High Accuracy," *Computers and Structures*, Vol. 33 (1), 1989, pp.1-5.
24. Song, B. F., "A Numerical Integration Method in Affine Space and a Method with High Accuracy for Computing Structural System Reliability," *Computers and Structures*, Vol. 42 (2), 1996, pp255-262.
25. Wang, D., Chowdhury, M. R., and Haldar, A., "System Reliability Evaluation Considering Strength and Serviceability Requirements," *Computers and Structures*, Vol. 62, No. 5, 1997, pp. 883-896.
26. Koucky, M., "Exact Reliability Formula and Bounds for General k-out-of-n Systems," *Reliability Engineering and System Safety*, Vol. 82, No. 2, 2003, pp. 229-231.
27. Kordecki, W., "Reliability bounds for multistage structures with independent components," *Statistics and Probability Letters*, Vol. 34, No. 1, 1997, pp. 43-51.

28. Penmetsa R.C., and Grandhi R.V., "Structural System Reliability Quantification using Multi-Point Approximations," *AIAA Journal*, Vol. 40, No. 12, 2002, pp. 2526-2531.
29. Levitin, G., and Lisnianski, A, "Structure Optimization of Multi-State System with Two Failure Modes," *Reliability Engineering and System Safety*, Vol. 72, No.1, 2001, pp. 75-89.
30. Melchers, R.E., Ahammed, M., "Estimation of failure probabilities of intersections of non-linear limit states," *Structural Safety*, Vol. 23 (2), 2001, pp. 123-135.
31. Mori, Y., Kato, T., "Multinormal integrals by importance sampling for series system reliability," *Structural Safety*, Vol. 25 (4), 2003, pp. 363-378.
32. Melchers, R. E., "Importance sampling in structural systems", *Structural Safety*, Vol.6, 1989, pp.3-10.
33. Zadeh, L., "Fuzzy Sets," *Information and Control*, Vol. 8, 1965, pp. 338-353.
34. Lallemand, B., Plessis, G., Tison, T., and Level, P., "Neumann Expansion for Fuzzy Finite Element Analysis," *Engineering Computations*, Vol. 16 (5), 1999, pp. 572-583.
35. Rao, S. S., and Weintraub, P. N., "Modeling and Analysis of Fuzzy Systems using Finite Element Method," *Proceedings of 41st AIAA/ ASME/ ASCE/ AHS/ ASC Structures, Structural Dynamics and Materials Conference*, Atlanta, GA, April-2000, AIAA-2000-1633.
36. Hanss, M., and Willner, K., "A Fuzzy Arithmetical Approach to the Solutions of Finite Element Problems with Uncertain Parameters," *Mechanics Research Communications*, Vol.27 (3), 2000, pp. 257-272.

37. Moore, R. E., *Methods and Applications of Interval Analysis*, SAIM Publ., Philadelphia, PA, 1979

38. Alefeld, G., and Herzberger, J., *Introduction to Interval Computations*, Academic Press, New York, 1983.

39. Hansen, E., *Global Optimization using Interval Analysis*, Pure and Applied Mathematics, Marcel Dekker, Inc., 1992, pp. 11-12.

40. Rao, S. S., and Berke, L., "Analysis of Uncertain Structural Systems using Interval Analysis," *AIAA Journal*, Vol. 35 (4), April 1997, pp. 727-735.

41. Chen, Su-Huan, and Yang, Xiao-Wei, "Interval Finite Element Method for Beam Structures," *Finite Elements in Analysis and Design*, Vol. 34, No. 1, 2000, pp. 75-88.

42. Dimarogonas, A. D., "Interval Analysis of Vibrating Systems," *Journal of Sound and Vibration*, Vol. 183, No. 4, 1995, pp. 739-749.

43. Guo, S., and Lu, Z., "Interval Arithmetic and Static Interval Finite Element Method," *Applied Mathematics and Mechanics*, Vol. 22, No. 12, 2001, pp. 1390-1396.

44. Gao, W., "Interval Natural Frequency and Mode Shape Analysis for Truss Structures with Interval Parameters," *Finite Elements in Analysis and Design*, Vol. 42, No. 6, 2006, pp. 471-477.

45. Briabant, V., Oudshoorn, A., Boyer, C., and Delcroix, F., "Nondeterministic Possibilistic Approaches for Structural Analysis and Optimal Design," *AIAA Journal*, Vol.37, No.10, October 1999, pp. 1298-1303.

46. Dong, W. M., and Wong, F. S., "Fuzzy Weighted Averages and Implementation of the Extension Principle," *Fuzzy Sets and Systems*, Vol. 21, 1987, pp.183-199.

47. Smith, S.A., Krishnamurthy, T., Mason, B.H., "Optimized Vertex Method and Hybrid Reliability," *Proceedings of 43rd AIAA/ ASME/ ASCE/ AHS/ ASC Structures, Structural Dynamics and Materials Conference*, Denver, CO, April-2002, AIAA-2002-1465.

48. Penmetsa, R. C., Grandhi, R. V., "Uncertainty Propagation using Possibility Theory and Function Approximations," *Mechanics Based Design of Structures and Machines*, Vol. 31, No. 2, 2003, pp. 257-279.

49. Moller, B., Graf, W., Beer, M., "Safety Assessment of Structures in view of Fuzzy Randomness," *Computers and Structures*, Vol. 81 (15), 2003, pp. 1567-1582.

50. Grandhi, R. V., Wang, L. P., "Reliability-Based Structural Optimization Using Improved Two-Point Adaptive Nonlinear Approximations," *Finite Elements in Analysis and Design*, Vol. 29, No. 1, 1998, pp. 35-48.

51. Kharmanda, G., Olhoff, N., El-Hami, A., "Optimum Values of Structural Safety Factors for a Predefined Reliability Level with Extension to Multiple Limit-States," *Structural and Multidisciplinary Optimization*, Vol. 27, No. 6, 2004, pp. 421-434.

52. Rais-Rohani, M., Singh, M. N., "Comparison of Global and Local Response Surface Techniques in Reliability-Based Optimization of Composite Structures," *Structural and Multidisciplinary Optimization*, Vol. 26, No. 5, 2004, pp. 333-345.

53. Wu, Y-T., Shin Y., Sues, R., and Cesare, M., "Safety Factor Based Approach for Probability-based Design Optimization," *Proceedings of the 42nd AIAA/ ASME/ ASCE/ AHS/ ASC Structures, Structural Dynamics and Materials Conference*, Seattle, WA, April-2001, AIAA 2001-1645.

54. Du, X., and Chen, W., "Sequential Optimization and Reliability Assessment Method for Efficient Probabilistic Design," *ASME Design Engineering Technical Conferences*, Montreal, Canada, 2002, DETC2002/DAC-34127.

55. Youn, B., Choi, K., and Du, L., "Enriched Performance Measure Approach (PMA+) and its Numerical Method for Reliability-Based Design Optimization," *Proceedings of the 10th AIAA/ISSMO Multidisciplinary Analysis and Optimization Conference*, Albany, NY, 2004, AIAA-2004-4401.

56. Eldred, M. S., Giunta, A. A., Wojtkiewicz, S. F., Jr., and Trucano, T. G., "Formulations for Surrogate-Based Optimization under Uncertainty," *Proceedings of the 9th AIAA/ISSMO Symposium on Multidisciplinary Analysis and Optimization*, Atlanta, GA, 2002, AIAA-2002-5585.

57. Box, G. E. P., and Draper, N. R., *Evolutionary Operation: A Statistical Method for Process Management*, John Wiley & Sons, Inc. New York. 1969.

58. Sacks, J., Welch, W. J., Mitchell, T. J., and Wynn, H. P., "Design and Analysis of Computer Experiments," *Statistical Science*, Vol. 4, No. 4, 1989, pp. 409-435.

59. Toropov, V.V., Filatov, A.A., and Polynkin, A.A., "Multiparameter Structural Optimization Using FEM and Multipoint Explicit Approximations," *Structural Optimization*, Vol. 6, No. 1, 1993, pp. 7-14.

60. *GENESIS Analysis Manual* Version 7.2, Vanderplaats Research & Development, Inc., Colorado Springs, CO.

61. Wang, L.P., and Grandhi, R.V., "Effective Safety Index Calculation for Structural Reliability Analysis," *Computers and Structures*, Vol. 52, No. 1, 1994, pp. 103-111.

62. Wang, L. P., and Grandhi, R. V., "Improved Two-Point Function Approximations for Design Optimization," *AIAA Journal*, Vol. 33(9), 1995, pp. 1720-1727.

63. Xu, S, and Grandhi, R. V., "Multi-Point Approximation for Reducing the Response Surface Model Development Cost in Optimization," *Proceedings of the 1st ASMO UK/ISSMO Conference on Engineering Design Optimization*, Ilkley, West Yorkshire, UK, July 8-9, 1999, pp. 381-388.

64. Cornell, J. A., *How to Apply Response Surface Methodology*, American Society of Quality Control, 1990, pp. 12-13.

65. Li, G., "Accuracy and Efficiency Improvement of Response Surface Models for Multidisciplinary Optimization," PhD Dissertation, Wright State University, Dayton, OH, USA, 2000.